2016

Enhancing Oncolytic Rhabdovirus Infection With Sunitinib In An IFN Responsive Tumour Model

Dastidar, Himika

UNIVERSITY OF CALGARY

Enhancing Oncolytic Rhabdovirus Infection With Sunitinib In An IFN Responsive Tumour Model

By

Himika Ghosh Dastidar

A THESIS

SUBMITTED TO THE FACULTY OF GRADUATE STUDIES

IN PARTIAL FULFILMENT OF THE REQUIREMENTS FOR THE

DEGREE OF MASTERS IN SCIENCE

GRADUATE PROGRAM IN MICROBIOLOGY AND INFECTIOUS DISEASES

CALGARY, ALBERTA

APRIL 2016

Abstract

Oncolytic virus (OV) therapy for cancer is an emerging biotherapeutic strategy that employs replicating viruses to selectively infect and kill cancer cells. While promising, host innate immunity, namely type I IFN signaling, remains a barrier to OV therapy as it eliminates the virus before it spreads efficiently through the tumour. Sunitinib (Su), a receptor tyrosine kinase inhibitor, was recently shown to enhance OV infection by inhibiting IFN signaling in tumour cells. We therefore hypothesized that Su might enhance oncolytic rhabdovirus (ORV) infection in tumours. Indeed, Su treatment improved ORV productivity, tumour regression and overall survival in an IFN responsive tumour model. Su reduced the number and function of IFN producing myeloid cells such as cDCs and MΦ and thereby improved tumour infection with ORV. Collectively, our findings provide further support for the clinical evaluation of Su/ORV co-therapy in OV refractory tumors.

Acknowledgements

I would like to express my sincere gratitude to my advisor Dr. Douglas Mahoney for the continuous support of my Masters of Science study and related research, for his patience, motivation, and immense knowledge. His guidance helped me in all the time of research and writing of this thesis. I could not have imagined having a better advisor for my MSc study.

Besides my advisor, I would also like to thank the rest of my committee: Dr. Don Morris and Dr. Donna Marie McCafferty, for their insightful comments and encouragement, but also for the hard questions which pushed me to broaden my research horizons and perceptions. I would also like to thank my external examiner Dr. Faisal Khan for taking the time to read and evaluate my thesis. I would also like to extend a special thanks to Dr. Paul Beaudry for stimulating discussion related to my particular research project and providing insightful comments, guidance and encouragement.

I thank my fellow lab mates for the stimulating discussions, the sound advice and company they provide during long days at the lab, and for all the fun we have had in the last three years. I would especially like to thank Dr. Chunfen Zhang (lab manager) for the extensive help with the *in vivo* studies. I am also grateful for Dr. Dale Balce (post-doctoral fellow) and Rhiannon Campden for kindly providing me with bone marrow derived macrophages and dendritic cells, Dr. Victor Naumenko and Dr. Dae Sun Kim for also providing assistance with animal work. I would like to thank Dr. Franz Zemp for critically reading this thesis.

Last but not the least; I would like to thank the 2013 iGEM crew as well as my family and friends for supporting me throughout the completion of my studies.

Table of Contents

List of tables

List of figures and illustrations

List of abbreviations

7-AAD: 7- Aminoactinomycin D

AKT: RAC-alpha serine/threonine-protein kinase

AML: Acute myeloid leukemia

APC: Antigen presenting cells

APC: Allophycocyanin

ATCC: American Type Culture Collection

ATP: Adenosine triphosphate

BAD: Bcl-2-associated death promoter

BCL-X_L: B cell Lymphoma Extra Large

BMDC: Bone Marrow Derived DCs

BMDM: Bone Marrow Derived Macrophages

BSA: Bovine Serum Albumin

CARD: Caspase activation and recruitment domains

CEA: Carcino- Embryonic Antigen

CLP: Common lymphoid progenitor

CMP: Common myeloid progenitor

CPE: Cytopathic effect

DAMP: Danger Associated Molecular Patterns

DC: Dendritic cells

eIF2α: Eukaryotic Initiation Factor 2 alpha

ELISA: Enzyme Linked Immunosorbent Assay

ERK: Extracellular signal-regulated kinases

FADD: Fas-Associated protein with Death Domain

FBS: Fetal Bovine Serum

FITC: Fluorescein Isothiocyanate

FLT3R: Fms-like tyrosine kinase 3

Fluc: Firefly luciferase

FSC: Forward Scatter

FSC-A: Forward Scatter Area

FSC-H: Forward Scatter Height

GIST: Gastrointestinal Stromal Tumor

GM-CSF: Granulocyte Macrophage Colony Stimulating Factors

GM-CSF: Granulocyte-Macrophage Stimulating factor

GFP: Green Flourescent Protein

Grb-2: Growth factor receptor-bound protein 2

HCC: Hepatocellular Carcinoma

HMGB-1: High-Mobility Group Protein 1

HPI: Hours Post Infection

HRP: Horse Radish Peroxidase

HSV: Herpes Simplex Virus

ICAM: Intracellular Adhesion Molecule

IFN: Interferon

IFNAR1/2: Interferon Alpha/Beta Receptor Subunit 1 And 2

IFN-γ: Interferon gamma

IL: Interleukin

IPS: interferon-β promoter stimulator 1

IRAK: Interleukin-1 Receptor-Associated Kinase

IRF: interferon regulatory factor

IRF: Interferon Regulatory Factors

ISG: Interferon Stimulated Genes

IT: Intra-tumoral

IV: Intravenous

JAK: Janus Kinase

JAM: Junction Adhesion Molecule

LDLR: Low Density Lipoprotein Receptor

LPC: Lymphoid progenitor cells:

MAGE: Melanoma Antigen E

MAPK: Mitogen-activated protein kinases

MAVS: Mitochondrial Antiviral Signaling Protein

M-CSF: Macrophage Colony stimulating factor

MDA: Melanoma Differentiation-Associated protein 5

MDSC: Myeloid derived suppressor cells

MEK: Mitogen-activated protein kinase

MHC: Major Histocompatibility Complex

MOI: Multiplicity of Infection

MPC: Myeloid progenitor cells

mRCC: Metastatic renal cell carcinoma

MTD: Maximum tolerable dose

MyD88: Myeloid differentiation primary response gene 88 κκκ

NDV: Newcastle Disease Virus

NEMO: NF-kappa-B Essential Modulator

NF-κB: nuclear factor kappa-light-chain-enhancer of activated B cells

NK: Natural Killer

NSCLC: Non-Small Cell Lung Carcinoma

TMB: 3'3'5'5' tetramethylbenzidine

TBST: Tris Buffered Saline with Tween 20

ORV: Oncolytic Rhabdovirus

OV: Oncolytic viruses

OVA: Ovalbumin

OVT: Oncolytic virus therapy

PAMP: Pathogen Associated Molecular Patterns

PCR: Polymerase Chain Reaction

PDGFR: Platelet-derived growth factor receptors

PE: Phycoerythrin

PerCP: Peridinin- Chlorophyll proteins

PFU: Plaque Forming Units

PI3K: Phosphatidylinositol-4,5-bisphosphate 3-kinase

PKR: Protein kinase R

RIG: RIG-I-like receptors

RIP: Receptor-interacting protein 1

RLR: RIG-I Like Receptor

RLU: Relative Luminescence Units

RNP: Ribonucleoprotein

SAR: Sialic Acid Receptor

SDS: Sodium Dodecyl Sulfate

SHIP: SH2 domain-containing inositol-5'-phosphatase

SHP2: Src homology-2 domain containing protein tyrosine phosphatase-2

SLAM: Signalling Lymphocytic Activation Molecule

Sos: Son of Sevenless

SSC: Side Scatter

SSC-A: Side Scatter Area

SSC-H: Side Scatter Height

STAT: Signal Transducer and Activator of Transcription

TAA: Tumour Associated Antigen

TAB: TAK-1 Binding Protein

TAK: TGF-β Activated Kinase

TBK: TANK-binding kinase 1

TGF-β: Transforming growth factor beta 1

TIF: Tumour Interstitial Fluid

TKI: Tyrosine Kinase Inhibitor

TLR: Toll-like Receptor

TME: Tumour Microenvironment

TNF-α: Tumour Necrosis Factor Alpha

TRAF: TNF receptor associated factors

TUNEL: Terminal deoxynucleotidyl transferase dUTP nick end labeling

TVEC: Talimogene laherparepvec

TYK: Tyrosine Kinase 2

VEGF: Vascular Endothelial Growth Factor

VEGFR: vascular endothelial growth factor receptor

VSV: Vesicular Stomatitis Virus

WT: Wild Type

CHAPTER 1: INTRODUCTION

1.1 Overview

OV therapy is a novel bio-therapeutic strategy that employs live, replicating viruses to selectively infect and kill tumour cells[1]. OVs target tumour cells due to their altered physiology such as mutations in apoptosis pathways, metabolism and anti-viral signalling pathways[2]. Oncolytic rhabdoviruses (ORV), such as VSVΔ51 and Maraba-MG1, preferentially infect and rapidly kill tumour cells[3,4]. However, ORVs are exquisitely sensitive to host anti-viral signalling, type I IFN. Virus infection induces the production of type I IFN which sets up an anti-viral state in the surrounding cells thereby making cells resistant to infection[5]. Sunitinib (Su) has recently been shown to inhibit type I IFN signalling in tumour cells thereby improving OV infection[6]. This thesis investigates the role of Su in improving ORV infection in an IFN responsive tumour model, 4T1.

1.2 Oncolytic viruses

Oncolytic virus therapy (OVT) employs viruses to preferentially target tumour cells without harming non-malignant tissue[1,7]. OVT has shown promise in pre-clinical models[8,9] as well as clinical trials. In 2006, Herpes simplex virus (HSV) expressing granulocyte macrophage colony stimulating factor (GM-CSF) (T-VEC) and adenovirus with an attenuating mutation (H101) was approved for human use in China[10]. Other viral platforms such as adenovirus, poxvirus, poliovirus, coxsackievirus, measles virus, reovirus and rhabdoviruses are also being developed as OV vectors. Most of these viral platforms are currently in early phase clinical trials or undergoing regulatory review[1]. A list of OVs and their clinical status is summarized in Table 1.

OVs can target tumour cells in different ways; some OVs display natural tropism towards cancer cells whereas others infect cells ubiquitously[1]. For example, OVs such as Newcastle Disease virus (NDV), myxoma virus and reovirus are more tropic to tumour cells and more likely to infect them compared to their non-diseased counterparts. These viruses are tropic to oncogenic signatures, which are common to tumour cells[1]. For example, Reovirus selectively infects cells that upregulate Ras activity, a common oncogenic signature[11]. Whilst some OVs are selective towards tumour cells, others infect tumour and normal cells ubiquitously. OVs that infect tumour and normal cells ubiquitously only survive in cells with anti-viral signalling defects. Whereas non-malignant cells can produce type I IFN to eliminate the infection[12,13]. Despite this, these OVs are considered too dangerous clinical use. For example, OVs such as VSV, adenovirus, measles, vaccinia virus and HSV ubiquitously infect tumour and normal cells without discrimination. Therefore they are attenuated to improve tumour selectivity or engineered to selectively infect cancer cells[1,7]. For example, oncolytic VSV, currently in phase I clinical trial has IFN-β engineered into its genome. Upon VSV-IFNβ administration non-malignant cells can respond to secreted IFN-β and protect themselves against VSV infection whereas tumour cells with IFN signalling defects will be infected[13]. Viruses can also be genetically altered to bind to antigens expressed by tumour cells. For example, an adenovirus platform, Adenovirus5/3-Δ24, binds to a specific integrin $\alpha_v\beta3$ upregulated on ovarian cancer cells[14]. Measles virus has been engineered to express an antibody that binds to carcinoembryonic antigen (CEA) an ectopic tumour antigen[1,7]. Different OV platforms, their genetic alterations clinical progress are summarized in Table 1. OVs selectively target tumour cells due to altered signalling pathways in tumour cells.

Table 1: Summary of different oncolytic virus mechanisms of action, genetic alterations and their clinical progress.[1,7,15]

Oncolytic virus	Receptor	Modification	Clinical trials	Types of cancers	Clinical Status
Adenovirus					
Onyx-015	ICAM-1 and CAR	E1B deletion to block p53 interaction	12	Head and neck, pancreatic, ovarian, colorectal cancers, gliomas, lung metastases, and liver metastases	Clinical studies were abandoned in 2000 due to lack of specificity and efficacy of the virus as a single agent in phase I and II clinical trials.[16]
H101		E1B deletion to avoid p53 interaction	4	Squamous cell carcinoma, head and neck cancer	Approved for use in China and marketed by Shanghai Biotech for head and neck cancer[17].
DNX-2401		24bp deletion and RGD insertion	4	Glioblastoma, ovarian cancer	Achieved orphan drug status for high-grade glioblastoma in the EU.
VCN-01		PH20 hyalouronidase insertion	2	Pancreatic cancer	Ongoing phase I dose escalation study with gemcitabine and abraxane in pancreatic tumours (NCT02045602).
Colo-Ad1			3	Colon cancer, NSCLC, renal cancer, bladder cancer, ovarian cancer	Ongoing phase I clinical trials in resectable tumors renal cancer, bladder cancer, colon cancer and NSCLC by Psioux Ltd (NCT02053220).
ProstAtak		Thymidine kinase insertion	6	Pancreatic, lung, breast, ovarian, prostate cancer and mesothelioma	Ongoing phase III trials in prostate cancer with standard radiation therapy (NCT01436968).
Oncos-102		24bp deletion, RGD and GM-CSF insertion	1	Solid tumours	Completed Phase I clinical trials and considered safe to use in malignant solid tumors (NCT01598129). Human trials also showed evidence of increase in tumor infiltrating lymphocytes after treatment[18].
CG0070		E3 deletion, to leave MHC production intact,	3	Bladder cancer	Ongoing phase I clinical trials in bladder cancer. CG0070 is well tolerated by

		GM-CSF insertion			patients and results indicate viral replication and virus mediated tumor regression (NCT02365818)[19].
Herpesvirus					
T-VEC	HVEM and Nectin	Deletion of ICP34.5, US11 deletion, GM-CSF insertion	7	Melanoma, head and neck cancers, pancreatic cancer	Approved by the FDA for use in inoperable melanoma[20].
G207		Deletion of ICP34.5, UL39 disruption	3	Glioblastoma	No dose-limiting toxicity observed in phase Ib trial in glioblastoma patients. Improvement in TILs after G207 infection, however the trial was too small to obtain statistical significance [21,22].
HF10		UL56 deletion, partial copy of UL52	3	Breast cancer, melanoma and pancreatic cancer	Phase I clinical trial complete in several cancers (NCT01017185). No adverse side effects observed in patients. Therapeutic potential observed due to TILs in the tumors[23–25]. Ongoing phase II clinical trial in malignant melanoma with ipilimumab (NCT02272855).
SEPREHVIR		ICP34.5 deletion	6	HCC, glioblastoma, mesothelioma, neuroblastoma	Ongoing Phase I/IIA trials indicate some anti-tumour therapeutic efficacy as measured by induction of Th1 cytokines and anti-viral and anti-tumour IgG production[26].
OrienX010		ICP3.45 deletion, ICP47 deletion, GM-CSF insertion	1	Melanoma, Liver Cancer, Pancreatic Cancer, Lung Cancer	Preclinical studies show that there was a reduction in pancreatic cancer growth[27]. Phase I development is ongoing in China by Oriengene Biotechnology (NCT01935453).

Vaccinia virus					
Pexa-Vec (JX-594)	?	GM-CSF insertion, TK disruption	13	Melanoma, liver, colorectal, breast and HCC	Several phase I/II clinical trials show signs of anti-tumor immune response with JX-549. Phase I trials indicate the virus in able to replicate in the tumor and improved survival in HCC patients[28]. Phase III randomized trial is currently recruiting for evaluation of Pexa-VEC with sorafenib in HCC (NCT02562755). Granted orphan drug status by the FDA for HCC.
GL-ONC1		TK disruption, hemaglutinnin disruptionF14.5L disruption	5	Lung, head and neck cancer, mesothelioma	Phase I clinical trial in GL-ONC1 showed reduced tumor burden in peritoneal carcinomatosis patients (NCT01443260).
Reovirus					
Reolysin	JAM	None	24	Glioma, sarcoma, colorectal cancer, NSCLC, ovarian cancer melanoma, pancreatic cancer, multiple myeloma, head and neck cancer	Early phase clinical trials with reovirus showed selective replication of reovirus in tumour cells. Additionally, no dose related toxicity in patients in doses upto $1x10^{11}$ [29,30]. Reolysin has achieved orphan drug status for ovarian cancer, pancreatic cancer and malignant glioma.
Paramyxovirus					
Measles virus	SLAM and CD46	MV-NIS^{+}, MV-CEA^{+}	6	Multiple myeloma, glioblastoma and brain malignancies, ovarian cancer	Phase I trials completed with MV-CEA in ovarian cancer. The virus was considered safe and improved median survival by 6 months in the patient population[31]. Phase I/II clinical trials ongoing in multiple myeloma and

					glioblastoma (NCT02192775, NCT00390299).
Newcastle Disease Virus		None	4	Neuroblastoma, glioblastoma and lung	Preclinical studies have shown promising potential as an oncolytic virus vector. NDV elicits an anti-tumour CD8+ T cell response in animal models[32]. Early phase I/II clinical trials have shown that NDV is safe for use in humans[33].
Coxackievirus					
Cavatak	ICAM-1	None	4	Melanoma, breast and prostate cancer	Pre-clinical studies with Cavatak treated C57/BL6 mice have shown evidence for the generation of CD8+ T cell mediated anti-tumour immunity[34]. Multiple phase trials are ongoing in melanoma (NCT02307149, NCT01227551) and bladder cancer (NCT02316171).
Rhabdovirus					
VSV-IFNβ	LDLR	IFN-β expressing	1	Hepatocellular carcinoma	Pre-clinical studies have shown promising results in safety and CD8+ T cell activation in mesothelioma model[13]. Phase I clinical trial is currently recruiting patients with HCC (NCT01628640).
Maraba-MG1-MAGE-A3		MAGE-A3 expression,	1	Lung, colon and melanoma	Maraba virus has shown oncolytic and anti-tumour potential in pre-clinical models of cancer[4,35]. Maraba-MG1-MAGEA3 is currently being evaluated with or without Adenovirus vectors for solid tumours (NCT02285816).

Poliovirus					
PVS-RIPO	CD155	IRES	1	Glioma	Pre-clnical studies have shown oncolytic potential of PVS-RIPO in xenograft models of GBM. Phase I clinical trial with PVS-RIPO shows that the virus was safe when injected directly into the tumour[36,37]. Currently ongoing clinical trial with grade IV recurrent glioblastoma (NCT01491893).

Tumour cells have mutations in signalling pathways which alter their cellular functions[1,7]. These include mutations cell-death pathways, anti-viral signalling pathways and altered proliferative and metabolic controls, all of which potentially make OV infection selective and sustainable. For example, tumour cells have mutated apoptosis machinery such as the B-cell lymphoma family of anti-apoptotic proteins (BCL-X_L). Normal cells undergo apoptosis when infected with virus. Inhibition of apoptosis allows cancer cells to survive and replicate infinitely. NDV targets cells that overexpress BCL-X_L and inhibit apoptosis allowing adequate time for the virus to replicate and spread[9]. Other oncogenic mutations such as Ras also result in apoptosis inhibition which allows for sustained OV infection and replication[38]. Additionally, tumour cells also have defects in anti-viral signalling pathways[2,3].

Anti-viral signalling, such as production of type I IFN, inhibits virus infection and replication as well as sets up an anti-viral state to protect neighbouring cells[39]. Tumour cells can have defects in anti-viral signalling pathways that enable OV infection. Normal cells secrete type I IFN, a key anti-viral cytokine, which orchestrates the production of anti-viral proteins[5]. Tumour cells can acquire loss of function mutations in components of the anti-viral signalling pathway. For example, tumour cells that have mutations in the IRF-3, IRF-7 upstream of IFN production pathway are susceptible to NDV infection[40] and VSVΔ51 infection[3]. Additionally, viruses are also reliant on host replication and translational machinery, for propagation[41]. Normal cells can regulate these pathways to limit viral replication, whereas tumour tells have mutations on these proteins which enable rapid replication[41].

Viruses usually lack protein translation machinery in their genome and therefore rely on the host protein translational machinery to effectively replicate[42]. Cells use eukaryotic initiation factor 2 α (eIF2α) for protein synthesis. Upon virus infection, normal cells phosphorylate eIF2α

and inhibit viral protein translation[43]. Tumour cells can have gain-of-function mutations on protein translation machinery such as eIF2α which enables them to divide rapidly[44]. For example, tumour cells can mutate Ser51, the key phosphorylation site in eIF2α, which enables for OV replication and protein synthesis[41]. Although, a key component of OV therapy is selective tumour cell infection, the mechanism of OV mediated anti-tumour response is not limited to tumour cell infection alone. OV therapy is multimodal and works by using three distinct yet interconnected mechanisms—(i) oncolysis, (ii) immune activation and (iii) vascular collapse[15]. These concepts are expanded upon in section 1.4. This thesis investigates the use of oncolytic rhabdoviruses (ORV), a class of OVs that consist of attenuated rhabdoviruses. ORVs are exquisitely sensitive to type I IFN due to their attenuating mutations (as discussed in section 1.3.3), which make them safe for clinical use but difficult to infect immune competent hosts with. This thesis studies the role of sunitinib, a small molecule tyrosine kinase inhibitor, in improving ORV therapy in an IFN responsive tumour model.

1.3 Oncolytic rhabdoviruses

Oncolytic rhabdoviruses (ORV) are negative sense single-stranded (-)ssRNA viruses that selectively target tumour cells with defects in IFN pathways[45,46]. Rhabdoviruses replicate quickly to reach high titres in tumour cells, which make them suitable oncolytic agents. The rhabdovirus genome is small (~10-12 kb), and amenable to genetic manipulation and effective transgene expression. For example, VSV expressing human IFNβ is currently in phase I clinical trials. ORVs are rhabdoviruses that express attenuating mutations, which allows IFN production[46]. As a result, ORVs target cells that are defective in IFN signalling, which enhances their safety as an

OV platform. ORV platforms that are currently under pre-clinical and clinical development are vesicular stomatitis virus (VSV), Maraba virus and Farmington. VSV was the first rhabdovirus to be developed as an ORV platform in early 2000s. Stojdl *et al* observed that VSV infected and killed tumour cells with defects in the IFN pathway[3,12]. Since then other ORV platforms, such as VSVΔ51 and Maraba-MG1, have been characterized *in vitro* and in pre-clinical mouse models[35]. VSV expressing human IFN-β and Maraba-MG1 expressing MAGE-A3, a melanoma antigen are currently in phase I clinical trials[15]. To understand the mechanism behind ORV function, we need to understand the structure and life cycle of rhabdoviruses.

1.3.1 *Rhabdoviruses*

Rhabdoviruses are (-) ssRNA viruses that belong to the order *Mononegalevirales*, family *rhabdoviridae*. They are classified as group V ssRNA virus according to the Baltimore classification system. There are over 200 different viruses in the *rhabdoviridae* family, which infect vertebrates, invertebrates and plants. Among rhabdoviruses, VSV, Maraba and Farmington are currently being developed as OV platforms[15]. Structurally, most rhabdovirus virions are shaped like a bullet measuring approximately 200 nm by 80 nm. Rhabdoviruses have a small genome (~10-12 kb) coding for five proteins—nucleoprotein (N), phosphoprotein (P), matrix protein (M), glycoprotein (G) and RNA dependent RNA polymerase (L). The viral capsid consists of M and G proteins. The viral RNA, P, N and L proteins are tightly wound in a coil within the capsid termed ribonucleoprotein (RNP)[47]. These five proteins have very specific roles in the rhabdoviral infection and replication.

1.3.2 *Lifecycle of rhabdoviruses*

The rhabdovirus lifecycle can be divided into three steps: (i) attachment and entry; (ii) uncoating and genome replication and (iii) packaging and budding of the daughter progeny. Rhabdoviruses such as VSV bind to host LDL receptor[48] via the G protein on the viral surface. VSVΔG mutants are unable to enter host cells, and VSV strains expressing G protein without any G transcript are able to undergo one round of replication in the host cell but unable to generate daughter progeny that can infect cells[49]. Upon attachment, VSV undergoes receptor-mediated endocytosis forming an early endosome. The early endosome acidifies and matures into a late endosome where the viral G protein fuses to the endosomal membrane and releases the viral ribonucleoprotein (RNP) into the host cytoplasm.

After release of viral RNP, VSV undergoes reverse transcription and translation to generate progeny. The L protein reverse transcribes rhabdoviral (-) ssRNA genome into (+) ssRNA, also known as the anti-genome or primary transcript, by the L protein and translated into viral proteins. The M protein blocks the transportation of IFN-β messages from the nucleus to the cytoplasm[50]. Reverse transcription and genome replication occurs simultaneously in the cytoplasm. Following this, the assembly and budding is initiated.

The viral progeny assembly starts approximately 2-3 hours after virus infection. The key players in viral assembly are the G and M proteins[51]. After translation, the G protein is transported into the Golgi/ER complex and folded with the help of chaperone proteins such as BiP and calnexin, glycosylated and fused into trimers. The G protein trimers then assemble at the cell membrane and form microdomains. Although important, G protein is non-essential for daughter progeny budding[49]. However, progeny production in ΔG virus is also reduced 10 fold compared to wild type VSV. However, the M protein is necessary for rhabdoviral budding. The

M protein is able to bind several viral and host protein to orchestrate budding. M proteins localize at the cell membrane; another set of M proteins also binds to the RNP and localize to the cell membrane. Rhabdoviruses then utilize host cellular machinery such as proteins that are used for vesicle formation[47]. Together, these components lead to budding of the progeny. The rapid replication cycle and the cytolytic capacity of rhabdoviruses make them suitable OV platforms.

1.3.3 *Development of clinically relevant ORVs*

Currently, VSV-IFNβ and Maraba-MG1-MAGEA3 are in Phase I clinical trials[15]. Rhabdoviruses enter the cell using LDLR[48], an ubiquitous receptor, and replicate rapidly causing cellular lysis which renders the use of wild type rhabdoviruses unsafe. Rhabdoviral platforms such as VSV and Maraba do not naturally infect humans and mice. However, at high doses necessary for OV therapy such as 10^9 plaque forming units, rhabdovirus infection has been shown to be lethal to mice[3]. To ensure safety, attenuating mutations, which allow type I IFN production, have been engineered into ORV platforms[3,35]. For the purpose of this thesis, only attenuating mutants VSVΔ51 and Maraba-MG1 will be discussed.

To enhance the safety of rhabdoviruses, attenuating mutations that reduce virulence have been engineered into rhabdoviruses. Host mRNA transport is inhibited by rhabdovirus infection; the M protein binds to a nuclear pore complex protein Nup98 and inhibits transportation of IFN-β message[31–34,]. Therefore, to generate attenuated VSV mutants, Desforges *et al*, generated VSV-M mutant. Among these, T1026R which had one mutation in the M protein, M51R, and TP3 which had two mutations on the M protein, V221F and S226R[55]. Stojdl *et al*, characterized these viruses as AV1 and AV2 respectively and created another mutant AV3 that has a deletion in the 51st amino acid on the M protein (ΔM51). The VSV-M mutants do not block host gene

expression and allowed IFN-β mRNA translation thereby targeting IFN-β defective cells. They also found that the maximum tolerable dose of AV1 and AV2 mutants were 100 to a 1000 fold higher in immune-competent mice compared to WT-VSV. Contrary to WT-VSV, the VSV-M mutants induced type I IFN signaling in host cells with intact IFN signaling molecules which makes VSV-M mutants safer than WT-VSV[3,12].

Following this, Brun *et al*, tested a library of rhabdovirus isolates to characterize their oncolytic potential and safety. Amongst these, they found Maraba virus, a rhabdovirus that shares 98% genomic identity with VSV, to be the most potent in the library. Maraba was also selective towards a NCI-60 cancer panel and had attenuated growth in normal fibroblasts. Similar to WT-VSV, Maraba was unsafe for use in mice at 10^7 PFU. Therefore, Maraba mutants were generated to further enhance safety of Maraba as an oncolytic vector. To this end, they generated single and double mutants of Maraba in both M and G proteins, M (L123W) and/or G (Q242R) and compared it to wt-Maraba. The double mutant (Maraba-MG1) was similar to M (L123W) in its ability to replicate in tumor cells, kill tumor cells and induce IFN production. However, the G Q242R mutant induced lower levels of IFN-β production, similar to WT-Maraba. The MG1 mutant produced high virus titers at early time-points compared to WT-Maraba and single mutants in tumour cells. MG1 infection was attenuated in fibroblasts; MG1 was also 100x safer in immune-competent mice compared to WT-Maraba. The maximum tolerable dose (MTD) of WT- Maraba was 10^7 and the MTD of Maraba-MG1 was 10^9. Taken together these data suggest that, MG1 was the safest and most effective oncolytic amongst the series of Maraba mutants[35]. ORVs are multimodal in nature and work using three different mechanisms: oncolysis, immune activation and vascular collapse[7].

1.4 Mechanism of oncolytic rhabdovirus therapy

1.4.1 Oncolysis

ORVs bind to the LDLR and enter the tumour cells, undergo replication and release progeny. A mechanism of ORV mediated tumour killing is oncolysis[7]. The cell death mechanisms in ORV are poorly understood. WT-VSV is known to activate caspase 9 to induce apoptosis, whereas VSV-M mutants are known to mediate cell death by activating caspase 8[56]. WT-VSV induces endoplasmic reticulum stress mediated apoptosis whereas VSV-M mutants activate three different apoptosis pathways such as the death receptor mediated apoptosis, mitochondria mediated apoptosis and ER stress mediated apoptosis[57,56]. Oncolysis leads to inflammation that breaks down immune tolerance and initiates the activation of anti-tumour immunity.

1.4.2 Immune Activation

Oncolysis releases viral PAMPs, cellular DAMPs such as ATP, high mobility group box 1 (HMGB-1) protein[58,59], tumour associated antigens (TAAs), neoantigens and inflammatory cytokines such as TNF-α, IL-12, IFN-γ and type I IFNs[1]. Type I IFN not only elicits an anti-viral response but also plays a key role in maturation of antigen-presentation by dendritic cells (DC), which prime cytotoxic T cells (CD8+ T cells) against TAAs. Type I IFN enhances DC maturation and activates cross presentation pathways to present TAAs. Cross presentation alters the signalling in DC antigen presentation pathways resulting in tumour antigens on major histocompatibility complex I (MHC-I) by altering the activation of STAT proteins as well as upregulating co-stimulatory molecule expression. For instance JAK/STAT signalling pathway is

activated upon IFN α/β binding to IFNAR1/2 receptor on DCs. In case of viral signalling JAK proteins phosphorylates STAT1/2 whereas in case of cross presentation of TAAs, STAT4 is phosphorylated activating a different cellular pathway[60,61]. Upon cross presentation of TAAs, CD8+ T cells are primed to recognize TAAs and kill tumour cells[62,63]. Treating immunocompetent tumour models with OV has shown the generation of anti-tumour CD8+T cell mediated immunity[8,13]. Treating B16 melanoma tumours with oncolytic VSV expressing tumour antigens ovalbumin (OVA) leads to an increase in tumour infiltrating CD8+ T cells mediated tumour regression. This indicates immune activation using with OV treatment. Furthermore, administration of VSV-OVA with neutralizing α-CD8 antibody was able to ablate the regression, which demonstrates that CD8 T cells were necessary for tumour regression[64]. Additionally, cytotoxic T cell activation also leads to the formation of memory T cells. For example, animals bearing B16-F10 tumours, that were treated with VSV expressing granulocyte macrophage colony stimulating factor (GM-CSF) and cured rejected a subsequent inoculation of B16-F10 cells[65]. In addition to immune activation, VSV has also been shown to infect tumour endothelium[46].

1.4.3 Vascular Collapse

ORVs can infect cells in a ubiquitous manner, and have been shown to infect tumour endothelium[66]. This phenomenon is termed vascular collapse and is poorly studied and understood. However, it is though that OVs infect the tumour endothelium thereby sequestering blood supply to the tumour causing tumour necrosis[67]. A study has shown reduced blood flow in the tumour subsequent to systemic VSV infection. This study suggests that that systemic

infection with oncolytic VSV leads to micro-clots as a result of leukocyte recruitment at the tumour endothelium leading to reduction in blood flow[68,69]. Additional evidence suggests that vaccinia virus infects tumour vasculature due to upregulation of VEGF signalling within the tumour. Increased VEGF signalling leads to transcriptional repression of type I IFN in the tumour endothelium thereby rendering these cells more prone to oncolytic vaccinia infection[70].

1.5 Barriers to oncolytic virus therapy

Although promising as a multimodal therapy, the clinical potential of OVs is limited in immune competent host. There are two barriers to OV therapy—host immunity and an immunosuppressive tumour microenvironment (TME) whereas tumour microenvironment inhibits the effective activation of CD8+ T cell mediate anti-tumour immunity[71,72]. Host immunity prevents the OV from reaching the tumour. There are two arms of immunity that orchestrate inhibition of OV infection, innate and adaptive. Virus-infected cells secrete innate anti-viral molecules such as type I IFN (IFNα/β). IFN-β limits OV infection by signalling in an autocrine and paracrine manner to set up an anti-viral state within the organism[73]. The tumour microenvironment is immunosuppressive and inhibits anti-tumour cytotoxic T cell response generated in response to OV therapy[74].

1.5.1 *Innate Immune responses that limit ORV*

The innate immune system has evolved to effectively protect the host from viral pathogens. Upon systemic administration of OVs, antibodies and phagocytic cells can prematurely eliminate OVs form the bloodstream. Upon viral entry, intracellular PRRs recognize viral pattern associated molecular patterns (vPAMPs), such as positive or negative strand DNA or RNA[75]. This leads to the induction of IFN production, which is a key regulator of anti-viral

signaling and orchestrates the set up of an anti-viral state in the host[39]. Two different types for PRRs detect viruses—TLRs and RLRs. TLRs 3,7 and 8 detect viral RNA (ssRNA or dsRNA) within the endosome. TLR7 and 8 bind to ssRNA whereas TLR3 binds to dsRNA. Upon binding to viral RNA, TLRs signal through a cytoplasmic adaptor protein MyD88 or without MyD88. These two mechanisms are known as MyD88 dependent and MyD88-independent signaling respectively. TLR7 and 8 signals through a MyD88 dependent mechanism whereas TLR3 signals through a MyD88 independent mechanism. TLR 7/8 recruits the IL-1 receptor associated kinase (IRAK-4), which further phosphorylates IRAK-1 or IRAK-2. The phosphorylated IRAK-4/1 or IRAK-4/2 complex then interacts with an E3 ubiquitin ligase, TRAF6 which poly-ubiquitinates the TAB/TAK-1 complex phosphorylating IKK-β. NEMO is a U3 ubiquitin ligase that poly-ubiquitinates p-IκB, which translocates to the proteasome to be degraded, releasing nF-κB (p50/p65). nF- κB translocates into the nucleus and induces the production of pro-inflammatory cytokines. The TAB/TAK complex simultaneously activates MAPK pathway that ultimately leads to the translocation of c-Jun and c-Fos complex (AP-1) into the nucleus and produces IFN-α/β. TLR3 on the other hand signals through a MyD88 independent manner. TLR3 signals through a different motif called TRIF. TRIF recruits TRAF3, which then activates IKKε and TBK-1 ultimately phosphorylating IRF-3 and IRF-7, which form a heterodimeric complex to enter the nucleus and produce IFN-β[76].

RLRs are cytosolic receptors that detect viral dsRNA. There are two receptors in the RLR family—the RIG-I receptor and the MDA-5 receptor. The RIG-I receptor binds specifically to 5'phosphorylated ends of short dsRNA fragments whereas MDA-5, a different RIG-I like receptor, binds to the long stretches of dsRNA. Upon binding dsRNA RIG-I and MDA-5 undergo an ATP dependent conformational change to activate the caspase recruiting domains

(CARD). The CARD domains then interacts with a signaling adaptor protein MAVS, also known as IPS-1, Cardif and VISA. MAVS then recruits TBK1/IKKε, which further phosphorylates IRF-3 and IRF-7 that translocate in the nucleus to produce of type I IFN. MAVS can also activate the NF-κB pathway by signaling through the IKKs[77,78]. MAVS can also activate NF-κB through an alternate pathway by signaling through RIP-1 and FADD. MAVS phosphorylates RIP-1, which interacts with FADD, activating TRAF6. TRAF6 then ubiquitinates NEMO leads to the degradation of IKKβ, translocation of NF-κB to the nucleus and production of pro-inflammatory molecules[79].

Upon secretion IFN-β binds to heterodimeric IFN receptor (IFNAR1/2) and signals in an autocrine and paracrine manner through the JAK/STAT pathway. IFN-β binds IFNAR1/2 and cytoplasmic proteins JAK/TYK are phosphorylated. The JAKs then phosphorylate STAT1/2, which forms a dimer and complexes with IRF9 to translocate in the nucleus, and stimulates the production of IFN stimulated genes (ISGs) by binding to the IFN stimulated response elements (ISRE) or GAS elements[80]. Some examples of ISGs include PKR, MxA, IRF-7, RNAseL, 2-5'OAS, and IFIT genes. These components work together to create an anti-viral state in the infected cell, surrounding cells and the organism[39,73]. The IFN production pathway and signaling is summarized in Figure 1.1. Additionally, the immunosuppressive tumour microenvironment also acts a barrier to ORV mediated anti-tumour immunity.

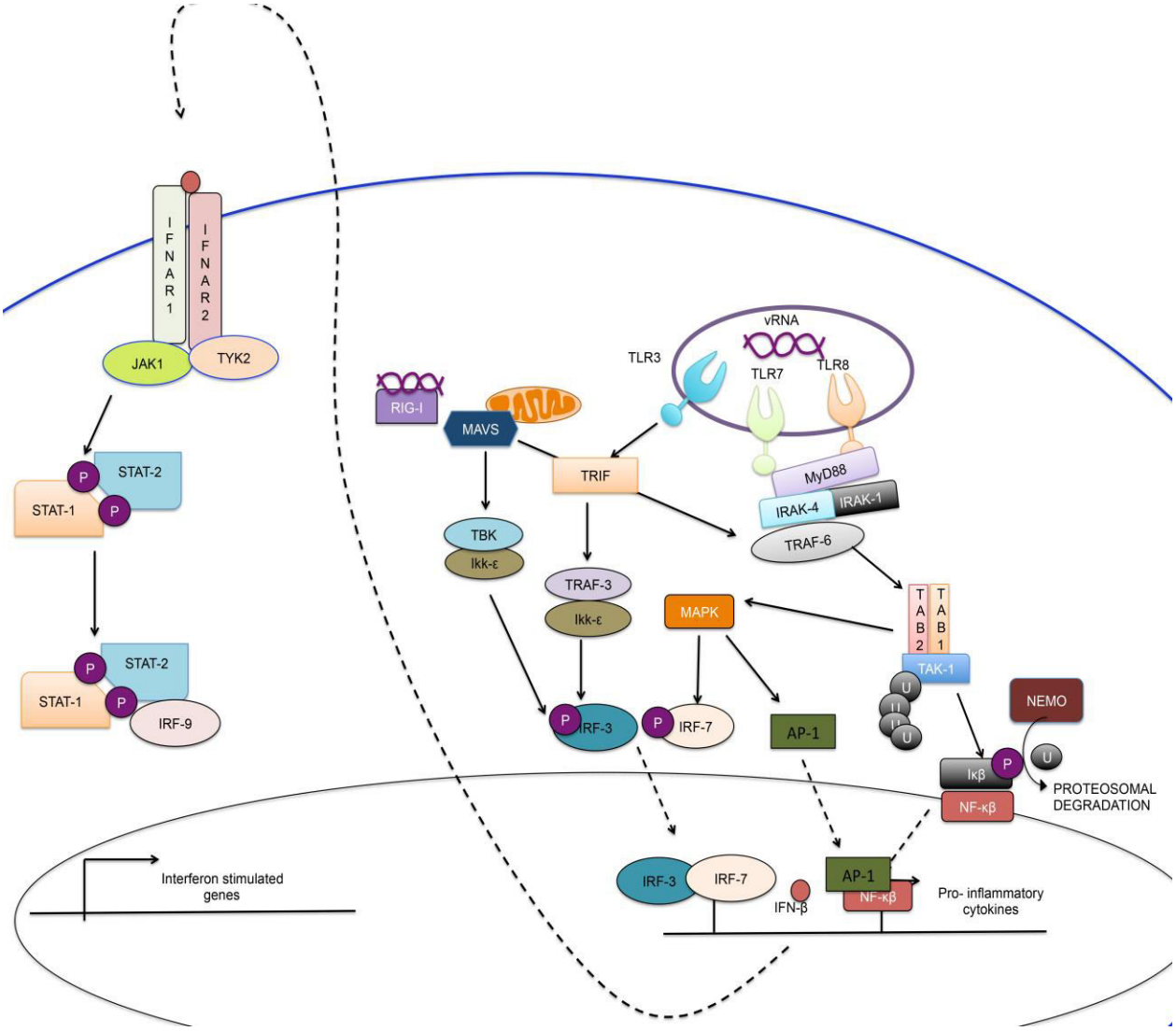

Figure 1.1 Toll-like receptor and RIG-I like receptor mediated anti-viral signaling in cells.

Upon RNA virus infection, TLRs 3, 7 and 8 detect RNA within the endosome and RLRs detect dsRNA in the cytoplasm. TLRs signal through MyD88 dependent or independent manner to activate the production of type I IFN (IFN-β) or NF-κB pathway which leads to the secretion of inflammatory cytokines. RLRs signal through MAVS, a mitochondrial protein to also lead to the production of type I IFN. When IFN-β is produced, it binds to the heterodimeric IFNAR1/2 on the cell itself and neighbouring cells. IFNAR1/2 phosphorylated JAK/TYK proteins which further phosphorylate STAT1/2 proteins. These translocate into the nucleus stimulating the production of interferon-stimulated genes (ISGs).

1.5.2 Tumour microenvironment as a barrier to ORV therapy

Formation of CD8+ T cell mediated adaptive anti-tumour response is an important aspect of OV mediated tumour clearance[62,64]. Various aspects of the tumour microenvironment inhibit CD8+ T cell activation[81]. The immune system surveys the body searching for malignant cells and eliminating them; to counteract this, tumour develop strategies to keep the immune system at bay. Tumours secrete cytokines such as GM-CSF that recruit immunosuppressive stromal cells such as myeloid derived suppressor cells (MDSCs)[82,62]. MDSCs are immature myeloid cells that display characteristics of granulocyte/monocyte[83] and supress inflammation. MDSCs orchestrate CD8+ T cell inhibition[81,84] by secreting immunosuppressive cytokines such as interleukin 10 (IL-10) and transforming growth factor beta (TGF-β)[85]. These cytokines block the production of cytolytic effector molecules from CD8+T cells such as IFN-γ and granzyme B[86] thereby negating the effects of OV mediated anti-tumour immune response. Taken together, innate IFN response and the tumour microenvironment limit ORV spread and impair ORV mediated anti-tumour immunity. Therefore, strategies to improve ORV infection and enhance anti-tumour immunity are necessary.

1.6 Sunitinib as an adjuvant for OV therapy

Strategies to improve ORV infection and ORV mediated immunotherapy in immunocompetent host are underway. Amongst these, one strategy is to genetically engineer ORV to express decoy receptors that bind IFN[87]. Others include combining ORVs with small molecules to improve the ORV mediated anti-tumour immunity. For example, combining ORV with small molecule LCL161 leads to improved CD8+ T cell immune infiltration and response in EMT6 breast tumour model[88]. In this study we investigate the role of sunitinib (Su), a small

molecule multi-tyrosine kinase inhibitor (TKI), in improving ORV mediated tumour control. Su was designed to be an anti-angiogenic TKI that targets several molecules in the angiogenic pathways. Su blocks phosphorylation of vascular endothelial growth factor receptor (VEGFR) 1/2/3 with the highest affinity but it also inhibits phosphorylation of platelet derived growth factor receptor (PDGFR)[89]. Anti-angiogenic drugs, now called "vascular normalizing agents" can improve perfusion within the tumour. Studies suggest that combining Su with other chemotherapeutics may lead to better delivery of the chemotherapeutic agents due to vascular normalization[90]. A study currently underway with oncolytic vaccinia has shown improved OV infection Rip-Tag2 pancreatic tumour model. This study suggests the improved OV infection is due to Su altering tumour vasculature; leading to improved delivery and infection[91]. Su is currently approved for use in human metastatic renal cell carcinoma (mRCC)[92], imatininb resistant gastro intestinal tumors (GIST), and acute myeloid leukemia (AML)[93]. In addition to being an anti-angiogenic drug, studies have also shown that Su targets c-KIT, c-RET, Fms-like tyrosine kinase 3 receptor (FLT3R)[94] and macrophage colony stimulating factor receptor (C-SFR1)[95]; and additional new targets have also been identified since. These newly identified targets include RNAseL and PKR, important IFN stimulated genes. RNAseL is an ISG; which can be found upstream of RIG-I after IFN production and leads to optimal activation of RLR signalling for the second wave of IFN signalling. Su has been shown to inhibit the phosphorylation and thereby activity of RNAseL[6,96]. These studies suggest suboptimal RLR signalling leads to an improvement in RNA virus productivity. Additionally, they also found that Su inhibits PKR phosphorylation; PKR binds to dsRNA in the cytosol. Upon binding dsRNA, PKR molecules dimerize and auto-phosphorylate which leads to phosphorylation of downstream eIF2α and inhibition of viral protein synthesis[5,43]. Su, has been shown to reduce the

phosphorylation of PKR and thereby eIF2α to improve RNA virus infection[96]. These two studies suggest that Su leads to inhibition of RNAseL and PKR in a cell-intrinsic manner to improve RNA virus productivity. In addition, Su has also been shown to relieve immunosuppression in tumour bearing hosts by reducing MDSCs[97,98].

MDSCs, as discussed previously, are putative immunosuppressive myeloid cells with granulocyte/monocyte characteristics[83]. MDSCs are recruited in the spleen and tumour of 4T1 bearing animals to promote systemic immunosuppression[97]. This immunosuppression leads to inhibition of CD8+ T cell mediated anti-tumour immunity[99]. Su treatment has been shown to reduce the population of MDSCs in the spleen and the tumour in mouse models such as 4T1, RENCA and CT-26[100]. Reduction in MDSC population has been linked to the generation of improved CD8+ T cell mediated anti-tumour immunity in animal models[100] as well as in patients[101]. Su treatment has shown a significant drop in the number of circulating neutrophils and thrombocytes in 20% of patients and a small percentage of them (5-8%) experience grade 3-4 neutropenia[102,103,104]. However, the mechanism by which Su reduces the MDSC population is unknown. Su is known to inhibit the phosphorylation of c-KIT, c-RET and FLT3R. These receptors are important players in the maturation of MPCs into mature myeloid cells[89,105]. FLT3R signalling is necessary for the survival of granulocyte/macrophage progenitor cells[106,107]. $FLT3^{-/-}$ mice have deficiencies in hematopoietic progenitor cells, conventional dendritic cells and NK cells[108]. FLT3R signalling phosphorylates SHIP/ SHP2 that then further phosphorylates PI3K and AKT. AKT inhibits the phosphorylation of pro-apoptotic BAD and induces signalling through anti-apoptotic Bcl-2 leading to cell survival. In addition, FLT3R can also phosphorylate Grb-2/Sos, which in turn activates Ras/Raf/MEK/ERK pathway, which leads to inhibition of BAD, a pro-apoptotic protein. Therefore, when FLT3 signalling is blocked, BAD is activated

and it leads to cell death in macrophage progenitor cells and DCs[109,110]. Since FLT3R signalling is crucial for haematopoiesis of the myeloid progenitor cells[107], Su treatment may lead to broad spectrum myelosuppression[103–105]. Patients treated with Su experience side effects such as neutropenia and thrombocytopenia[103,104]. Thereby, it is possible that Su treatment can also alter the population of other myeloid cells such as IFN producing macrophages and DCs. Since DC progenitors express FLT3R, treating animals with Su will reduce the number of DC progenitors ultimately reducing the number of dendritic cells[111], reducing IFN production and thereby improving virus infection.

Taken together, published evidence suggests that Su treatment can improve ORV infection by reducing the efficacy of ISGs such as PKR in a cell intrinsic manner[6,96]. In addition to dampening IFN signalling, Su may also reduce the number of IFN producing myeloid cells such as cDCs[111], reducing IFN and viral productivity *in vivo*. Furthermore, Su has been shown to alleviate immunosuppression by reducing the number of MDSCs in several tumour models such as CT-26, RENCA and 4T1. Taken together, these factors led us to hypothesize that Su may improve ORV infection and therapy in an IFN responsive and highly immunosuppressive tumour model, 4T1.

1.7 Research Objectives

HYPOTHESIS: Sunitinib (Su) will improve oncolytic rhabdovirus (ORV) infection in IFN responsive tumors.

AIM 1: To determine if Su improves ORV mediated tumour control in an IFN responsive tumour model.

AIM 2: To determine if Su treatment dampens IFN production and improves ORV infection in an IFN responsive tumour.

AIM 3A: To determine whether Su acts in a tumour cell dependent manner.

AIM 3B: To determine whether Su acts in a tumour cell independent manner.

CHAPTER 2: EVALUATING SUNITINIB AS AN IMMUNO-ADJUVANT TO ONCOLYTIC RHABDOVIRUS THERAPY IN AN IFN RESPONSIVE TUMOUR MODEL

2.1 Introduction:

Oncolytic virus therapy is novel bio-therapeutic strategy that uses live viruses to selectively infect and kill tumour cells without harming normal cells. There are several OV platforms that are currently being developed[1,7]. Among these, oncolytic rhabdoviruses (ORV) such as VSVΔ51 and Maraba-MG1, have shown potential in pre-clinical syngeneic mouse models[3,35], and are currently in phase I clinical trials. ORVs are multi-mechanistic and work using three major mechanisms---oncolysis, immune activation and vascular collapse. Oncolysis is the direct infection and lysis of tumour cells. Oncolysis leads to the release of TAAs and inflammatory cytokines that activate the immune system[112]. The TAAs are engulfed by APCs and cross-presented to cytotoxic CD8+T cells which leads to the activation and proliferation of anti-tumour CD8+ T cells[113]; the generation of a robust anti-tumour adaptive immune response which leads to tumour regression. Additionally, ORVs can also infect the tumour endothelium causing vascular collapse and tumour necrosis[67]. Although promising, the host immune system, namely type I IFN signalling[45,46], and the immunosuppressive tumour microenvironment[25] are barriers to ORV therapy.

ORVs are sensitive to anti-viral signalling[45,46], namely type I IFNs, which orchestrate the production of interferon stimulated genes (ISGs) and anti-viral proteins such as RNAseL and PKR. Together these proteins work together to inhibit viral replication and protein synthesis[5]. IFN signals to surrounding cells and sets up an anti-viral state, which limits ORV infection in

neighbouring cells. Some tumour cells can produce type I IFN; although, immune cells such as conventional dendritic cells (cDC)[114], F4/80$^+$ macrophages, CD169$^+$ macrophages and plasmacytoid dendritic cells (pDCs)[115] are also major IFN producers. Additionally, CD169$^+$ MΦ also allow virus gene-expression which aids anti-viral T cell priming in a controlled manner [116]. Despite being an important regulator of anti-viral signalling, CD169$^+$ MΦs are only characterized in the spleen, but we also aimed to characterize CD169$^+$ cells in the tumour with ORV and Su. In addition to type I IFN, the immunosuppressive tumour microenvironment is also a barrier to ORV mediated anti-tumour immunity[117].

ORV mediated anti-tumour immunity can be negated by the immunosuppressive tumour microenvironment[62,118]. Tumours often recruit immunosuppressive cells such as myeloid derived suppressor cells (MDSCs) that inhibit CD8+ T cell activation[25,83] to escape immune detection[119]. MDSCs secrete cytokines such as IL-10 and TGF-β that transcriptionally repress the release of IFN-γ and GzmB from anti-tumour CD8+ T cell[86]. Together these factors inhibit the effective activation of anti-tumour immunity. Therefore, strategies are overcome these barriers are necessary.

Studies have shown that sunitinib (Su), a tyrosine kinase inhibitor, can inhibit the activation of molecules downstream of IFN signalling in tumour cells[6,96] as well as reduce MDSCs in several tumour models[98,120]. Su has been shown to inhibit the phosphorylation and activation of PKR and eIF2α in response to RNA virus infection in a cell intrinsic manner[96] which leads to an improvement in rhabdovirus productivity. However, this study used WT-VSV, a virus already capable of inhibiting IFN signalling[6]. Therefore, we aimed to determine whether combining Su with clinically advanced rhabdoviruses, such as VSVΔ51 and Maraba-MG1, would also lead to an improvement in viral productivity and tumour regression. Su not only

blocks type I IFN signalling but also affects myeloid cell viability[109,121]. Su is known to target FLT3R[121], a cytokine receptor important for maintaining the population of the common myeloid progenitor cells (MPCs)[107]. MPCs give rise to cells such as cDCs, F4/80$^+$ Mϕ and CD169$^+$ Mϕ, which are important IFN producers. However, the role of Su in reducing the number of the aforementioned IFN producing cells is not well understood. Therefore, we wanted to test whether Su treatment also reduces the population of cDCs, F4/80$^+$ Mϕ and CD169$^+$Mϕ. Additionally, the immunosuppressive tumour microenvironment is also a barrier to ORV mediated tumour regression. Su has been well documented to reduce the population of MDSCs, a putative immunosuppressive cell, in several tumour models such as CT-26 colon carcinoma model, RENCA renal cell carcinoma model and 4T1 breast cancer model leading to an improved CD8+ T cell mediated anti-tumour immunity[100]. Together these studies suggest that Su may be able to inhibit both IFN production and immunosuppression, which may lead to tumour regression in IFN responsive ORV resistant tumour models.

Thereby we hypothesized that Su may improve the productivity of ORV in an IFN responsive tumour model, namely 4T1 (Figure S1). To this end, we tested the efficacy of Su in improving VSVΔ51 and Maraba-MG1 mediated tumour control and infection. Since VSVΔ51 and Maraba-MG1 have not been compared in the same tumour model, we also characterized VSVΔ51 against Maraba-MG1 *in vitro* and *in vivo*. We found that treating 4T1 tumours with VSVΔ51/ Maraba-MG1 and Su leads to an improved viral productivity and reduced type I IFN. We also found that Su acts on tumour infiltrating cDCs and CD169+ MΦs by reducing both the number and IFN producing function of DCs and MΦs that leads to an improvement in viral titres within the tumour.

2.2 Materials and Methods:

2.2.1 Reagents:

Sunitinib Malate was purchased from Selleckchem in powder form in 500 mg aliquots (Catalogue# S1042). 4T1, mouse breast carcinoma cells (ATCC Catalogue#: CRL-2539) and Vero, monkey kidney cells (ATCC Catalogue#: CCL-81) were obtained from ATCC and propagated in Dulbecco's Modified Essential Medium (DMEM, VWR Catalogue# 10565-018) supplemented with 10% fetal bovine serum (FBS, ThermoFisher Catalogue# 12484-010). 4T1 and Vero cells were cultured in DMEM+10% FBS and frozen at passage two and thawed for further use. ACHN, human renal carcinoma cells (ATCC Catalogue#: CRL-1611) were kindly donated by Dr. Don Morris (University of Calgary) and maintained in Eagles Modified Essential Medium (EMEM, VWR Catalogue# 10128-608) supplemented with 10% FBS, as recommended by ATCC. All cells were tested for mycoplasma contamination using polymerase chain reaction (PCR) amplification using a kit (Sigma Aldrich, Catalogue# MP0035) before use, and mycoplasma free stocks were stored in the -80^{o}C freezer for subsequent use.

Viruses used in this study were VSVΔ51 expressing green fluorescent protein (GFP) (VSVΔ51-GFP, Indiana Serotype)[3], VSVΔ51 expressing firefly luciferase (Fluc) (VSVΔ51-Fluc, Indiana Serotype), wild type (WT)-VSV (Indiana Serotype), Maraba-MG1[35] expressing GFP (Maraba-MG1-GFP) and Maraba-MG1-Fluc. Dr. David Stojdl from the Children's Hospital of Eastern Ontario (CHEO) research institute kindly provided viruses used in this study.

Primary antibodies for western blots were purchased from Cell Signalling technology, Santa Cruz and Milipore and secondary antibodies were purchased from Bio-Rad. The antibodies used in this study were total-PKR (Catalogue# sc-6282), phospho-PKR (Thr451, Catalogue# sc-

101784), which were purchased from Santa Cruz and total eIF2α (Catalogue# CST#9722), phospho-eIF2α (Ser51, clone D9G8; Catalogue# CST#3398) were purchased from Cell Signalling technology. β-actin was used as a loading control and purchased from Milipore (Clone C4, Catalogue# MAB1501). Secondary antibodies conjugated to horseradish peroxidase (HRP) were purchased from Bio-Rad, goat anti-rabbit (Catalogue# 1706515) and goat anti-mouse (Catalogue# 1721011).

Antibodies used for flow cytometry were purchased from eBiosciences, BD Pharmingen and Biolegened. Antibodies used in this study were Fc block (α-CD16/32 antibody, Biolegend Catalogue# 101302), CD11b (clone: M1/70, PE-Cy7 conjugated: eBio Catalogue# 25-0115-82, FITC conjugated: eBio Catalogue# 11-0112-82), CD45R/B220 (clone: RA3-6B2, APC conjugated: eBio Catalogue# 17-0451, APC-e-Flour780 conjugation: eBio Catalogue# 47-0451), CD8-a (clone 53-6.7, PE-conjugation: BD Catalogue #553032), CD4 (clone RM 4-5, PerCP-Cy5.5 conjugated, eBio Catalogue# 45-0042-82), Gr1 (clone RB6-8C5, PE conjugated: BD Catalogue# 553812, PerCP-Cy5.5 conjugated: eBio Catalogue# 45-5931-80), CD11c (clone N418, APC conjugated: eBio Catalogue# 17-0114-82), CD45 (clone 30-F11, APC conjugated: eBio Catalogue# 17-0451-82), CD19 (clone eBio1D3, APC-Cy7 conjugated: eBio Catalogue# 47-0193-80) and CD169 (clone 3D6.112, Biolegend Catalogue# 142404). Alamar Blue dye (Catalogue# DAL1025) and ACK lysis buffer (Catalogue# A1049201) were purchased from Thermofisher Scientific and IFNβ ELISA kit was purchased from PBL Assay Science (Catalogue# 42400-1).

2.2.2 Dissolving Sunitinib Malate:

Sunitinib malate was dissolved in sterile PBS supplemented with 1% DMSO to achieve a concentration of 8 mg/mL and stored in -20^{o}C. These stocks were used for both *in vitro* and *in vivo* studies. Stocks were thawed a maximum of two times for *in vivo* studies and thawed only once for *in vitro* studies. 100 µL of 8 mg/mL sunitinib stock was administered per 20 g mouse to achieve a concentration of 40 mg/kg.

2.2.3 Purifying Oncolytic Rhabdoviruses:

VSVΔ51-GFP, VSVΔ51-Fluc, Maraba-MG1-GFP, Maraba-MG1-Fluc and WT-VSV were propagated using Vero cells as described previously[122]. Briefly, Vero cells were seeded in 15 cm dishes and grown until the plates were approximately 95% confluent. Vero cells were then infected with VSV or Maraba-MG1 strains at a multiplicity of infection (MOI) of 0.01. The supernatant was harvested when approximately 50% of the cells were observed to have cytopathic effect (CPE) and rounded up. This was approximately 18 hours post infection (HPI) after Maraba-MG1 and WT-VSV infection and 18-20 HPI after VSVΔ51 infection. Following this the supernatant was collected in 50 mL falcon tubes and centrifuged at 780xg for 5 minutes at 4^{o}C to pellet cellular debris. After centrifugation, the supernatant was collected using a 25 mL serological pipette and filtered through a 0.2 µm membrane to remove all debris from the media. To concentrate the virus, the filtered supernatant was placed in polypropylene bottles and centrifuged at 28,000xg for 1.5 hours (longer if necessary) at 4^{o}C until virus pellets formed. To purify the virus, the supernatant was carefully removed from the bottles using a 25 mL serological pipette without disturbing the pellet. The virus pellet was then washed with PBS

twice to remove any remaining media and resuspended in 2 mL of solution C (1mM EDTA, 1mM NaCl, 1mM Tris, pH 7.4). Following this, an Optiprep gradient (Sigma Aldrich, Catalogue# D1556) was prepared using 5 mL of 15% Optiprep (1.5 mL of 50% Optiprep and 3.5 mL of solution C), 5 mL of 35% Optiprep solution (3.5 mL of 50% Optiprep and 1.5 mL of Solution C) in thin-walled ultracentrifuge tubes (Beckman Coulter Catalogue# 344059). Virus resuspended in solution C was then loaded on to the top of the gradient and the tube was centrifuged at 160,000xg for 1.5 hour at 4^{o} C. This yielded a single band of concentrated virus particles, which was collected by first removing solution from the top and then a P1000 pipette was used to collect the concentrated virus. The virus was then placed into a 5 mL eppendorf tube and aliquoted into 1.5 mL eppendorf tubes in volumes of 50-100 µL and stored at -80^{o} C and titered at a later time using plaque assay (described below in section 2.2.6). The purified virus was then diluted in the appropriate solutions for use in both *in vitro* and *in vivo* studies.

2.2.4 4T1 subcutaneous tumour model:

BALB/c (H-2d) mice were obtained from the Charles River Laboratory Inc. (Wilmington, MA) and were maintained under specific pathogen free (SPF) conditions in Biohazard Level 2 facility, Animal Housing Centre, University of Calgary. The mice used in these studies were female and between 6-8 weeks of age. All mouse experiments were conducted according to the guidelines approved by The University of Calgary Conjoint Health Research Ethics Board (Protocol# AC13-0271).

4T1 cells were thawed five days prior to the injection day. Media was refreshed one day after thawing the cells and the cells were then passaged (1:3) once and plated in 10 cm dishes

with DMEM+10% FBS the day before injection. On injection day, media was aspirated and 4T1 cells were washed twice with PBS to remove any remaining media on the plate. Following this, cells were treated with pre-warmed 0.01% Trypsin EDTA solution and incubated in 37^{o}C incubator for 5 minutes. Upon detachment of 90% of cells, as observed under a light microscope, media was dispensed on the cells and pipetted several times to detach all cells from the plate. 100 µL of cells were then diluted 1:10 in PBS in an eppendorf tube and counted using a cell counter or haemocytometer. The cell solution with media was then placed in a 15 mL falcon tube and centrifuged at 300xg for 5 minutes. Following this the media was aspirated and the cell pellet was washed with PBS twice before resuspending the cells at a concentration of $2x10^6$ cells/mL in PBS. Cells were then kept on ice until injection and 50 µL of cells ($1x10^5$ cells) were injected into the bottom right mammary fat pad of Balb/c mice using 28G, ½ inch long 500 µL insulin syringe (BD: Catalogue# 329424).

2.2.5 In vivo survival experiments:

4T1 tumours were established as previously described (section 2.2.4). Mice bearing established (5 day old) 4T1 tumours were then treated with sunitinib, which was administered intra-peritoneally (I.P.) using a 26G, ½ inch long needle with an insulin syringe daily for 14 days at a dose of 40 mg/kg. $5x10^8$ plaque forming units (PFU) of VSVΔ51 or Maraba-MG1 was injected intra-tumorally (I.T.) in 20 µL of PBS using a 27G, ½ inch long 500 µL tuberculin syringe directly into the tumour mass on days 8, 11 and 14-post tumour inoculation. Tumour dimensions, length and width, were measured twice a week using vernier calipers. Additionally, mice were weighed twice a week and monitored for signs of sickness due to tumour burden or side effects

of treatment such as lack of movement and grooming. Mice were euthanized using cervical dislocation when the tumour burden was >500 mm^3. Tumour volume was measured as $½L*W^2$ where L= length and W= width of the tumour. An n= 17 mice were used for control group, n= 19 mice were used for Su treated animals, n= 10 mice were used for MG1 treatment group, n= 9 mice were used for MG1+Su treatment group, n= 5 mice were used for each of VSVΔ51 and VSVΔ51+Su treatment groups.

2.2.6 Quantification of virus particles within the tumour:

Tumours were excised at 72 HPI using sterile forceps, scalpel, and scissors and any remaining skin was removed from the tumour. The tumour was then placed in 1.5 mL eppendorf tubes. The tubes were then flash frozen by placing them in 95% EtOH and dry ice for storage in -80^oC until analysis. For analysis, eppendorf tubes containing tumours were thawed on ice and the tumours were then weighed, chopped into small pieces (approximately 1 mm in diameter) and homogenized using Fisher Scientific Homogenizer Model 125 in serum free DMEM at a concentration of 50 mg tissue per mL using careful sterile technique. The homogenate was then centrifuged at 12,000 rpm for 5 minutes at 4^oC and the supernatant was serially diluted to perform plaque assays to quantify the virus in the solution.

Briefly, $5x10^5$ Vero cells were plated in six well plates overnight to establish a confluent monolayer of cells. The following day, the solution containing the unknown concentration of virus was serially diluted in 1:10 increments. This diluted solution was vortexed at high speed and 100 μL of the solution at different concentration was pipetted on to Vero cells. The Vero cells were then incubated at 37^o C, 5% CO_2 for one hour, and shaken every 15 minutes by hand.

Following this 2 mL of media and agarose mixture (1:1, 1.2% agarose with 2x DMEM with 20% FBS+ 2x Penicillin and Streptomycin) was overlaid using a serological pipette. These plates were then incubated at 37^{o}C, 5% CO_2 for 18-20 hours and the GFP^{+} plaques were counted under an epiflourescent microscope. An n= 5 mice were used in each group for this experiment.

2.2.7 Bioluminescence Imaging:

4T1 tumours were established as previously described (section 2.2.4). Sunitinib was administered I.P. daily starting 5 days after inoculation for 14 consecutive days. 5x10^{8} PFU VSVΔ51-Fluc and Maraba-MG1-Fluc were administered I.T. in a volume of 20 μL on day 8-post tumor inoculation. D-Luciferin (15 mg/mL, GoldBio Catalogue# LUCK-100) diluted in sterile PBS was administered I.P. at a dose of 200 μL per 20 g of mouse at 6, 12, 24, 48, 72, 96, 120 hours after virus infection. Mice were then anesthetized to prepare them for imaging. To this end, mice were anesthetized with isoflourane 10 minutes after D-luciferin injection and placed in the induction chamber, which was then filled with 5% isoflourane for 10 seconds to induce anaesthesia. Anaesthesia was maintained with the supply of 1-2% isofourane in the induction chamber. When the mice stopped moving, they were and placed into the Xenogen IVIS Imaging System 200, which was supplied with 1-2% isoflourane to maintain anasthesia. Images were then taken using exposure times of 1 second, 10 seconds and 30 seconds and mice were placed back into their cages. Data was analysed using the images obtained by the 30-second exposure. For analysis, images from all time points were opened in the IVIS software and the intensity scale was adjusted such that the range of firefly luciferase signal could be represented accurately over time. All images were set to have the same intensity scale, which allowed for direct comparison

between images. For example: all the images were opened in the IVIS software and the intensity was set from 300-3000 to ensure the range of signals was captured over time. Following this, a region of interest (ROI) around the tumour was set for analysis on each animal and each time point individually and the signal was measured by the software and expressed as relative luminescence units (RLU). An n= 5 mice/group were used for this experiment.

2.2.8 Bone marrow derived macrophage and DC cultures:

Bone marrow derived macrophages (BMDM) and dendritic cells (BMDCs) were kindly provided by Dr. Dale Balce and Rhiannon Campden from Dr. Robin Yates Lab (University of Calgary) respectively.

C57/BL6 mice were sacrificed using cervical dislocation. Following this, the mouse was dissected; intestines and rectum were carefully removed to minimize the contamination of the surrounding musculature. The lower half of the mouse including femur, ilium and tibia as well as the surrounding musculature was removed outside of the tissue culture hood. Following this, the tissues were transferred to the sterile tissue culture hood and the muscles and bones were placed in 70% ethanol for 10 seconds, flamed briefly to sterilize the tissue and placed into DMEM+10% FBS. The muscles were then removed using sterile forceps and scissors to expose the bones. The bones, femur, ilium and tibia, were then collected and the ends were cut using a pair of sterile scissors. The bones were then flushed with 20 mL of DMEM+10% FBS using a 21G needle. The bone marrow cells were then suspended in media to obtain a single cell suspension by gently pipetting them with a 10 mL serological pipette. Following this, the bone marrow cells were counted using a cell counter, centrifuged at 300xg for 5 minutes at 4^{o}C suspended in appropriate

medium for culture in 37°C, 5% CO_2 incubator at an appropriate concentration of cells for an appropriate amount of time (as described below).

To derive BMDMs, bone marrow cells were isolated as described above and red blood cells were lysed using sterile ACK lysis buffer. Briefly, bone marrow cells were centrifuged at 300xg for 5 minutes at 4°C to form a pellet. Following this, 3 mL of ACK lysis buffer was administered on to the bone marrow cells, resuspended and incubated for 3-5 minutes at room temperature. The ACK lysis buffer and bone marrow cells were then centrifuged at 300xg for 5 minutes at room temperature. The supernatant, which contained lysed red blood cells, was discarded. The bone marrow cells were then gently mixed with 5 mL of cold PBS and centrifuged at 300xg for 5 minutes at 4°C and the supernatant was removed. The bone marrow cells were then suspended in DMEM supplemented with 10% FCS, 2 mM L-glutamine, 1 mM sodium pyruvate, 20% L929-cell-conditioned media, as previously described[123]. To obtain L929 conditioned media, L929, mouse fibroblast cells (ATCC Catalogue# CCL-1) were plated in DMEM-F12 with Glutamax (ThermoFisher Scientific, Catalogue# 10565-018) supplemented with 10% FBS and 1x penicillin-streptomycin. The media was harvested 3 days after culture and filtered through 0.2 μm filter to remove cellular debris and stored in 4°C for future use. L929 conditioned media contains macrophage colony stimulating factor (M-CSF), which is an important cytokine that stimulates the differentiation of bone marrow cells into macrophages. Additionally, 1x penicillin-streptomycin antibiotic cocktail was also added to the media. Following this, the cells were counted, pelleted by centrifugation at 300xg for 5 minutes and resuspended in complete media to achieve a concentration of $2x10^6$ cells/mL. The media was refreshed every three days and differentiated bone marrow derived macrophages ($CD11b^+$ $F4/80^+$) were obtained after 5-7 days of culture[123].

Similarly, to derive BMDCs bone marrow cells were isolated using the same procedure as described above. Following this red blood cells were lysed using ACK lysis buffer (as described above). Cells were then counted and seeded at $3x10^6$/mL in media. The media consisted of RPMI supplemented with 10% FBS, 2 mM L-glutamine, 50 µM β-mercaptoethanol and 1000 U/mL recombinant mouse GM-CSF (Peprotech, Catalogue# 900-K30), or 10% conditioned media derived from Ag8653 myeloma cells transfected with murine GM-CSF cDNA[124] and 1x penicillin-streptomycin antibiotic cocktail. Media was refreshed four days after the culture and loosely adherent cells were transferred to a new petri dish with fresh media on day 6. DCs ($CD11b^+$ $CD11c^+$) cells were used from day 6 onwards for experiments[125]. An n= 3 independent biological replicates were used in both viability experiments as well as ELISAs.

2.2.9 IFN-β assay (Eve Technologies):

Tissue culture supernatants were collected from bone marrow derived macrophages (BMDMs) and sent to Eve Technologies (University of Calgary) for analysis. Briefly, $1x10^6$ BMDMs were plated per well in 12 well plates overnight. The next day the BMDMs were treated with sunitinib at different concentrations (0, 0.07µM, 0.625µM, 5µM) for 2 hours in 500 µL of media. Following this BMDMs were treated with VSVΔ51-GFP at an MOI of 10 in 500 µL. Supernatant was collected at 6 HPI and sent to Eve technologies for cytokine analysis. An n= 3 independent biological replicates were performed and analysed in this experiment.

2.2.10 Measuring IFN-β using ELISA:

Serum and tumour interstitial fluid (TIF) were collected from mice at 6 HPI with VSVΔ51 and Maraba-MG1 at a dose of $5x10^8$ PFU (I.T.). To collect the serum, the mouse was anesthetized with ketamine, xylazine cocktail (100mg/kg, 10mg/kg) and blood was drawn using a 26G, 1-inch needle with 1 mL insulin syringe by cardiac puncture. After completing blood collection mice were euthanized using cervical dislocation. The blood was incubated at room temperature for 30 minutes and centrifuged at 10,000 rpm for 10 minutes and the supernatant (serum) was collected for further analysis.

TIF was collected using a protocol described previously[126]. Briefly, the tumour was excised and any skin left on the excised tumour was removed. Following this, the tumours were weighed; chopped into small pieces approximately 1 mm in diameter using a scalpel blade. Following this, the tumour was placed in a 15 mL falcon tube and 1mL of PBS was added per 250 mg of tumour. The tumour and PBS was then incubated for 1 hour at 37°C, 5% CO_2. Following this the tubes were centrifuged at 1000 rpm for 3 minutes at 4°C, the supernatant was collected and further centrifuged at 5000 rpm for 20 minutes at 4°C. Following this, the supernatant was collected into 1.5 mL eppendorf tubes and frozen in -80°C prior to further processing.

IFN-β was also measured from *ex vivo* bone marrow derived DCs and 4T1 cells. $2x10^6$ BMDC or $2x10^4$ 4T1 cells were plated per well in a 12 well-plate overnight using their respective medium. The next day media was aspirated and the cells were treated with 0, 0.07 µM, 0.625 µM and 5 µM concentration of sunitinib for two hours in 500 µL of media. Following this, VSVΔ51 was administered at an MOI of 10 in 500 µL. 200 µL of supernatant was collected

6 HPI and stored in -80^{o}C until analysis. An n= 3 biological replicates were used in this experiment.

Samples were then analysed using Mouse IFN-β ELISA kit according to the manufacturer's protocol. Briefly, 100 µL of sample was put into the wells, incubated for 1 hour at room temperature without shaking and washed three times using wash solution in the ELISA kit. Following this, 100 µL of antibody cocktail was prepared as per manufacturer's instruction and added to each well. The plate was incubated for 1 hour at room temperature without shaking and washed three times using wash solution. Following this, HRP solution was prepared according to manufacturer's protocol and 100 µL of HRP solution was added into each well. The plate was then incubated for 1 hour at room temperature without shaking and washed three times using wash solution. Following this 100 µL 3'3'5'5'-tetramethylbenzidine (TMB) substrate, provided by the manufacturer, was added per well and the plate was incubated for 15 minutes in the dark without shaking; 100 µL of stop solution, provided by the manufacturer, was added and the plate was read at a wavelength of 450 nm in the spectramax i3 (Molecular Devices) spectrophotometer. An n=5 mice were used to analyse the serum and TIF from Ctrl, Su, MG1, MG1+Su groups and an n=2 mice was used for VSVΔ51 and VSVΔ51+Su *in vivo* and an n=3 independent replicates were used for BMDM and BMDC ELISAs.

2.2.11 In vitro viability assay:

$3x10^3$ 4T1 cells and $5x10^3$ ACHN were plated per well in a 96 well plate overnight to achieve a density of 60-80% the following day prior to starting the experiment. The cells were then treated with sunitinib (0 µM to 5 µM) for 2 hours in 50 µL of media. Following this, cells were infected

with VSVΔ51-GFP, Maraba-MG1-GFP and WT-VSV-GFP at several MOIs ranging from $1x10^{-4}$ to 10 in an additional 50 µL of media. Cells were then incubated from 18-72 hours after virus infection and alamar blue assay was performed at various time points in each cell line (Figure S6 and S7). 1/10 volume of alamar blue dye was administered into each well using a multi-channel pipette at various time points and cells were further incubated at 37^{o} C, 5% CO_2 for 3-4 hours or until the control wells had just changed colour from blue to pink which indicated cellular metabolism of the dye. The absorbance of each sample was then measured at 570 nm and 600 nm using the spectramax i3 spectrophotometer. Data was expressed as percent viability compared to control/ untreated group.

$$\%\text{viability}=\frac{\text{Abs(570nm-600nm)sample}}{\text{Abs(570nm-600nm)control}}*100$$

Viability assays were also performed using BMDMs and BMDCs. BMDMs were plated at a concentration of $1x10^6$ cells/well and BMDCs were plated at a concentration of $2x10^6$ cells/well in a 12 well-plate overnight. The next day media was aspirated and the cells were treated with 0, 0.07 µM, 0.625 µM and 5 µM concentration of sunitinib for two hours in 500 µL of media. Following this, VSVΔ51 was administered at an MOI of 10 in 500 µL. Viability assays were performed using alamar blue assay at 24 HPI and analyzed using the same method as stated above. An n= 3 biological replicates were performed and analysed in this experiments.

2.2.12 Multistep viral growth curves:

$2.5x10^5$ 4T1 cells and $5x10^5$ ACHN cells were plated per well in 6 well plates overnight to achieve a density of 60-80% the following day. The cells were then treated with 0 µM, 0.078 µM, 0.625 µM and 5 µM of sunitinib for 2 hours. Following this, the media containing sunitinib

was removed and cells were then infected with VSVΔ51-GFP at a MOI of 0.1 in 200 µL of media for one hour. The plates were incubated in 37°C, 5% CO_2 for one hour and shaken every 15 minutes by hand. Following this, media containing the appropriate concentrations of sunitinib was added back into the appropriate wells. 100µL supernatant was collected from these cells at 8, 12 and 22 HPI and replenished until the end of the experiment. The supernatants collected were stored in -80°C until they were analysed using plaque assays (as described in section 2.2.6). An n= 3 biological replicates were used in this experiment.

2.2.13 Western blot analysis:

$1x10^6$ 4T1 cells and $4x10^6$ ACHN cells were plated in 10 cm dishes overnight. The next day cells were treated with sunitinib at 0 µM, 0.07 µM, 0.625 µM, 1.25 µM and 5 µM concentrations for two hours. Following this, sunitinib-containing media was removed and the cells were treated with VSVΔ51 (MOI 10) in 1 mL complete medium for 1 hour at 37°C, 5% CO_2 incubator and shaken every 15 minutes by hand. Media containing sunitinib was then replenished at appropriate concentrations and incubated for 24 hours. Lysates were collected 24 HPI in total lysis buffer (50 mM Tris-HCl (pH 8.0), 150 mM NaCl, 1% Triton X-100, and 1% SDS) with phosphatase and protease inhibitor (Sigma Aldrich, cOmpleteMini, Catalogue# 4693159001) and boiled at 95°C until they could be run smoothly through a P1000 pipette tip. Samples were then either frozen at -20°C or protein assay was performed to determine the concentration of protein in each sample using the Bio-Rad DC Protein Assay Kit (Bio-Rad Catalogue# 5000112) as per manufacturer's protocol. Briefly, 5 µL of sample or bovine serum albumin (BSA, Sigma Aldrich Catalogue # A9418) standard ranging from 0.2 mg/mL to 1.5 mg/mL was loaded on to flat

bottom 96-well plate. Following this, 25 µL of reagent A' (20 µL of reagent S+ 1 mL of reagent A) was added into each well. Following this, 200 µL of reagent B was added into each well. The plate was incubated at room temperature for 15 minutes and read at 750 nm using the spectramax i3 spectrophotometer.

After protein concentration was determined, 20 µg of protein was diluted in 30-40 µL of solution containing lysis buffer and 5x SDS (sodium dodecyl sulphate) loading dye (Bromophenol blue 0.25%, β-mercaptoethanol 0.5 M and 10% SDS) was loaded per lane in a 8% SDS-polyacrylamide gel electrophoresis (SDS-PAGE) gel and samples were ran using 1x SDS PAGE running buffer (25 mM Tris, 190 mM glycine and 0.1% SDS, pH 8.3) until the dye front reached the bottom of the gel. Samples were then transferred on to a 0.2 µm nitrocellulose membrane (Bio-Rad Catalogue# 162-0112) using Bio-Rad Trans-turbo semi-dry transfer apparatus at 25V, 1 Amp for 1 hour in transfer buffer (25 mM Tris, 190 mM glycine, 20% Methanol, pH 8.3). Membranes were then stained with 0.05% (w/v) ponceau red dye diluted in 5% acetic acid to ensure proper transfer of protein. Following this, the membranes were washed with 1x Tris Buffered Saline with Tween-20 (TBST, 20 mM Tris and 150 mM NaCl, pH 7.6). Membranes were then blocked with 5% BSA in TBST or 5% skim milk in TBST overnight at 4^{o}C on a shaking platform rotating at 100 rpm and probed the following day with p-PKR (1:1000), p-eIF2α (1:500), PKR (1:1000), EIF2α (1:500), actin (1:5000) overnight at 4^{o}C on a rotating platform at 100 rpm. Membranes were then probed with appropriate secondary antibodies conjugated to HRP for two hours at room temperature and visualized using the Chemidoc-IT Imager. This experiment was repeated three times to ensure reproducibility of the blots.

2.2.14 Flow cytometry:

Spleens were isolated from mice and homogenized using the thumb end of a 1mL insulin syringe and passed through a 70 µm cell strainer. The cell suspension was then centrifuged at 300xg for 5 minutes at 4^{o}C followed by red blood cell lysis using ACK lysis buffer (as described previously). Splenocytes containing white blood cells were then resuspended in 5 mL cold FACS PBS (PBS+2% FCS, 0.01% NaN_3). Splenocytes were diluted 1:100 in FACS PBS and counted using a cell counter. 1x10^{6} cells were placed into an eppendorf tube and concentrated into 100 µL of FACS PBS. Splenocytes were blocked with 1 µL of Fc block for 5 minutes and stained using the appropriate antibodies at a concentration of 1:100 stationary for 30 minutes at 4^{o}C in the dark. Following staining, the cells were washed 3x with FACS PBS and antibody stained cells were quantified using the Attune Flow Cytometer.

Tumours were isolated from mice and chopped up in pieces approximately 1mm in diameter using a sterile scalpel at room temperature. The tumours were then incubated in a 37^{o}C-shaking incubator with 0.1 mg/mL of Collagenase IV (Sigma Aldrich, Catalogue# C5138) and DNAseI (Sigma Aldrich, Catalogue# DN25) in 1x HBSS with Ca^{2+} and Mg^{2+} (ThermoFisher Scientific, Catalogue# 14025-076) for 45 minutes. The samples were then homogenized using GentleMACS (Miltenyi Biotech) for 1 minute and the samples were centrifuged at 800xg for 10 minutes. Following this the supernatant was removed and the pellet containing single cell suspension from the tumour was collected. The samples were further washed twice with FACS PBS, counted using a haemocytometer, blocked using Fc block and stained (same as above) with appropriate antibodies, washed 3x with FACS PBS and antibody stained cells were quantified using the Attune Flow Cytometer.

Cells from both spleen and tumours were passed through the flow cytometer where their size, granularity and marker-profile were detected. Firstly, the unstained control was passed through the flow cytometer and the forward scatter (FSC) and side scatter (SSC) were set up by adjusting the voltages on the flow-cytometer. Following this, single colour controls were run through the machine to set up compensation. Compensation is important to ensure dyes that have similar or overlapping emission spectra do not produce a false positive signal. For example, both fluorescein isothiocynate (FITC) and phycoerythrin (PE) are both excited by the same laser, the blue laser, and emission spectra of FITC and PE overlap, which may lead to a false positive FITC signal in the PE channel. Compensation allows for correction of errors due to the spectral overlap. Once compensation was set up and samples were collected, the cells were gated (R1) excluding blood clots, red blood cells and cellular debris (low FSC, low SSC) and cellular clumps (high FSC, high SSC) and then doublets were excluded. To exclude doublets, the gated cells were further plotted as side scatter area (SSC-A) vs side scatter height (SSC-H) and all cells that were in a cluster at a 45^{o} line in the plot were selected in a gate (R2) and cells that were scattered beyond the 45^{o} line were excluded from analysis. R2 was then plotted as forward scatter area (FSC-A) vs forward scatter height (FSC-H) and single cells were selected using the same method as above (R3). R3 was considered to be single cells only. Following this, single cells were also further gated to be $CD45^{+}$. An n= 10 animals were used per group in two separate experiments. Data is represented from one replicate where n=5 mice/group, as mean ±SEM of $\%CD45^{+}$ cells.

2.2.15 Statistical Methods:

Survival curves were analysed using the Log-Rank analysis to test for trend. The Log-Rank analysis was further analysed to determine differences between groups using the Bonferonni correction. Briefly, the total number of combinations was determined between groups, 15 possible combinations. The significance level was set for the test to be <0.05. Then each of the curves was compared to determine a p value. The significance value, which was set at $p<0.05$, was divided by the number of possible combinations (15) to obtain an adjusted p value that was corrected. If the adjusted p value was smaller than [0.05/15=0.003] then the comparison was determined to be significant.

Further animal experiments were analysed using parametric one-way ANOVA or the non-parametric equivalent of ANOVA, the Kruskal-Wallis test. Bartlett's test was applied to the samples to determine whether samples had equal variances and normal distribution. Bartlett's test was significant if the samples did not have equal variances. If Bartlett's test was $p<0.05$ then ANOVA was applied. In the event that the Bartlett's test was significant ($p<0.05$, in Bartlett's test), then the non-parametric Kruskal-Wallis test was applied. When ANOVA analysis was performed, further post-hoc test namely Tukey's was applied to determine the statistical differences between each of the treatment groups.

2.3 Results

2.3.1 Sunitinib improves ORV mediated tumour control in the 4T1 model

ORVs are exquisitely sensitive to type I IFN and therefore are unable to effectively infect tumours that secrete type I IFN[45,46]. Su, has been shown to inhibit virally induced IFN effector molecules such as PKR in a tumour cell intrinsic manner[6]. Additionally, Su may also reduce the number of myeloid progenitor cells, resulting in reduced numbers of IFN producing cells such as conventional dendritic cells (cDCs) and macrophages (MΦ) by inhibiting FLT3R signalilng [111,121]. Therefore to determine the role of Su in IFN signalling, we had to choose a tumour model that is responsive to IFN.

The 4T1 model was chosen due to its ability to produce virally induced type I IFN and respond to type I IFN (Figure S1). We infected 4T1 cells with no virus (Ctrl), UV inactivated-VSVΔ51 and VSVΔ51 (MOI 0.1) and collected the supernatant at 18 hpi. This supernatant was then UV-inactivated to remove any live virus particles. Naïve 4T1 cells were then treated with supernatant for 24 hours after which they were infected with VSVΔ51 at MOIs 0, 1 and 10. We found that 4T1 cells that were treated with supernatant from VSVΔ51 were able to protect themselves from the subsequent VSVΔ51 infection. This data suggests VSVΔ51 infected 4T1 cells are able to produce factors in the media that will protect neighbouring cells from infection, likely type I IFN[5]. Additionally, these factors signal to the naïve 4T1 cells activating anti-viral response. This results in naïve cells being able to protect themselves from virus infection. These protective factors were absent in media collected from 4T1 cells treated with supernatant from UV inactivated VSVΔ51 and non-infected cells. Then we proceeded to characterize whether Su improved ORV mediated tumour control.

To start this study, we needed to determine the dose of Su and ORV co-therapy that 4T1tumor bearing Balb/c mice could tolerate. The tolerated dose of Su in Balb/c mice is determined in the literature to be 40 mg/kg[97,127]. However, the maximum tolerated dose (MTD) of ORV+ Su co-therapy is unknown. To determine the MTD of ORV and Su combined, we conducted a study with Maraba-MG1±Su. Since Maraba-MG1 is more virulent and has higher cytotoxicity towards cancer cells *in vitro*[35], we chose Maraba-MG1 for the MTD studies. To this end, 4T1 tumours were established in the right mammary fat pads of Balb/c mice. Upon establishment of a palpable mass at five days, mice were treated with Su and Maraba-MG1 was injected intravenously at various doses--5x 10^8, 1x 10^9 and 2x10^9 PFU ± Su treatment. We chose 5 x10^8 PFU to start, as it was half-MTD in Balb/c mice as established by Brun *et al*[35]. We monitored mice daily for virus related toxicity using symptoms such as hind leg paralysis and poor grooming. All mice showed signs of virus related illness such as pyloerection as previously documented. All mice also experienced weight loss due to the virus infection, but weight was gained back 72 HPI. We did not observe a difference in the toxicity when mice were treated with 5x10^8 PFU Maraba-MG1±Su (Figure S2). Mice that were treated with 5 x 10^8 PFU Maraba-MG1±Su did not experience any fatal virus related symptoms such as >20% weight loss or hind leg paralysis and were sacrificed due to tumour burden. However, 1 of 5 mice treated with 1x10^9 and 2x10^9 PFU Maraba-MG1+Su died one day earlier compared to Maraba-MG1 alone at the same doses, which may indicate a marginal increase in toxicity of Maraba-MG1 with Su. Based on this experiment, we chose 5x10^8 PFU to characterize Su and ORV co-therapy in subsequent experiments.

To assess whether sunitinib improves ORV mediated tumour regression and survival in the 4T1 model, 6-8 week old female Balb/c mice were inoculated with 1x10^5 4T1 cells in the

mammary fat pad. The outline of the experimental schedule is displayed in Figure 2.1A. Briefly, there were four groups in this experiment—control, Su, ORV and ORV+Su. The control group was treated with PBS+ 1% DMSO, I.P.; Su (40 mg/kg I.P.) for 14 days starting at five days upon establishment of a palpable tumour mass (~2 mm x 2 mm), ORV (5×10^8 PFU of Maraba-MG1 or 5×10^8 PFU of VSVΔM51) were injected I.T. on days 8, 11 and 14 post tumour inoculation. Mice were monitored for signs of morbidity and mortality and tumours were measured twice a week using calipers and mice were sacrificed when the tumour reached a volume of 500 mm^3. The outline of the experiment and schedule is summarized in Figure 2.1A. The treatments were generally well tolerated however Su treated mice were more excitable and hyperactive compared to the vehicle treated group. However, these mice did not lose weight or show signs of morbidity and mortality. ORV treated animals showed transient signs of virally induced illness such as pyloerection and weight loss for up to 48 hours after treatment (Figure S3).

Mice treated with Su or ORV monotherapy showed modest yet significant improvement in life span compared to control animals (Figure 2.1B, D). Tumours treated with sunitinib had slower average rate of growth compared to control and co-therapy treatment slowed down the tumour growth more significantly than monotherapy treatment (Figure 2.1 C, E). Mice treated with Su/ORV co-therapy showed significant improvement in survival compared to monotherapy ($p<0.01$, Figure 2.1F). There was no significant difference between VSVΔ51 vs. Maraba-MG1 ($p=0.33$) and VSVΔ51+Su vs. Maraba-MG1+Su ($p=0.34$) in terms of survival outcomes. Together this data led us to conclude that Su+ORV therapy was well tolerated in Balb/c and improved the survival outcome in an IFN responsive model compared to ORV alone.

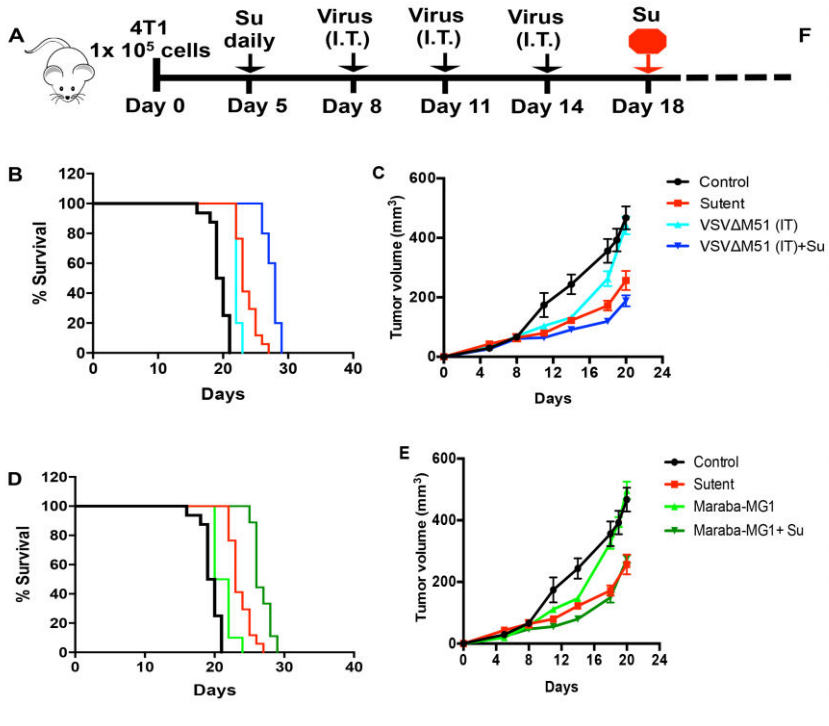

F

Groups	p	*
Ctrl vs Su	p<0.01	**
Ctrl vs MG1	p<0.05	*
Ctrl vs VSVΔ51	p<0.01	**
Ctrl vs VSVΔ51+Su	p<0.01	**
Ctrl vs MG1+Su	p<0.01	**
Su vs. MG1	p<0.01	**
Su vs. VSVΔ51	p>0.05	N.S
Su vs VSVΔ51+Su	p<0.01	**
Su vs MG1+Su	p<0.01	**
MG1vs MG1+Su	p<0.01	**
VSVΔ51 vs. VSVΔ51+Su	p<0.01	**

Figure 2.1: Su improves ORV mediated tumour control in the 4T1 model.

Balb/c mice were injected with $1x10^5$ 4T1 cells and treated with ORV (VSVΔ51 or Maraba-MG1)±Su as displayed in (A). Animals were divided into four groups, Ctrl (n=16, PBS+1%DMSO, I.P.), Su (n=17, 40mg/kg, I.P.), ORV ($5x\ 10^8$ PFU, I.T) and ORV+Su. Animals were sacrificed when the tumour size reached 500 mm^3. Kaplan-Meier curve depicting the survival (B) and tumour growth curve (C) of mice treated with VSVΔ51 (n=5) and VSVΔ51+Su (n=5). Kaplan-Meier curve depicting the survival (D) and tumour volume (E) treated with Maraba-MG1± Su, MG1 (n=10), and MG1+Su (n=9). (F) Depicts the p value between groups as determined by Log-Rank analysis (*p<0.05, ** p<0.01).

2.3.2 Sunitinib treatment improves ORV infection and reduces production of type I IFN in the tumour and serum of ORV treated animals

After we determined that Su improves ORV mediated survival, we wanted to determine whether Su reduced IFN production and improved ORV infection in the tumour. Sunitinib inhibits the phosphorylation of IFN effector molecules such as PKR and RNAseL. This attenuates the second wave of IFN-β production resulting in improved viral productivity[6,96]. Additionally, Su mediated inhibition of PKR phosphorylation leads to an inhibition on eIF2α phosphorylation and improves viral productivity in the tumour cell[96]. Su may also induce apoptosis and reduce the number of myeloid progenitor cells thereby reducing cDCs and MΦ that produce IFN[111,128] This prompted us to test whether sunitinib blunted the production of IFN-β *in vivo* in response to VSVΔ51 and Maraba-MG1 infection. To this end, 4T1 tumours were established and mice were treated with CTRL, Su, ORV (I.T) or ORV (I.T)+Su. Cardiac puncture was performed to collect blood and tumours were excised 6 HPI. Following this, serum and tumour interstitial fluid (TIF) were obtained from the blood and tumour respectively and IFN-β was measured using an ELISA. As predicted, ORV infection induced the production of IFN-β in both serum and TIF when compared to the control groups ($p<0.001$, Figure 2.2). We found that IFN-β levels were higher in the TIF compared to the serum, which might be as a result of the virus being injected I.T. rather than systemically. Sunitinib treatment reduced the production of type I IFN in response to VSVΔ51 in the serum (Figure 2.2 A, $p=0.07$) and in the TIF (Figure 2.2 B, $p<0.01$) as well as in response to Maraba-MG1 in the serum (Figure 2.2C, $p<0.05$) and TIF (Figure 2.2 D, $p=0.09$). Although this data suggests that Su reduces the ORV mediated IFN-β production in the TIF and serum, some of the data is not statistically significant. More samples are required in this case to reach statistical significance. Interestingly, Maraba-

MG1 infection induced about 50% less IFN-β compared to VSVΔ51. Following this, we wanted to determine whether Su improves ORV infection or replication in the tumour.

To this end, 4T1 tumours were injected with firefly luciferase expressing ORVs and virus infection was measured using Fluc signal at 6, 12, 24, 48 and 72 hpi. The region of interest (ROI) was defined around the tumour and the relative luminescence units (RLU) was quantified in the tumor. We found that there was a significant increase in the luminescence signal in the ORV+Su groups compared to ORV alone at 6 hpi, which suggests that Su improves initial ORV infection (Figure 2.3 A-C, Figure S4). The improved infection was maintained throughout the 72 hours, which also suggests that the rate of viral clearance may be reduced when Su treatment is continued. Furthermore, we performed plaque assays 72 hpi to quantify viral particles in the tumour. We found that sunitinib and ORV treated mice still had higher viral titres at 72 hpi (3 logs with MG1 treatment, $p<0.01$, 2 logs with VSVΔM51, $p<0.05$ Figure 2.3 D, E). Taken together, this data led us to conclude that Su reduced the IFN production in the 4T1 tumour as well as improved viral infection in the 4T1 tumours.

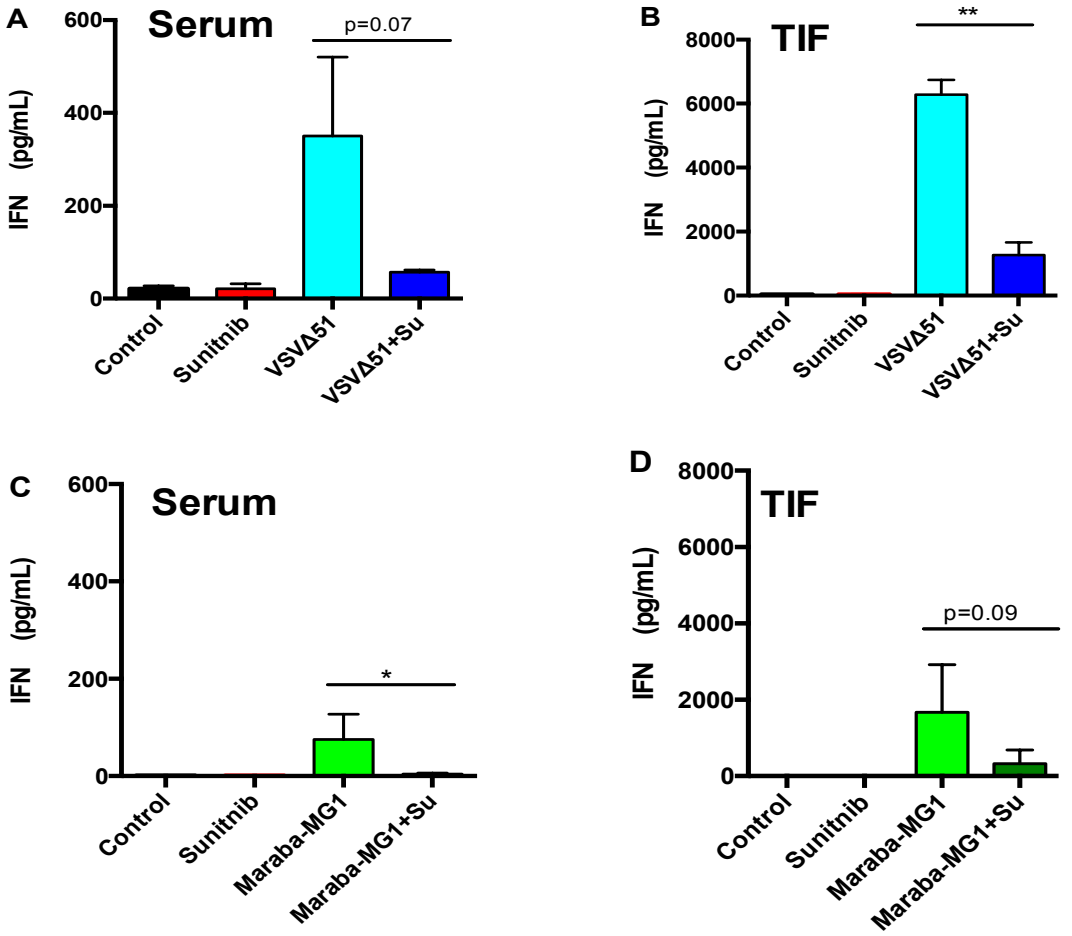

Figure 2.2: Sunitinib reduces the production of ORV induced type I IFN in vivo.

4T1 tumour bearing mice were treated with ORV (I.T) ±Su as described in Fig 2.1A. Blood was collected and tumours were excised 6 hpi and IFN-β levels were measured. IFN-β levels in the serum (A) and tumour interstitial fluid (TIF) (B) of animals treated with VSVΔ51±Su (n=2/ group); IFN-β levels in the serum (C) and TIF of animals treated with Maraba-MG1±Su (n=5/ group). Data represented as mean±SEM. One-way ANOVA was applied to determine statistical significance (*$p<0.05$, **$p<0.01$).

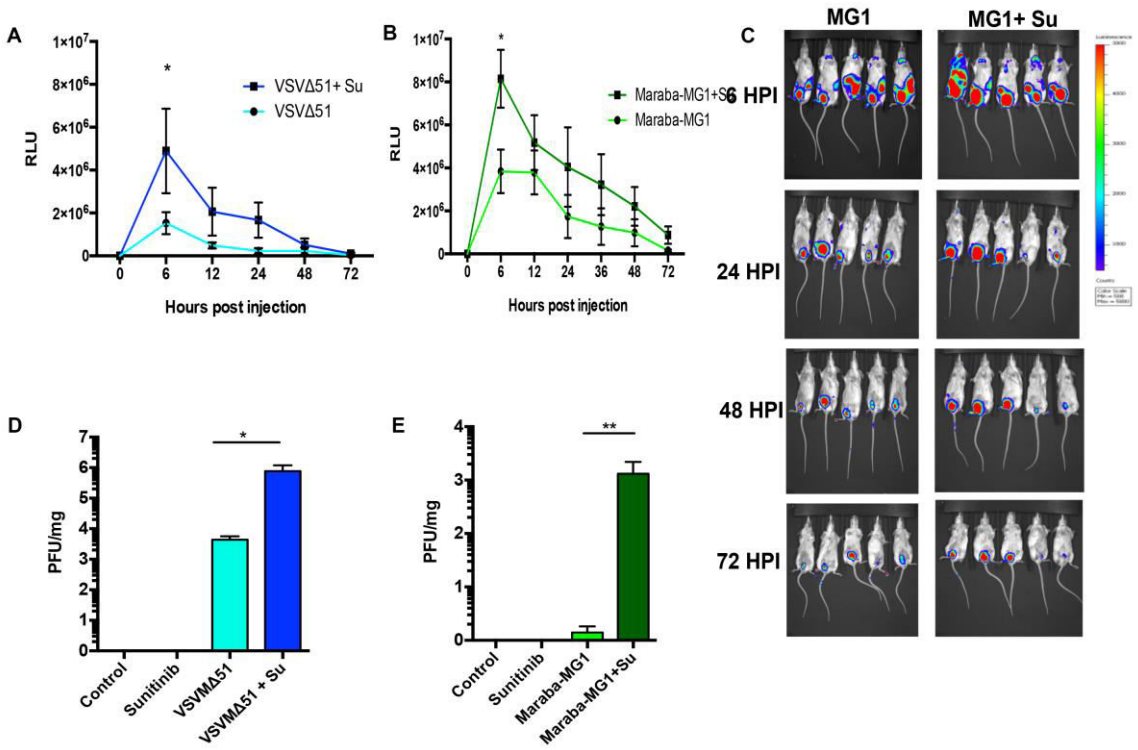

Figure 2.3: Sunitinib improves ORV infection in vivo

4T1 tumour bearing mice were treated with VSVΔ51 and Maraba-MG1 (I.T)±Su as described in Fig 2.1A. Tumours were collected on day 8, 72 hpi, to measure viral productivity. Viral productivity as relative luminesce units (RLU) in mice treated with VSVΔ51-Fluc±Su (A) and Maraba-MG1-Fluc (B) (n=5 mice/ group); data represented as mean±SEM. (C) Bioluminescence images representing Maraba-MG1-fluc±Su infection in 4T1 tumour bearing animal upto 72 hpi. Viral productivity represented as PFU/mg in mice treated with VSVΔ51±Su (D) and Maraba-MG1±Su (E); data represented as mean ±SEM (n=5 mice/ group). Image representing VSVΔ51-Fluc±Su is shown in Figure S4. One-way ANOVA was performed to determine statistical significance (* $p<0.05$, ** $p<0.01$).

2.3.3 Sunitinib does not inhibit IFN-β production in 4T1 cells

After determining that Su reduces ORV induced IFN production in the tumour and improves ORV infection in the tumour, we aimed to determine the source of the IFN. 4T1 tumour cells (Figure S1) as well as surrounding stromal cells such as cDCs, pDCs and MΦ produce IFN. We first aimed to determine whether Su is acting in on the 4T1 cells to reduce IFN production and improve viral productivity.

Jha *et al* conducted studies that suggest Su treatment inhibits activation of ISGs such as RNAseL and PKR by reducing phosphorylation[6,96]. This in turn leads to reduction in phosphorylation of eIF2α, which relieves the inhibition on viral translation. This study showed that there was an improved infection of VSVM51R with Su, a virus that is closely related to VSVΔ51 in a human renal cell carcinoma line, ACHN. They also showed that Su treatment reduced the phosphorylation of VSVM51R induced PKR and eIF2α in ACHN with 5μM Su. However, they did not show the same data in 4T1 cells. Therefore, we first tested whether Su reduced the phosphorylation of PKR and eIF2α in response to VSVΔ51 infection in 4T1 cells. ACHN cells were used as a positive control because Jha *et al*, showed Su inhibits PKR and eIF2α phosphorylation in response to VSVM51R infection. VSVM51R is closely related to VSV Δ51. VSVM51R has a methionine to arginine mutation on the 51st amino acid instead of a deletion. To this end, ACHN and 4T1 cells were treated with vehicle 0.078, 0.625, 1.25 and 5μM with VSVΔ51 at an MOI of 10. Cell lysates were collected 24 hours after infection and samples were analysed using western blots for phospho-PKR and phospho-eIF2α (Figure 2.4 A, B). We found that VSVΔ51 induced the phosphorylation of PKR and eIF2α in both ACHN and 4T1 lines. Su treatment led to a reduction in the levels of p-PKR and p-eIF2α in the ACHN line as

reported. Interestingly, Su treatment reduced the levels of virally induced p-PKR in a dose dependent manner but did not reduce the levels of p-eIF2α in 4T1 cells. Together this data led us to conclude that sunitinib was active *in vitro*. Next we wanted to determine whether Su reduced VSVΔ51 induced IFN production in 4T1 cells. To this end, 4T1 cells were treated with three different concentrations of sunitinib (0.078μM, 0.625 μM and 5μM) two hours prior to infecting cells with VSVΔ51 at an MOI of 10. Supernatant was collected at 8 hpi, 16 hpi and analysed to measure the levels of IFN-β. Interestingly, we found that Su did not reduce the levels of IFN-β production in the 4T1 cells at both time points (Figure 2.5 A, B).

This finding did not fit our hypothesis. However, we did not test IFN production at lower concentrations of VSVΔ51 at various time-points. To determine whether Su increased the productivity of VSVΔ51 in the 4T1 cell line, we performed plaque assays. Jha *et al*, showed that there was a one-log increase in viral productivity in ACHN when the cells were treated with VSVM51R+Su compared to VSVM51R alone at 13 hpi using an MOI of 1. Therefore, we chose to use ACHN cells as a positive control. To this end, 4T1 and ACHN cells were treated with vehicle, 0.078μM, 0.6 μM and 5μM of sunitinib for two hours following infection with VSVΔ51 at an MOI of 0.1. Supernatant was collected at 8, 12 and 22 hpi and plaque assays were performed to quantify the virus titre in the media. There is no difference between the titres of VSVΔ51 alone and VSVΔ51+Su at 0.078 μM and 0.625 μM (Figure 2.6 A). However, the virus titre is reduced in 4T1 cells treated with VSVΔ51+5μM Su. This was likely due to the cells being unhealthy at this high dose (Figure 2.5C). This data suggests that sunitinib does not enhance the productivity of VSVΔ51 in 4T1 or ACHN cells. We also performed viability experiments with all three viruses (VSVΔ51, Maraba-MG1 and WT-VSV) in both ACHN and 4T1 lines at several time points, using several concentrations of Su and viruses (Figures 2.7; Figure S7 and S8).

Using the conditions described we were unable to achieve the synergistic cytotoxicity Jha *et al* observed by combining Su and wt-VSV in 4T1 and ACHN lines. Taken together, this data led us to conclude that Su does not dampen IFN production in the tumour cell itself.

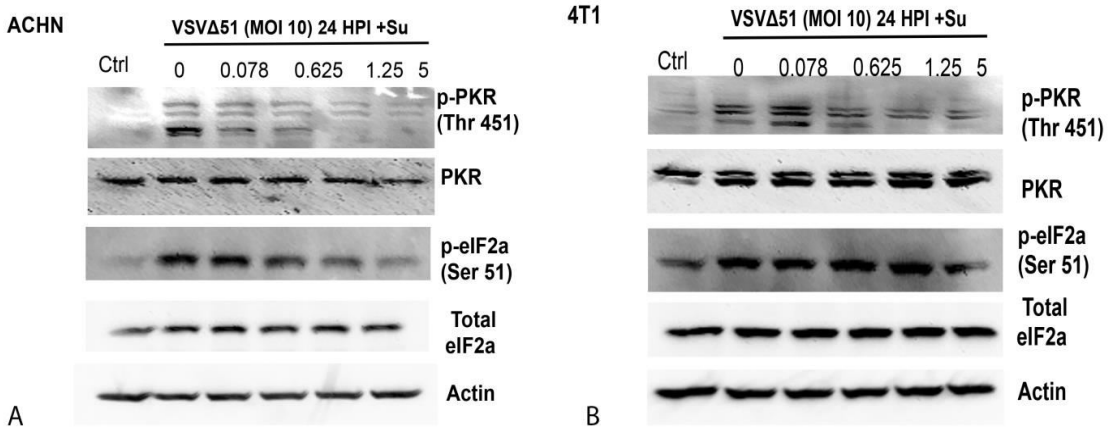

Figure 2.4: Sunitinib reduces phosphorylation of PKR and eIF2α in response to VSVΔ51 infection.

ACHN and 4T1 cells were treated with Su at 0.078μM, 0.625μM, 1.25μM and 5μM concentration for two hours prior to VSVΔ51 infection (MOI 10). Cells were then harvested; western blots were run to detect the phosphorylation of PKR and eIF2α in (A) ACHN (B) 4T1 cells. Actin was used as a loading control.

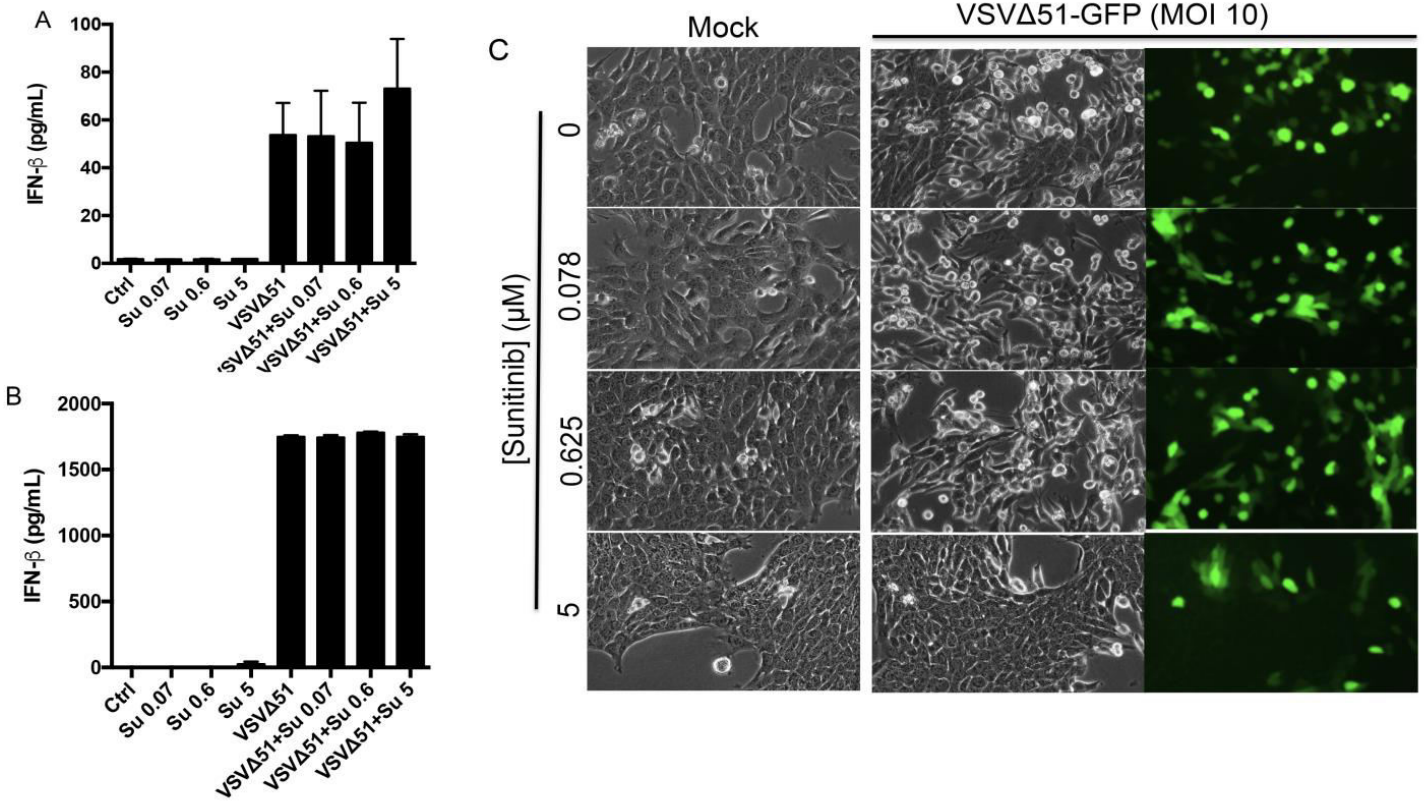

Figure 2.5: Sunitinib does not reduce the production of type I IFN in 4T1 cells.

4T1 cells were treated with Su at 0.078μM, 0.6μM and 5μM concentration for 2 hours prior to VSVΔ51 (MOI 10) infection. IFN-β levels were measured in the supernatant at 8 hpi (A) and 16 hpi (B), data represented as mean±SEM (n=3 samples/ treatment group)±. (C) Images depicting 4T1 cells treated with VSVΔ51 (MOI 10)±Su at 12 hpi.

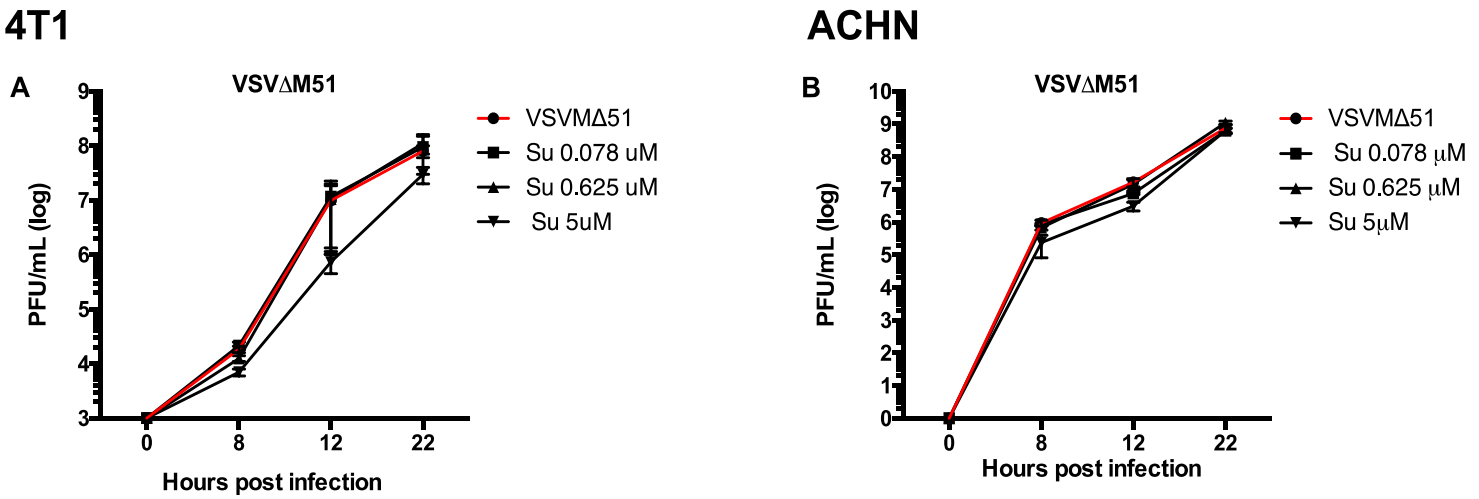

Figure 2.6: Sunitinib does not improve VSVΔ51 productivity and infectivity in vitro.

Two-step growth curve VSVΔ51 ±Su in 4T1 and ACHN cells. Cells were treated with Su at 0.078μM, 0.625μM and 5μM concentrations and then treated with VSVΔ51 (MOI 0.1).Plaque assays were performed to assess viral productivity of VSVΔ51±Su expressed as plaque forming units/mL of media at 8, 12 and 22 hours post infection in (A) 4T1 and (B) ACHN cells. Data represented as mean±SEM (n=3/ timepoint).

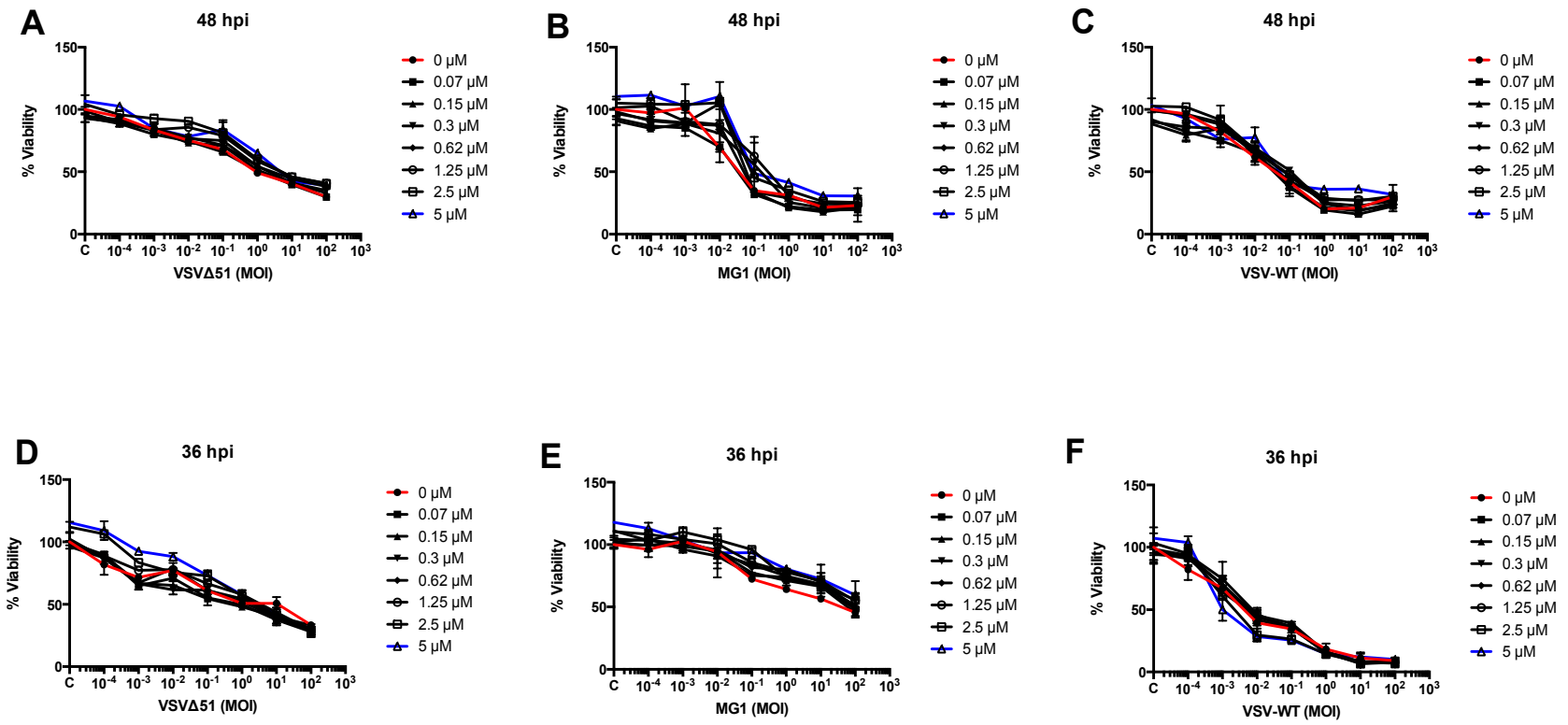

Figure 2.7: Sunitinib does not enhance VSVΔ51, Marba-MG1 or WT-VSV mediated cytotoxicity in 4T1 and ACHN lines in vitro.

4T1 and ACHN cells were treated with Su from 0.078μM-5μM for 2 hours prior to virus infection with VSVΔ51, Maraba-MG1 or WT-VSV from MOI 0.0001 to 100. Alamar blue assays were performed to measure cytotoxicity at 48 hpi for 4T1 cells (A-C) and 36 hpi for ACHN cells (D-F). Data depicted mean±SEM as percent viability compared to control (n=2/virus).

2.3.4 Sunitinib treatment reduced the number of IFN producing cells in the tumour and spleen of 4T1 tumour bearing animals

In addition to the 4T1 tumour cells, the tumour microenvironment can also harbour cells that produce high levels of type I IFN in response to virus infection. 4T1 tumors secrete high levels of GM-CSF which recruit myeloid cells from the bone marrow into the spleen and the tumour[129]. Among these, the myeloid derived suppressor cells have been characterized in the 4T1 tumour[97,127]. However, other myeloid cells can be recruited into the tumour. For example, EMT6 breast tumour model similar to 4T1 has been shown to harbour CD68+ macrophages which renders them difficult to infect[130]. Myeloid cells such as F4/80$^+$ macrophages, CD169$^+$ Mϕs and DCs are major producers of type I IFN[131,132]. Su has been shown to inhibit Flt3R signalling which plays an important role in the proliferation and survival of common myeloid progenitor (CMP)[133]. Since myeloid progenitor cells (MPCs) differentiate Mϕs and cDCs that produce type I IFN, and lymphoid progenitor cells give rise to pDCs, a major producer of type I IFN[132,134], we hypothesize that sunitinib may reduce the number of type I IFN producing cells cDCs and CD169$^+$ Mϕs in 4T1 tumour bearing animals resulting in the reduced levels of IFN-β. CD169$^+$ Mϕs allow viral gene expression to prime anti-viral T cell response[116,135]. Although an important regulator of anti-viral responses, CD169$^+$ Mϕs have not been characterized in the tumour. Therefore, we chose to look at cDCs, CD169$^+$ Mϕs and pDCs.

To determine whether Su reduces the number of cDCs, CD169$^+$ Mϕs and pDCs in the tumour and spleen flow cytometry was performed at two different time points, day 8 and day 11 after tumour implantation. We chose two time points to understand the kinetics of tumour growth in the 4T1 model as well as understand the impact of continuous Su treatment on this model. We also wanted to determine whether Su and ORV treatment altered 4T1 tumour micro and macro environment and therefore we measured cell population in both tumour and spleen. Balb/c mice

were injected with 4T1 cells and treated with Su (40 mg/kg intra peritoneally, 5 days after tumour implantation) and MG1 (5E8 PFU intra tumorally, 8 days after tumour implantation). As reported we found that 4T1 tumour bearing mice undergo splenomegaly[129] (observed data, data not shown), an enlargement of the spleen, which is partially ablated with Su treatment. As previously reported there is an infiltration of myeloid cells in the spleen as the 4T1 tumour grows (Figure S8). Studies suggest that splenomegaly may be due to 4T1 tumours secreting the cytokine GM-CSF[129] to set up an immunosuppressive tumour microenvironment[97]. Following this, we wanted to characterize the effect of different treatments on cells such as F4/80$^+$ Mϕ (F480$^+$ CD11b$^+$), CD169$^+$ Mϕ (CD169$^+$ CD11b$^+$), cDCs (CD11b$^+$ CD11c$^+$), pDCs (CD11c$^{lo/int}$ Gr1$^+$ B220$^+$).

Three days of sunitinib treatment reduce CD169 MΦ and cDCs in the tumour (Figure S9) or spleen (Figure S10). However, six consecutive days of Su significantly reduces myeloid cell counts such as cDCs and CD169$^+$ Mϕs in the tumour (Figure 2.8). To analyse tumour samples, all cells were gated and we excluded doublets by plotting cells on SSC-H vs SSC-A and then FSC-H vs FSC-A. Following this, the cells were further gated on CD45+ cells and markers and analysed.

We found that cDC population was significantly reduced in the tumour after 6 days of Su treatment alone (CTRL=53.6%, Su= 27.5% of CD45$^+$ cells, $p<0.05$) and co-therapy (MG1= 47.5%, MG1+Su= 24.1% of CD45$^+$ cells, $p<0.05$). CD169$^+$ MΦs reside in the splenic subcapsular sinus are important for response to virus infection, cross presentation and cross priming of T cells[135]. Interestingly, we found CD169+ MΦs in 4T1 tumours (Figure 2.7, 5.8% of CD45+ cells in CTRL and there is a 50% reduction in the CD169+ MΦ population with Su treatment (Su=2.36% of CD45+ cells). We also found that intratumoral MG1 treatment

significantly increases the number of CD169+ cells in the tumour compared to CTRL (MG1= 13.8% of $CD45^+$ cells, $p<0.05$) whereas Su treatment leads to a trend in reduction of in $CD169^+$ MΦ with MG1+Su treatment (MG1+Su =4.5% of $CD45^+$ cells, $p=0.07$). More animals are necessary to gain statistical significance. Interestingly we found no difference in the population of pDCs, a lymphoid IFN producing cell, in the tumour with sunitinib treatment (CTRL= 7.7%, Su= 7.5% of $CD45^+$ cells).

Virus infection can stimulate the activation of cDCs, MΦs and pDCs that not only reside in the tumour but also in the spleen. We see a reduction in VSVΔ51 and Maraba-MG1 induced IFN-β production in the serum with Su treatment, which may be due to the reduced number of the aforementioned cells in the spleen. Since majority of cDCs, $CD169^+$ MΦs and pDCs reside in the spleen, we hypothesized that Su may lead to a reduction in the splenic cDC, $CD169^+$ and pDCs contributing to reduced IFN production in the serum (Figure 2.2).

Similar to the tumour data, three days of Su treatment trends to reduce cDCs, $CD169^+$MΦ and $F4/80^+$ MΦ (Figure S10). Levels of cDCs and $CD169^+$ MΦs were significantly reduced after 6 days of treatment in the spleen. This is consistent with the tumour data. We find that Su treatment significantly reduces the number of compared to control animals (Figure 2.9, CTRL=7.8%, Su=4.5% of $CD45^+$ cells, $p<0.05$). $CD169^+$ MΦ is recruited or proliferates in the spleen upon virus infection (CTRL=1.3%, MG1=2.7% of $CD45^+$ cells). However, when animals are treated with MG1+Su co-therapy the population of splenic CD169+ MΦ is significantly reduced compared to MG1 (MG1+Su= 0.8%, $p<0.05$). pDC population in the spleen remained unchanged.

Together this data suggests that Su treatment reduces the number of IFN producing cDCs and $CD169^+$ MΦ in the spleen and tumour, which may explain the reduced IFN production and

improved viral productivity. However, we do not see a change in the pDC population with Su treatment, which is a key IFN producer[131,132]. Additionally, we also do not see a dramatic drop in the number of cDCs and $CD169^+$ MΦ after three days of Su treatment which is when we observe an improved virus infection with bioluminescence imaging (Figure 2.3A-C). This led us to wonder whether Su might be altering the function of DCs and MΦs.

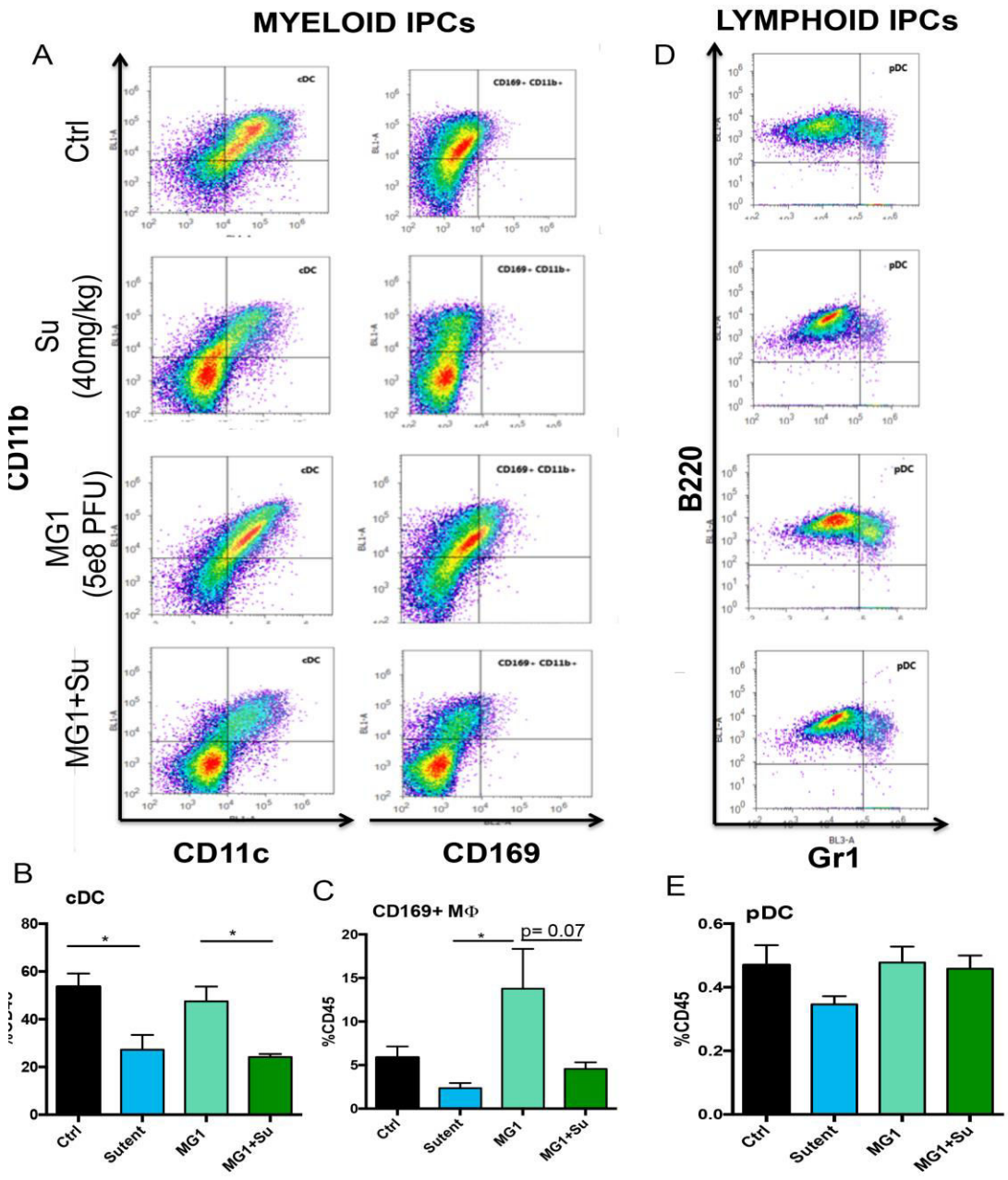

Figure 2.8: Sunitinib reduces the number of cDCs and CD169+ MΦ in the tumour.

4T1 tumours were treated with vehicle (Ctrl), Su, 5E8 PFU MG1 (MG1) on day 8, or combination therapy (MG1+Su). Tumours were harvested on day 11 and initial gate was set to include all cells and doublets were excluded, daughter plots were generated based on $CD45^+$ cells. Representative plots of cDCs ($CD11b^+$ $CD11c^+$), $CD169^+$ Mϕ ($CD169^+$ $CD11b^+$), in the spleen (L→R)(A). cDCs (B) $CD169^+$ MΦ (C) calculated as % $CD45^+$ cells. (D) Representative plots of pDCs. pDCs calculated as % $CD45^+$ cells (E). Data represented as mean± SEM of % $CD45^+$ cells. One-way ANOVA was applied to whether data was statistically significant (n=5/ group, * $p<0.05$, ** $p<0.01$, *** $p<0.001$).

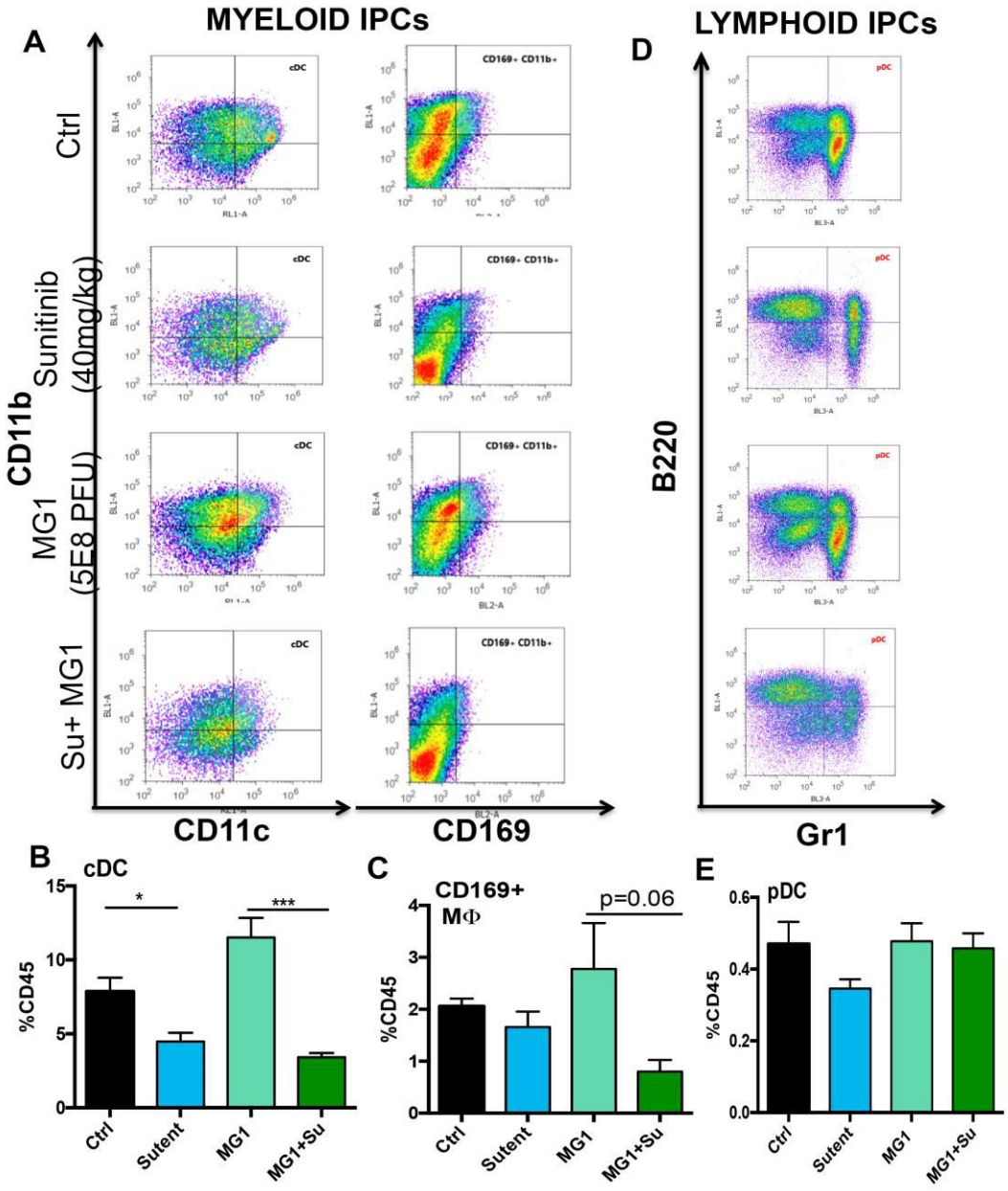

Figure 2.9: Sunitinib reduces the number of cDCs and CD169+ MΦ in the spleen.

4T1 tumours were treated with vehicle (Ctrl), Su, 5E8 PFU MG1 (MG1) on day 8, or combination therapy (MG1+Su). Spleens were harvested day 11 post tumour implantation and flow cytometry was performed. Initial gate was set to include all cells and doublets were excluded, daughter plots were generated based on CD45+ cells. Representative plots of cDCs (CD11b+ CD11c+), CD169+ Mϕ (CD169+ CD11b+), in the spleen (L→R)(A). cDCs (B) CD169+ MΦ (C) calculated as % CD45. (D) Representative plots of pDCs. pDCs calculated as % CD45 (E). Data represented as mean± SEM of % CD45+ cells. One-way ANOVA was applied to whether data was statistically significant (n=5/ group, * $p<0.05$, ** $p<0.01$, *** $p<0.001$).

2.3.5 Sunitinib reduces type I IFN production from BMDM and BMDCs ex vivo

Although IFN production was decreased significantly with three days of Su treatment (Figure 2.2), we found that Su treatment did not reduce the number of cDCs or macrophages on day 8 (Figure S8 and S9). This prompted the hypothesis that Su may be reducing not only the number of cDCs and Mϕ s in the tumor and spleen, but also altering IFN production in the individual cells. To this end, bone marrow was harvested from mice and treated with M-CSF and GM-CSF to differentiate them into macrophages and DCs respectively[124]. BMDMs and BMDCs were then treated with sunitinib (0.078μM, 0.625μM and 5μM) for two hours and infected with VSVΔ51 or Maraba-MG1 (MOI 10). We chose high doses of virus to emulate direct intratumoral infection in the tumour. The Su doses were chosen to be able to directly compare the tumour cell data with BMDM/ BMDC data. Supernatant was collected 6 hpi, analysed for type I IFN (IFN-β) and viability assays were performed at 24 hpi.

As predicted, VSVΔ51 infection induced IFN-β production in BMDMs compared to untreated controls (Figure 2.9 A). Interestingly, Su treatment reduced IFN-β production in a dose dependent manner from BMDMs (Figure 2.9 A). No GFP expression was observed with VSVΔ51 infection (Figure 2.9 C) or Maraba infection (Figure S10). BMDMs do not support productive ORV infection. Sunitinib treatment also reduces the viability of BMDMs after 24 hours of treatment (Figure 2.9 B). Although there is Su mediated cell-death in BMDMs at 24 hours, there was no observable cell death at 6 hpi (Figure S13), when IFN is measured. This finding supports our hypothesis that Su may be reducing the production of type I IFN in BMDMs.

Similar to BMDMs, VSVΔ51 infection also induced IFN-β production in BMDCs at 6hpi (Figure 2.10 A). Additionally, Su treatment reduced the production of IFN-β in a dose dependent manner from BMDCs (Figure 2.10 A). Interestingly, Su did not affect the viability of BMDCs whereas ORV infection reduced the viability of BMDCs (Figure 2.10 B). VSVΔ51 infection (Figure 2.10 B) and Maraba MG1 infection (Figure S12) reduces the viability of BMDCs. Contrary to BMDMs, evidence suggests that BMDCs are susceptible to a virus infection[136]. Indeed, we found that BMDCs allowed for gene expression VSVΔ51; the BMDCs were GFP^+ with VSVΔ51 infection (Figure 2.10 C).

Taken together, this data suggests that Su reduces IFN production in BMDMs and BMDCs.

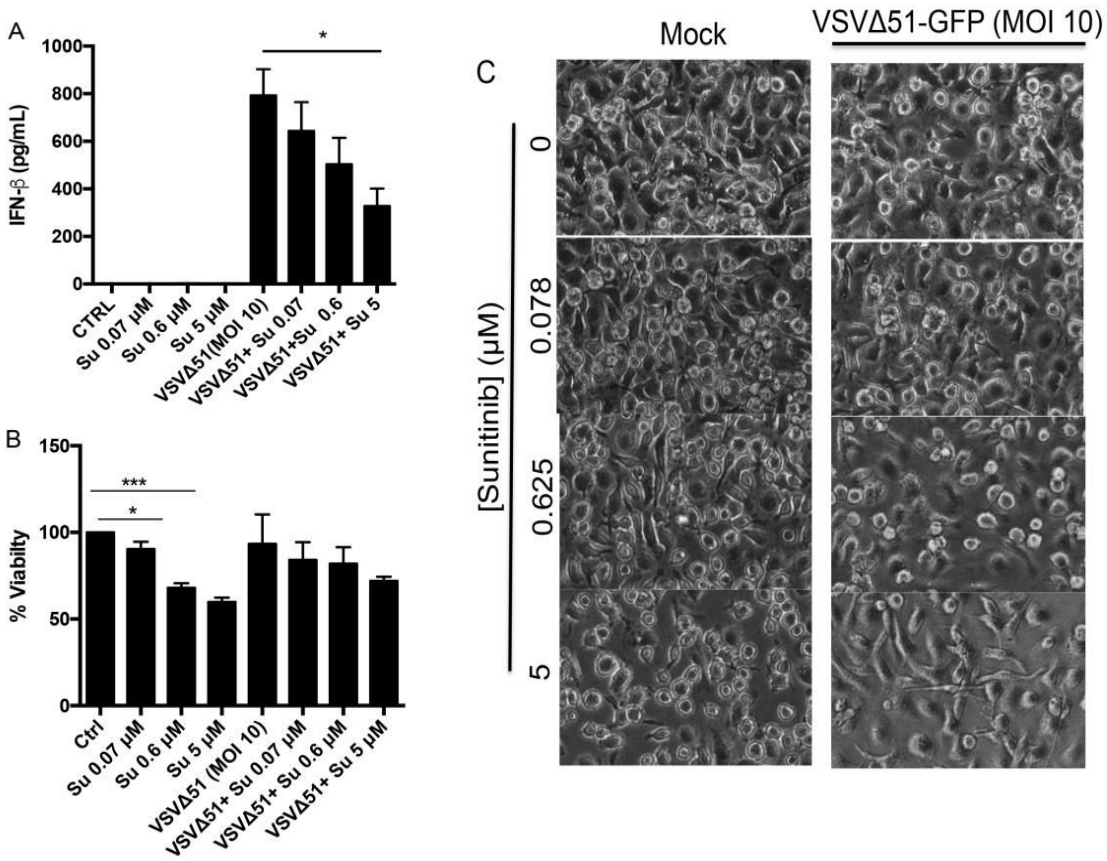

Figure 2.10: Sunitinib reduces IFN-β production in BMDMs in response to VSVΔ51 infection.

BMDMs were derived from bone marrow of C57/BL6 mice and treated with Su at 0.078µM, 0.625µM and 5µM for 2 hours prior to VSVΔ51 infection (MOI 10). (A) IFN-β levels 6 hpi (n=4/group), (B) Viability of BMDMs at 24 hpi calculated as % control (n=3/ group), (C) Representative images of BMDMs 24 hpi with VSVΔ51 (MOI 10) ±sunitinib. Data represented as mean± SEM (*p<0.05, ** p<0.01, ***p<0.001).

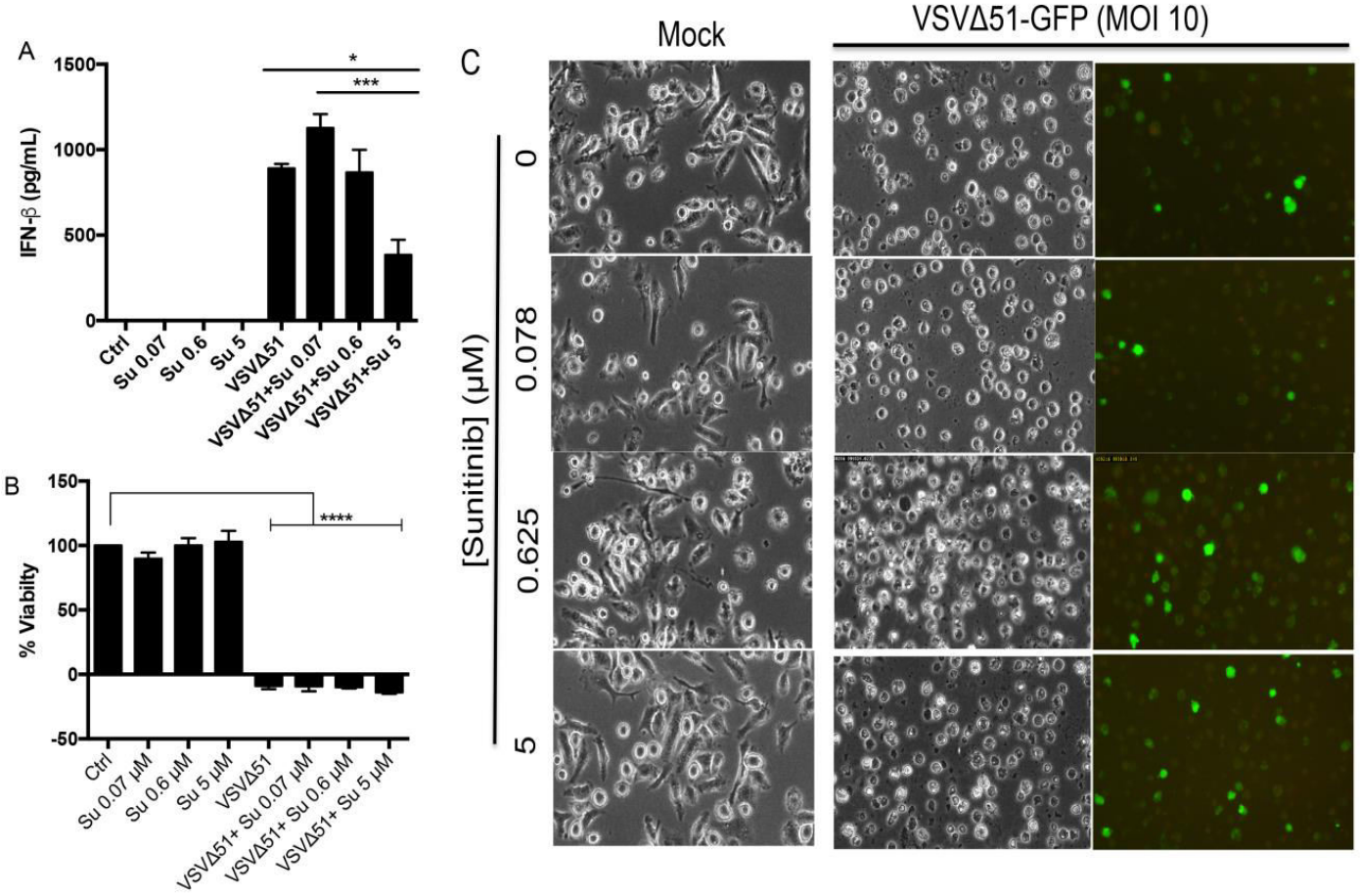

Figure 2.11 Sunitinib reduces IFN-β production in BMDCs in response to VSVΔ51 infection.

BMDCs were derived from bone marrow of C57/BL6 mice and treated with Su at 0.078μM, 0.625μM and 5μM for 2 hours prior to VSVΔ51 infection (MOI 10). (A) IFN-β levels 6 hpi, (B) Viability of BMDCs at 24 hpi calculated as % control, (C) Representative images of BMDCs 24 hpi with VSVΔ51 (MOI 10) ±sunitinib. Data represented as mean± SEM (n=3/ group, *p<0.05, ** p<0.01, ***p<0.001).

2.3.6 Sunitinib treatment may make the tumour microenvironment more immune-permissive

Oncolytic virus therapy induces the activation of anti-tumour $CD8^+$ T cells which are important for OV mediated responses[25,64]. The tumour microenvironment often acts as a barrier to anti-tumour $CD8^+$ T cell responses[118] and studies have shown that relieving immunosuppression in the microenvironment may lead to enhanced $CD8^+$ T cell responses [98]. 4T1 tumours are comprised of tumour and stromal cells, which include immunosuppressive cells (MDSCs and Tregs) that serve to protect the tumour from immune detection and also inhibit T cell responses[83,97]. Splenic MDSC population is increased in several tumour models such as RENCA, CT26 and 4T1[97]. MDSCs inhibit $CD8^+$ T cell function in the host by secreting cytokines such as IL-10 and TGF-β[84,97]. Sunitinib treatment has shown to reduce the number of MDSCs in both spleen (Personal communication, Dr. Don Morris) and tumour in RENCA, CT26 model leading to an improved outcome[97] Therefore, we sought to determine whether Su and ORV treatment leads to an improvement in the 4T1 tumour contexture. To this end, flow cytometry was performed on the spleen and tumour to measure the levels of MDSCs and lymphocytes ($CD4^+$, $CD8^+$ T cells and B cells). As previously reported, Su treatment reduced the number of MDSCs in the spleen ($p<0.05$, Figure 2.12 A, B)[98]. There was a small increase in the percentage of $CD4^+$, $CD8^+$ T cells and B cells with Su treatment. However, this was not statistically significant. Interestingly, there was a significant reduction in the percentage of lymphocytes upon MG1 treatment. The percentage of splenic lymphocytes, $CD4^+$ and $CD8^+$ cells, were also increased with sunitinib treatment (Figure 2.13 A, B). This data suggests that Su treatment may lead to the host immune system becoming more immune permissive to OV therapy. As previously documented[127], Su treatment in the tumour did not reduce the percentage

of MDSCs (Figure 2.14 A, B). However, there is a small but statistically insignificant increase in the percentage of tumour infiltrating lymphocytes (TILs). Taken together, this data suggests that sunitinib treatment may make the tumour micro and macro environment more immune permissive.

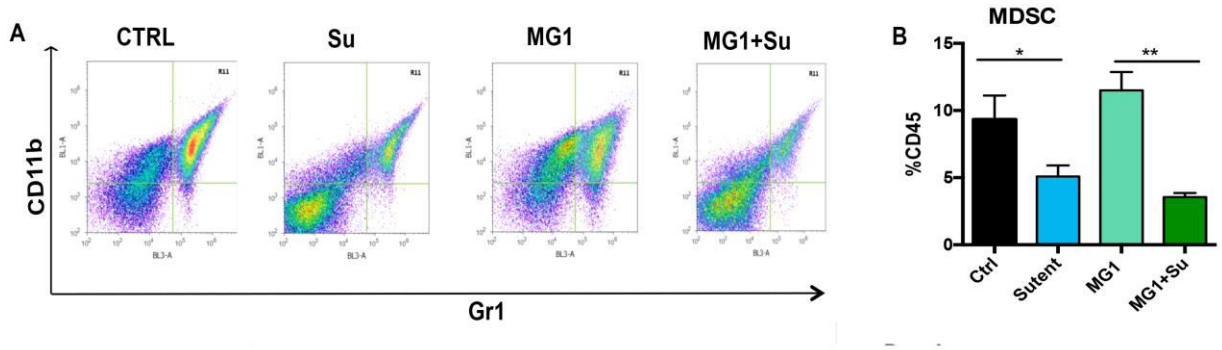

Figure 2.12 Sunitinib reduces the number of MDSCs in the spleen.

4T1 tumours were treated with vehicle (Ctrl), Su, 5E8 PFU MG1 (MG1) on day 8, or combination therapy (MG1+Su). Spleens were harvested day 11 post tumour implantation and flow cytometry was performed. Initial gate was set to include all cells and doublets were excluded, daughter plots were generated based on CD45+ cells. Representative plots of MDSCs with different treatment groups (A). MDSCs calculated as % $CD45^{+}$ cells (B). One-way ANOVA was applied to whether data was statistically significant (n=5/ group, * $p<0.05$, ** $p<0.01$, *** $p<0.001$).

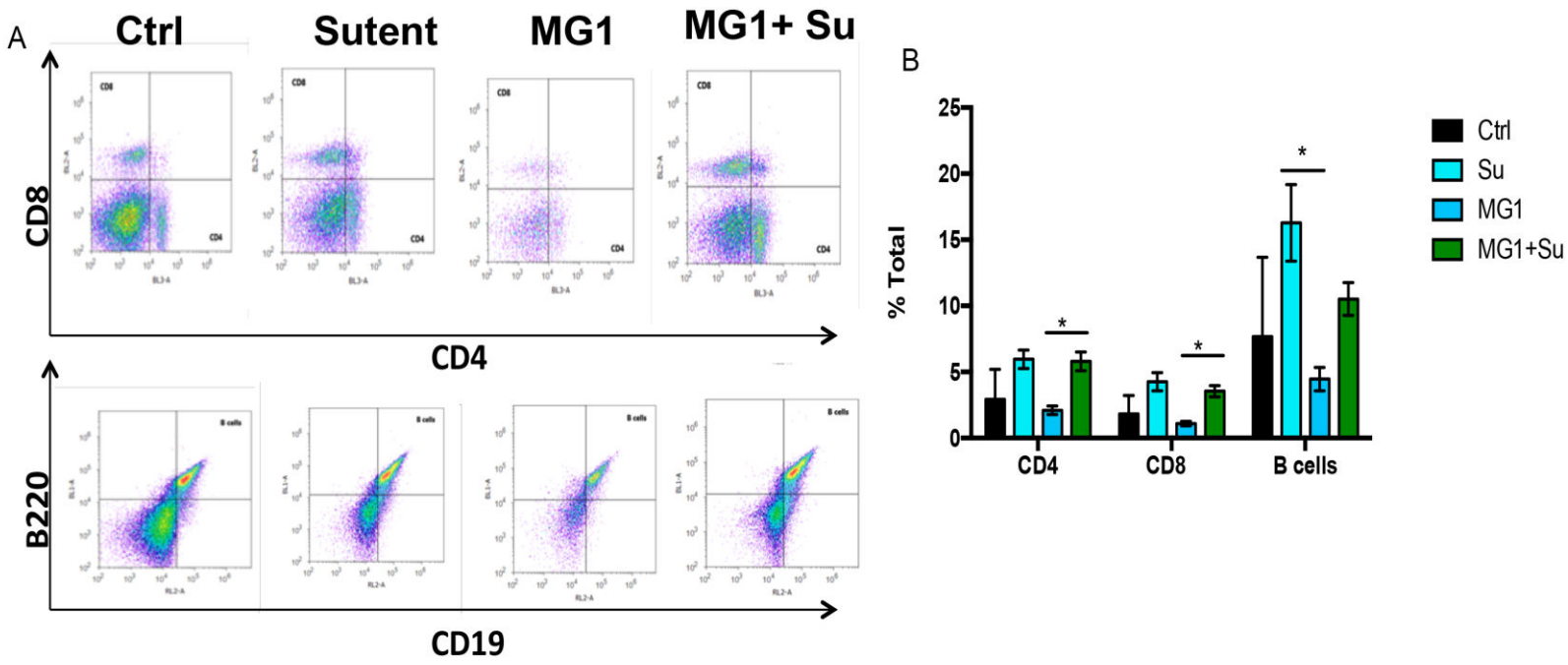

Figure 2.13 Sunitinib treatment increases the number of lymphocytes in the spleen.

4T1 tumours were treated with vehicle (Ctrl), Su, 5E8 PFU MG1 (MG1) on day 8, or combination therapy (MG1+Su). Spleens were harvested day 11 post tumour implantation and flow cytometry was performed. Initial gate was set to include all lymphocytes based on FSC and SSC; doublets were excluded, daughter plots were generated based on $CD45^+$ cells. Representative plots of $CD4^+$ and $CD8^+$ T cells and B cells with different treatment groups (A). MDSCs calculated as % $CD45^+$ cells (B). One-way ANOVA was applied to whether data was statistically significant (n=5/ group, * $p<0.05$, ** $p<0.01$, *** $p<0.001$).

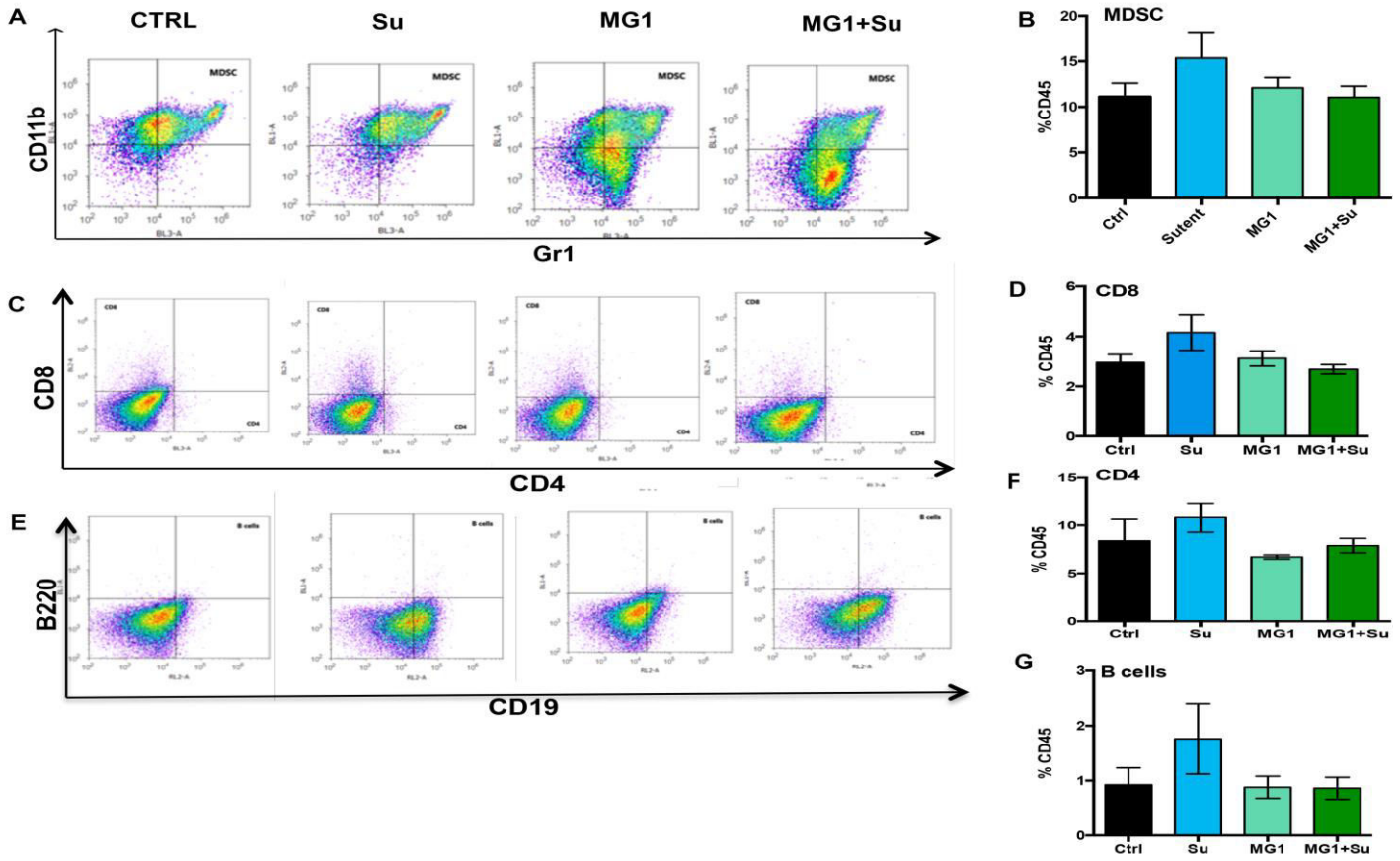

Figure 2.14 Sunitinib does not alter the population MDSC and lymphocyte in the tumor.

4T1 tumours were treated with vehicle (Ctrl), Su, 5E8 PFU MG1 (MG1) on day 8, or combination therapy (MG1+Su). Spleens were harvested day 11 post tumour implantation and flow cytometry was performed. Initial gate was set to include all cells and doublets were excluded, daughter plots were generated based on $CD45^+$ cells. Representative plots of MDSCs (A) MDSCs calculated as % $CD45^+$ (B); representative plots of $CD4^+$ and $CD8^+$ cells (C), $CD8^+$ expressed as % CD45 (D), $CD4^+$ expressed as % CD45 (F); representative plots of $B220^+$ $CD19^+$ cells (E) and B220+ CD19+ expressed as % CD45 (G). Data shows as mean±SEM (n=5/ group).

CHAPTER 3: DISCUSSION

3.1 Summary of findings

Type I IFN is a barrier to ORV therapy and strategies are necessary to improve the oncolytic and immunotherapeutic potential of ORV. In this study we assessed the efficacy of sunitinib (Su) as an adjuvant for ORV. Studies show that Su dampens anti-viral signalling by reducing the activity of IFN effector molecules in the tumour cell, and improving viral productivity[6,96]. Su also alleviates immunosuppression in mouse models by reducing the population of immunosuppressive cells such as MDSCs[101]. Therefore, we hypothesized that Su may improve ORV infection and ORV mediated immunotherapy. To test this hypothesis we chose a tumour model which responds to type I IFN, namely 4T1 (Figure S1).

We found that combining Su with ORVs VSVΔ51 and Maraba-MG1 improved tumour control in 4T1 bearing animals (Figure 2.1). Since studies suggest that Su may inhibit IFN signalling in the tumour cell, we tested whether Su blunted IFN response *in vivo* (Figure 2.2). We found that Su does indeed reduce the production of ORV induced IFN. Then, we also tested whether Su improves viral productivity in the tumour. Su does indeed improve ORV infection in the tumour (Figure 2.3). Following this, we sought to determine whether Su reduces type I IFN production in the tumour cell itself, or in the surrounding stromal components. To this end, we tested virus induced IFN production in 4T1 cells *in vitro* (Figure 2.5). We found that Su did not reduce the IFN production or improve viral productivity in 4T1 cells (Figure 2.5-6). Contrary to this finding, *ex vivo* cultured macrophages and DCs treated with Su had impaired IFN production (Figure 2.10-11). We also investigated whether Su altered the number of cDCs, pDCs and $CD169^+$ MΦ in the organism. We found that Su treatment reduces the number of cDCs and

$CD169^+$ macrophages in both the tumour and spleen (Figure 2.8, 2.9). Together our data suggests that Su inhibits IFN production *in vivo* by limiting the number of IFN producing cells in the tumour and spleen, as well as their ability to produce IFN.

In addition to IFN production in the tumour, the immunosuppressive microenvironment is also a barrier to OV therapy. The immunosuppression within the tumour inhibits the activation of anti- tumour $CD8^+$ T cell mediated immunity[62]. Studies suggest that Su alters the immune contexture of tumour bearing animals, by inhibiting cells such as MDSCs[97,98]. As reported, Su reduced the number of MDSCs in the spleen (Figure 2.12) and increased the number of lymphocytes in the spleen (Figure 2.13). However, Su treatment did not reduce the number of MDSCs in the 4T1 tumor[127] (Figure 2.14) or increase the number of tumour infiltrating lymphocytes.

In conclusion, we found that Su improved the ORV infection in an IFN responsive tumour model in a tumour cell independent manner. Su treatment reduced both the number of and the IFN production in cDCs and CD169+ MΦ thereby making the 4T1, an IFN responsive tumour, more susceptible to ORV infection.

3.2 Discussion of findings

3.2.1 Sunitinib improves ORV infection in a tumour cell independent manner

Sunitinib improves VSVΔ51 and Maraba-MG1 mediated tumour control and infection in an IFN- responsive tumour model. Tumour control with co-therapy was modest yet statistically significant; Su+VSVΔ51/Maraba-MG1 treated animal lived on average 25-30% longer than tumour bearing controls (Figure 2.1). We believe that the survival outcomes seen in this model can be further improved by optimizing the treatment schedule. The therapy schedule used in this

study (Figure 2.1A) was established in the renal cell carcinoma (RENCA) model treated with Reovirus ± Su (Personal communication, Dr. Don Morris). RENCA bearing animals underwent tumour regression using Su (40 mg/kg)+Reovirus *in vivo* (Unpublished data, Dr. Don Morris). Similarly a neuroblastoma model, Neuro2A treated with VSVΔ51±Su co-therapy using the same dosing strategy also had significant tumour regression with co-therapy (Unpublished data, Dr. Doug Mahoney). However, the schedule was not further optimized for the 4T1 tumour model. The optimal scheduling of Su alone is still being debated amongst clinicians and further studies are necessary to determine the best possible schedule. Su was approved for human use in 2006 and is usually used at a dose of 50 mg daily for 4 weeks on and 2 weeks off[105,137] unless the patient experienced drug-related toxicity. Upon experiencing adverse events, the dose is reduced to 37.5 mg or 25 mg[105,138]. Studies comparing traditional Su treatment schedule (50mg daily, 4 weeks on/2weeks off) with lower dose of sunitinib and a prolonged schedule (37.5mg daily for 6 weeks) have been inconclusive[137,139]. Some studies have suggested lower more prolonged dosing of Su leads to the same therapeutic effect with reduced toxicity[140,141] whereas others have argued that there is no significant difference between the two treatment regimens[138]. These studies suggest that the optimal dosing of Su mediated tumour regression remains unknown. However, Su treatment schedule used in this study did improve VSVΔ51 and Maraba-MG1 mediated tumour regression and we wanted to determine the mechanism behind this.

Studies suggested that Su might improve viral infectivity in tumour cells *in vitro*[6,96]. Therefore, we examined whether sunitinib blunted IFN production in response to VSVΔ51 and Maraba-MG1 infection. Since IFN is a key component of the anti-viral signalling pathway, we wanted to determine whether Su treatment reduced ORV induced IFN production. We found that Su reduced virally induced IFN production both in the tumour and in the serum of in VSVΔ51

and Maraba-MG1 infected animals six hours after infection (Figure 2.2). Interestingly we found that Maraba-MG1 infection induced lower levels (~10 fold) of IFN production in the 4T1 tumours or spleen compared to VSVΔ51. This was interesting and novel as IFN-β production in response to VSVΔ51 and Maraba-MG1 have never been compared before. The G protein mutation on Maraba-MG1 (Q242R) might be a gain of function mutation as the G mutant itself blocks IFN production *in vitro.* However, the Maraba-MG1 mutant has been shown to produce same levels of IFN-β as the Maraba-Δ51 mutation[35]. To further understand the differences between VSVΔ51 and Maraba-MG1, we need to conduct studies comparing VSVΔ51, VSV-MG1, MarabaΔ51 and Maraba-MG1. This would require careful characterization of these mutants extensively over time. We would need to characterize the IFN production, and also the anti-viral signalling pathways these mutants activate to fully understand the difference between these mutants. Additionally, we could also characterize the differences between these viruses *in vivo*.

Next we wanted to determine if Su improved VSVΔ51/ Maraba-MG1 productivity *in vivo.* To this end, we quantified VSVΔ51 and Maraba-MG1 infection using plaque assays in the tumour 72hpi ± Su. We found Su treatment improved the initial infection of both VSVΔ51 and Maraba-MG1 in 4T1 tumours (Figure 2.3 A-C, S4). This is also maintained at 72 hours post infection (Figure 2.3 D-E). Improvement virus productivity with Su treatment has been seen in other tumour models. For example, Su improves the infection of VSVΔ51 in Neuro2A tumours (Unpublished data, Dr. Doug Mahoney). Additionally, Donald McDonald`s group published an abstract suggesting that Su improves the productivity of oncolytic vaccinia virus (Pexa-Vec) in a pancreatic cancer model. This study suggested that viral infection is improved due to Su improving perfusion and viral delivery within the tumour[91]. Although a key component in

sunitinib mediated infection improvement[90,142], studying the effects of sunitinib on viral delivery was beyond the scope of this study. We focused on the role of Su as an immune adjuvant to ORV therapy[6]. Together this data suggests that Su reducing IFN may be responsible for improvement in viral productivity. IFN can be produced by both 4T1 cells as well as supporting stromal cells within the tumour.

The tumour microenvironment can be resistant to virus infection due to production of IFN. IFN can be secreted by tumour cells (Figure S1), or by the supporting cells such as cDCs[143], MΦs[117] and pDCs[144]. A recent study suggested Su treatment inhibits the phosphorylation of IFN effector molecules such as RNAseL, PKR and eIF2α leading to improved viral productivity in tumour cells *in vitro*[6,96]. Based on this data, we wanted to test whether Su inhibited phosphorylation of PKR in response VSVΔ51 infection in 4T1 cells. Since this study did not demonstrate the effect of Su on 4T1 cells, we used ACHN cells as a positive control. ACHN cells were used to characterize the inhibition of phosphor-PKR and eIF2α in the aforementioned study. We found that Su indeed did reduce the phosphorylation of PKR in a dose dependent manner in ACHN, as reported, as well as in 4T1. Su also blocked the phosphorylation of eIF2α in ACHN but not 4T1 (Figure 2.4). Following this, we aimed to determine whether Su reduces the IFN production in 4T1 cells. We found that Su did not reduce IFN production in the 4T1 cells (Figure 2.5).

Further experiments were then conducted to determine whether Su improves the productivity of VSVΔ51 in 4T1 cells, we found that Su did not improve viral productivity in 4T1 cells. Once again, ACHN was used as a positive control and we found Su treatment did not improve productivity of VSVΔ51. Additionally, Neuro2A, a neuroblastoma cell line was tested for VSVΔ51 productivity with Su treatment at various time points as well. Yet again, there was

no improvement in viral productivity in Neuro2A with Su treatment (Personal communication, Dr. Mahoney, data not shown). Additionally, this study demonstrated that Su treatment improved WT-VSV mediated cytotoxicity in a panel of cell lines including 4T1 and ACHN. However, the experiment in this study was based on one MOI of virus (MOI 1) at a single time point (8 hpi). We tested Su at eight different concentrations starting at 5μM, as the study used, and tittered down to 0.078μM with WT-VSV, VSVΔ51 and Maraba-MG1 at eight different MOIs at various time points in both 4T1 and ACHN lines (Figure 2.7 and Figure S5-6). We were unable to observe synergy under any of the aforementioned conditions.

There may be several reasons why our findings may differ from the findings published in Jha *et al*. 4T1 cells produce and respond to type I IFN (Figure 2.5, S1), but the RNAseL activity and status in 4T1 cells is unknown and 4T1 cells may have a gain of function mutation in RNAseL. For instance, studies suggest that 13% of prostate cancer cells can have gain of function mutation in RNAseL[145]. However, we did not test the RNAseL activity or RLR activation in 4T1 cells. Future experiments could be conducted to test this; we could treat 4T1 cells with VSVΔ51 and various Su concentrations and check for the phosphorylation of MAVS, the RIG-I adaptor protein[146]. Additionally, cells may have other PRRs that detect viral components. For instance, 4T1 cells express TLR3, a PRR that detects viral RNA[147]. This may also induce sufficient levels of IFN-β upon VSVΔ51 infection. To understand whether Su treatment truly inhibits IFN production through inhibiting RNAseL and sub-optimally activating RIG-I, we need to obtain $TR3^{-/-}$, $7^{-/-}$, $8^{-/-}$ cell lines and test whether Su reduces RNAseL mediated RIG-I activation by probing for phosphorylation of downstream MAVS and IRF-3. Additionally, we could obtain an $RNAseL^{-/-}$ cell line to test the negative regulation of Su in this line. To this

end, we could compare a wild type line (RNAseL^{+}), RNAseL$^{-/-}$ and RNAseL$^{-/-}$+Su and compare the levels of virally induced IFN and ISGs. If Su blocks RNAseL there should not be any differences in IFN and ISG production between RNAseL$^{-/-}$ and RNAseL$^{-/-}$+Su.

The other mechanism of Su mediated viral productivity is the inhibition of PKR activation. PKR is a cytosolic protein, which binds to ds-RNA and is constitutively expressed in uninfected cells[43] (Figure 2.4). PKR is phosphorylated upon binding ds-RNA and IFN signalling. PKR then phosphorylates eIF2α inhibiting viral RNA translation[43]. However, we do not observe a reduction in eIF2α phosphorylation with Su treatment in 4T1 cells (Figure 2.6). Therefore, despite the reduction in phosphorylation of PKR upon Su treatment in 4T1 cells, the levels of p-eIF2α remains the same in 4T1 cells (Figure 2.4) with or without Su treatment. This may account for the unchanged levels of virus productivity in 4T1 cells in response to VSVΔ51±Su. Additionally, eIF2α can be phosphorylated by PKR-like ER kinase (PERK) in response to virus mediated ER stress[148]. Therefore, redundant phosphorylation of eIF2α may explain the unaltered levels of p-eIF2α in 4T1 cells with Su+VSVΔ51 treatment.

Taken together, this evidence suggests that Su does not reduce IFN production and improve VSVΔ51 productivity in 4T1 cells *in vitro*. However, 4T1 tumours produce ORV induced type I IFN, which is dampened by Su treatment and results in an improved viral productivity *in vivo* (Figure 2.3), which led us to further investigate the composition of 4T1 tumors. The tumour microenvironment is complex and consists of macrophages[130] and DCs that produce IFN and can potentially inhibit ORV infection[130].

Similarly, the 4T1 tumours are also populated with myeloid cells[129]. 4T1 tumours secrete GM-CSF[129], and recruit myeloid cells into the tumour to escape immune detection[149]. Some myeloid cells such as cDCs and MΦ produce type I IFN in response to virus infection[150,151]

which differentiate from myeloid progenitor cells. Common myeloid progenitor cells express FLT3R which promotes survival of these progenitor cells[107,128,152]. FLT3R receptor signalling blocks a downstream apoptosis pathway by inhibiting proteins such as BAD, a pro-apoptotic protein[109]. A study showed that Su can inhibit cDC expansion in mouse models by inhibition of FLT3R dependent signaling[111]. Additionally pDCs, a major IFN producer, also express FLT3R[153]. Therefore, blocking FLT3R signalling with Su may lead to apoptosis of the progenitor cells thereby reducing the number of mature DCs and macrophages[154]. However, the effect of Su in cDCs, CD169+ MΦ and pDCs are not characterized in the context of 4T1 tumours or ORV therapy. This led us to investigate whether Su treatment may be reducing the number of DCs and MΦ in the tumour microenvironment reducing production of type I IFN and improving OV infection.

To this end, we performed flow cytometry to determine whether Su altered the population of IFN producing cells in the tumour microenvironment. We found that the tumour microenvironment consisted of largely $CD11b^+$ $CD11c^+$ cDCs (~50% of leukocytes); upon Maraba-MG1 infection, there is an increase in the number of CD169+ cells within the tumour (13.8%). This may be due to recruitment or expansion of $CD169^+$ cells. Su reduced the number of cDCs by half and decreased the number of Maraba-MG1 induced $CD169^+$ macrophages (Figure 2.8). We also found that the number of pDCs was not reduced with Su treatment. Although pDCs are considered to be a major IFN producer[131,132], cDCs and $CD169^+$ macrophages are also able to produce large amounts of type I IFN. pDCs only make up a very small fraction of the tumour (~0.5%) therefore observing the reduction in pDC population is difficult when measured as $\%CD45^+$ cells. Therefore, we also expressed pDCs as absolute numbers (Figure S14) in the tumour. We found that there was a decrease in the absolute number

of pDCs in the tumour with Su treatment. However, this correlates with the tumour size and therefore could be a result of reduced total cells in the tumour with treatment. Additionally, the genesis of pDCs is incompletely understood. pDCs undergo convergent rather than divergent differentiation[155]; pDCs are generated from both myeloid and lymphoid progenitor cells[156]. Adoptive transfer of either common myeloid progenitor cells (CMP) and lymphoid progenitor cells (CLP) into sub-lethally irradiated mice both generates pDCs[155]. CMPs produce both cDCs and pDCs via a common DC precursor whereas CLPs differentiate into an intermediate B cell like phenotype, which further differentiate into pDCs. Flt3R is expressed by lymphoid primed multipotent progenitor but not in the committed lymphoid progenitor cell[153]. Studies shown that the IFN producing potential of the MPC generated pDC is higher than LPC generated pDCs upon stimulation with CpG, a TLR9 agonist[156]. Taken together, these studies suggest that pDCs may require further immune phenotyping to differentiate them based on their origin. Currently, there are no distinguishing features to differentiate myeloid and lymphoid derived pDCs. Additionally, cDCs and macrophages are also able to produce large amounts of IFN. For example, a study by Diebold *et al* showed that when cDCs were infected with LCMV directly in the cytosol, cDCs produced as much IFN-α as pDCs. However, when splenic cDCs were infected with virus in the media, they produced reduced levels of IFN. The authors speculate that electroporation of the virus simulated cytosolic RNA binding. The authors also show that high levels of IFN production upon electroporation maybe due to activation of the PKR signalling rather than TLR signalling[114]. This suggests that albeit pDCs being major IFN producers, cDCs may alter their phenotype and become larger IFN producers in response to virus infection.

We found that Su did not reduce the number of cDCs and $CD169^{+}$MΦ and $F4/80^{+}$ MΦ on day eight (Figure S9). However, we find that there is reduced IFN production and improved viral infection on day 8. This led us to hypothesize that Su may be altering the IFN producing function of cells in the tumour. To this end, we derived MΦ and DCs from bone marrow of C57/BL6 mice and treated them with ORV+/- Su. As predicted, the BMDMs and BMDCs produced IFN-β upon virus infection (Figure 2.10-2.11). Interestingly, Su treatment reduced the production of type I IFN in a dose dependent manner in both BMDMs and BMDCs. Su treatment alone leads to a reduction in viability in BMDMs at 24 hpi. However, we do not observe BMDM cell death with Su treatment at 6 hpi when we measure IFN (Figure S13). This suggests that the reduction in IFN with Su treatment was not due to the loss of cell viability. However, it is possible that Su treatment may alter PRR mediated signalling in the BMDMs. We have not explored the mechanism by which Su may reduce IFN production in BMDMs and BMDCs but not in 4T1 cells themselves.

It is possible that Su acts on an IFN producing pathway that is common to both BMDMs and BMDCs but absent in 4T1 cells. For example, RLRs are ubiquitous in cells; however, not all cells have TLRs or the full repertoire of TLRs. Interferon producing cells such as cDCs, macrophages and pDCs express varying combination of TLRs including TLRs 3, 7 and 8 whcihc detect viral RNA. cDCs, MΦ and pDCs all express and use TLR7 to induce anti-viral production. Thereby, it is possible that sunitinib may be targeting TLR7 signalling in order to reduce IFN production by DCs[157] and MΦs. However, evidence also suggests that cDCs preferentially use RLRs to induce IFN-β[143,158], therefore it is also possible that Su targets a component of the IFN signalling pathway downstream of the PRRs. Future experiments to

determine the intracellular targets of Su in 4T1 cells, BMDMs and BMDCs are necessary. To this end, we could perform a kinome analysis to determine which signalling pathway is activated when these cells are infected with VSVΔ51. Following this, we could treat cells with VSVΔ51+Su to determine which kinases, in the IFN production/ signalling pathway, are down-regulated with Su treatment in each cell line compared to VSVΔ51 alone. We could then perform secondary validation on these molecules using knockout mouse models.

We also found, BMDMs do not allow VSVΔ51 gene expression, as we could not observe any GFP^+ cells (Figure 2.10 C). However, BMDCs allow gene expression, as measured by expression of viral GFP, when infected with VSVΔ51 and undergo ORV mediated apoptosis. Interestingly, we found that BMDC viability is unaffected by Su treatment whereas Su treatment is toxic to BMDMs. The mechanism of BMDM cell death upon Su treatment is not understood. Su is known to target M-CSFR signalling[95]. BMDMs might be undergoing Su mediated apoptosis due to M-CSFR signalling inhibition by Su. M-CSF is a cytokine that is pivotal for differentiation of BMDMs from bone marrow monocyte-macrophage precursor cells. Upon binding M-CSF ligand, M-CSFR activates ERK signalling through GRB2 and AKT through PI3K. This ultimately induces the activation of Bcl-2 that promotes cell-survival. Thereby inhibiting M-CSF signalling with Su may be promoting cell death pathways downstream of M-CSFR in BMDMs which leads to cell death[159]. Interestingly, Su does not cause cell death in BMDCs, which are differentiated using the cytokine GM-CSF[124]. Studies suggests that GM-CSF signalling may confer Su resistance in cells such as MDSCs[97]. This supports our finding that GM-CSF signalling in *ex vivo* BMDCs may render them resistant to Su treatment.

Taken together, this data suggests that Su treatment reduces the number of IFN producing cells such as cDCs and $CD169^+$ MΦ in the TME. Additionally, Su treatment also reduces the IFN production from BMDMs and BMDCs. Due to reduced IFN levels in the tumour microenvironment the surrounding cells such as tumour cells and endothelial cells are unable to defend themselves from the virus infection, which results in improved viral productivity. Additionally, due to a reduction in the number of tumour infiltrating cDCs and MΦ in the tumour, they may not be able to clear the virus quickly, which may explain the difference in virus titres in the tumour 72 hpi. The model is summarized in Figure 3.1.

Although this data strongly suggests the improvement in virus productivity *in vivo* is due to Su reducing IFN, we have not directly proven this. To do so, we would need to determine whether replenishing IFN in the tumour would ablate the improved viral productivity we see with Su treatment. To this end, we could obtain IFNAR1/2 knockout mice and treat them with Su and ORV. These mice can be treated with VSVΔ51+Su and the IFN levels should be measured in the serum and TIF. The $IFNAR1/2^{-/-}$ mice are capable of producing IFN but not signalling through IFN. Therefore, if Su were truly responsible for reducing the production of IFN, $IFNAR1/2^{-/-}$ mice would have reduced production of IFN. However, if Su were responsible for dampening IFN mediated signalling, there would not be any difference between the levels of virally induced IFN in $IFNAR1/2^{-/-}$ knockout mice and wild type mice.

In addition to viral infection, the generation of an adaptive anti-tumour response is also important for ORV mediated tumour clearance. It is known that type I IFN play an important role in maturation of cDCs, and cross presentation of tumour antigens to CD8+ T cells[160,46]. IFN leads to DC maturation by upregulating co-stimulatory molecules on DCs such as CD80, CD86,

IFN[161] also increases antigen presentation by upregulating expression of MHC class I and II on DCs. Therefore, albeit being permissive for ORV infection, reduction in number and function of cDCs with Su treatment may be a double-edged sword for OV mediated immunotherapy. Jaini *et al*, argue that although Su may hinder priming of T cells depending on the administration schedule. When animals are treated with Su and vaccine vector concurrently, there is a reduction in the number of IFN-γ producing T cells. Although upon terminating Su treatment during priming phase, there is a significant increase in the number of IFN-γ producing T cells[162]. However, a study conducted by Hipp *et al*, 2008 demonstrated that Su treatment did not reduce the expression of antigen presentation markers such as CD1a, CD86, CD80 and CD83 on DCs. Additionally they also demonstrated that T cell activity was not blunted with Su treatment at 20 and 40 mg/kg[163]. Taken together, it is likely that Su may inhibit maturation of DCs, however it is inconclusive whether that is truly the case *in vivo*. To test whether Su reduces the maturation of DCs, we could test the DC phenotype with or without Su treatment *in vivo.* We could measure DC maturation markers such as CD80, CD86 and CD83 in splenic and intra-tumoral DC. In addition to reduced DC maturation, another barrier to T cell priming in tumour bearing hosts is the immunosuppressive micro and macro-environment.

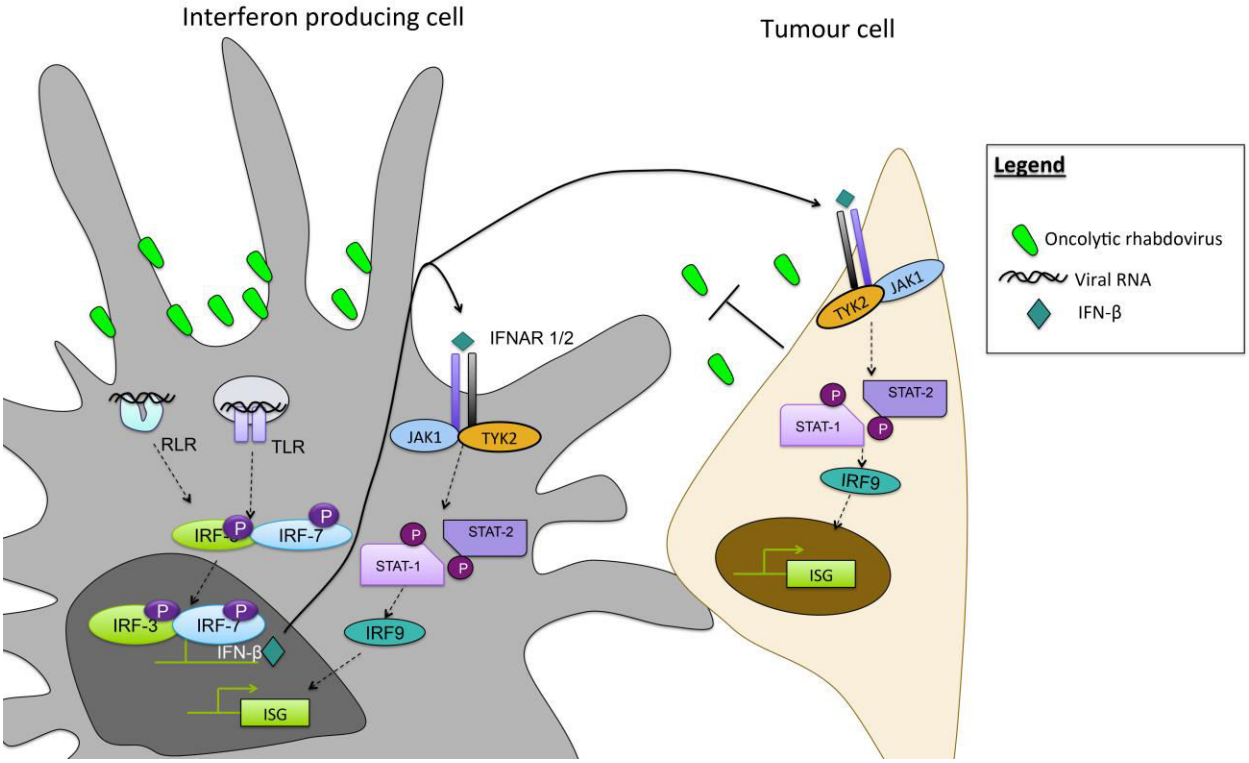

Figure 3.1 Working model of Su and ORV interaction in the tumour microenvironment.

Upon ORV infection of 4T1 tumors, the virus induces type I IFN production from 4T1 cells, DCs and MΦ. ORV binds to TLRs and RLRs in IFN producing cells to produce type I IFN, which is secreted and protects surrounding cells from an impending virus infection. However, with Su treatment the numbers and IFN production of DCs and MΦ is reduced. Su treatment leaves the tumours vulnerable to ORV infection.

3.2.2 Su treatment may improve immune contexture of 4T1 tumours

The tumour microenvironment is immunosuppressive and a barrier to OV immunotherapy[62]. 4T1 tumours recruit MDSCs into the spleen and tumour[100,127] which produce immunosuppressive cytokines to inhibit T cell mediated anti-tumour immunity[84]. Su treatment has shown to reduce splenic and intra-tumoral MDSC population in several tumour models such as RENCA and CT-26 to aid $CD8^+$ T cell activity leading to tumour regression[83]. Therefore, we wondered whether Su improved T cell infiltration and reduced MDSCs in the 4T1 tumors. We found that 4T1 tumour bearing animals undergo splenomegaly (observed data) due to the recruitment of myeloid cells into the spleen as the tumours grow (Figure S7). As published, we found that Su reduces the number of MDSCs in the spleen upon treatment. We found that there is a reduction in the number of MDSCs in the spleen (Figure 2.12) and a modest but insignificant increase in the number of lymphocytes in the spleen (Figure 2.14). Su treatment did not reduce MDSC population in the tumour after 6 days of treatment (Figure 2.14). This is consistent with previously published report[127]. Su treatment also did not appear to increase the number of tumour infiltrating lymphocytes in the 4T1 tumours (Figure 2.14). These results alone do not provide any information about the T cell activity within the tumour microenvironment. Future experiments to determine whether $CD8^+$ T cell function is improved with co-therapy, ELISPOT assays should be performed measuring IFN-γ production. Additionally, IFN-γ and TNF-α can be measured using intracellular flow cytometry from splenic and intra-tumoral T cells. Ko *et al* published a study characterizing IFN-γ production from $CD8^+$ T cells isolated from the spleen of a 4T1 tumour-bearing animal treated with Su. They found that these $CD8^+$ T cells produced more IFN-γ with Su treatment. This study found that Su treated animals had more IFN-γ producing T cells in

the spleen however these cells were highly anergic as they needed α-CD3 and α-CD28 *ex vivo* to produce IFN- γ. However, when they extracted T cells from the tumour they were unable to detect IFN-γ production with even with *ex vivo* stimulation[97]. This further emphasizes the role of the tumour microenvironment as a barrier to immunotherapy. In addition to altering the immune contexture of tumour bearing animals, Su is also a vascular normalizing agent[90,142].

3.2.3 Su treatment may improve viral delivery to the tumours

Su was primarily designed to be an anti-angiogenic agent that inhibits formation of neo-vessels. Recently, it has been found that anti-angiogenic agents increase the perfusion within the tumour vasculature. This is now termed "vascular normalization". An on going study shows that Su improved productivity of oncolytic vaccinia (JX-549) in a pancreatic tumour model and they attribute the findings to Su improving tumour vasculature[91]. Although, vascular normalization is an important aspect of Su treatment, we did not study viral delivery. Therefore we attempted to minimize this effect by delivering ORV into the tumour directly.

Taken together this study showed that Su improves ORV infection and tumour control in an IFN responsive model in a tumour cell independent manner. We showed that Su did not inhibit the IFN production, or improve the viral productivity in the 4T1 cell itself; instead Su reduced the IFN production in stromal cells such as DCs and MΦ.

3.3 Limitations of this study

One of the limitations to this study is the use of a single model system. The 4T1 cells produce IFN and were therefore ideal for understanding the interactions of Su and IFN in the context of ORV therapy. However, we could extend the relevance of this study by testing Su/ORV interaction in other IFN competent tumour models such as EMT6[117] or B16. Although,

similar findings of improved OV infection were reported in other models such as Rip-Tag2[91] and Neuro-2A (unpublished data), the association of IFN has not yet been tested in these model system. For example, the Rip-Tag2 study suggests that Su mediated improvement of viral infection may be due to improvement in delivery. However, we also did not study the role of Su in delivery.

Additionally, we did not study the effect of ORV±Su on metastatic lesions. Human patients diagnosed with breast cancer undergo mastectomy removing the primary tumour and are treated with chemotherapy thereafter to eliminate any remaining lesions. The metastatic lesions and systemic disease are often fatal to the patient. We did not study the metastatic aspect of 4T1 tumours. Su improved ORV mediated survival in the primary 4T1 tumour, however this survival enhancement was modest with no cures. Future experiments could be done to optimize the therapy. Despite the modest improvement in survival, our experiments strongly suggested that the improved viral productivity phenotype seen in the tumour is due to Su reducing the numbers of and IFN production in DCs and macrophages. However, we did not elucidate the mechanism of Su mediated improvement in ORV infection completely. Further experiments are necessary to determine whether Su mediated IFN reduction is responsible for improved virus infection in tumours. Additionally, our studies do not delve into ORV infection completely; we did not determine which cells are infected when ORV is injected directly into the tumour.

The most interesting finding in this study is that Su selectively inhibits IFN production in the BMDM and BMDCs but not in 4T1 cells. However, further experiments are necessary to elucidate the mechanism by which Su inhibits IFN production in BMDM and BMDCs but not in 4T1 cells. Additionally, we do not completely understand the differences between VSVΔ51 and Maraba-MG1. Although they are share 98% genetic identity, there were some discrepancies in

the IFN production between VSVΔ51 and Maraba-MG1 *in vivo*. Future studies are necessary to determine the differences between these two viruses. Despite the limitations of this study, our studies strongly suggest that Su can improve ORV infection in an ORV refractory tumour model. However, further studies are necessary to completely understand the mechanism.

3.4 Future Directions

While this study investigated the innate immune modulation by Su, further experiments are necessary to prove that Su mediated reduction in IFN is responsible for improved viral productivity in the tumour. To this end we could treat IFNAR1/2 knockout mice with Su and ORV. These mice are capable of producing the first wave of IFN-β[164] in response to TLR/RLR signalling pathways. IFNAR1/2$^{-/-}$ cells and animals are unable to signal through IFNAR1/2 receptors to activate ISGs and produce IFN-α[165] and the second wave of IFN signalling. Therefore, if Su is acting on a molecule upstream of the IFN-β production pathway by targeting TLR or RLR signalling, there will be a reduction in the TIF and serum of IFNAR1/2$^{-/-}$ mice. However, if Su were responsible for dampening IFN mediated signalling or induction of the second wave of IFN production, there would not be any difference between the levels of virally induced IFN in IFNAR1/2$^{-/-}$ knockout mice and wild type mice.

The most interesting and novel finding in this study is that Su does not reduce IFN production in the tumour cell, but Su reduces IFN production in the stromal cells. However, additional experiments are necessary to determine which kinases Su is inhibiting. In order to determine the mechanism by which sunitinib is affecting the ORV induced IFN production in MΦ and DC *ex vivo* but not the tumour cells, it would be necessary to understand which IFN production pathway Su targets. Since Su has a wide range of targets, to understand the effect of

sunitinib on MΦ, an intracellular kinome analysis would be performed comparing BMDMs/BMDCs and 4T1 cells treated with VSVΔ51±Su to determine which anti-viral pathway may be targeted by Su to reduce the production of IFN-β in BMDMs. To this end, we could add radioactive [γ-^{32}P] ATP into the media. Therefore, all substrates that are phosphorylated in response to virus infection would incorporate [γ-^{32}P] ATP whereas the proteins that are inhibited by Su treatment will not have [γ-^{32}P] ATP [166]. We can then analyze proteins bound to [γ-^{32}P] ATP using mass spectrometry. The most likely targets in this case would be kinases in the TLR signalling pathways that are phosphorylated in response to virus infection. Following this, we could also perform secondary validation to confirm positive hits using BMDMs from knockout lines. In addition to reducing IFN production, Su also reduced the number of MΦ and DCs in the tumour micro and macroenvironment. Although blocking of FLT3R signalling may be at play, we have yet to show this connection in this particular case.

To understand the mechanism by which sunitinib reduces the number of macrophages and dendritic cells *in vivo*, experiments could be performed to determined whether sunitinib blocks the recruitment of myeloid cells in the spleen or leads to the apoptosis of the myeloid cells that are in the spleen. 4T1 tumours are known to secrete GM-CSF[129] that can recruit myeloid cells from the bone marrow. Based on our experiments it is unclear whether Su inhibits the recruitment of myeloid cells into the spleen or actually kills the myeloid cells that are already in the spleen. Therefore we could experiments using neutralizing GM-CSF antibodies mice to determine whether Su has an impact on the resident splenocytes or it blocks the recruitment of additional myeloid cells into the spleen and tumour. For instance, 4T1 tumour bearing animals can be treated with Ctrl, Su, α-GM-CSF antibody and α-GMCSF antibody+ Su. α-GM-CSF antibody would inhibit the recruitment of bone marrow cells into the spleen; this may result in a

similar reduction in numbers as Su treatment. However, if we observe further reduction in splenic myeloid cells in the animals treated with α-GM-CSF+Su, this would suggests that Su is cytotoxic to splenic cells. However, if α-GMCSF+Su yields the same results as Su alone or α-GM-CSF alone, then Su is blocking recruitment of bone marrow cells into the spleen in the 4T1 model. Similarly, non-tumour bearing animals could be treated with Su to determine the effect of sunitinib when cells are not being recruited to the tumour. Su could also potentially target FLT3R signalling and cause apoptosis of myeloid progenitor cells and DCs *in vivo*.

Upon binding of FLT3, FLT3R phosphorylates a series of proteins such as SHIP, SHP2 which further activate PI3K and AKT. AKT inhibits the phosphorylation of BAD and induces signalling through Bcl-2 promoting cell survival. Additionally, Flt3R can phosphorylate Grb-2/Sos, which in turn activates Ras/Raf/MEK/ERK pathway, which leads to inhibition of BAD. Therefore, when Flt3 signalling is blocked, BAD is activated and it leads to cell death in macrophage progenitor cells and DCs[109,110]. Flow cytometry experiments could be performed to staining for apoptosis markers such as 7-AAD and TUNEL in myeloid progenitor cells in mice treated with Su.

To confirm these findings, we could also perform competitive inhibition assays *ex vivo* with myeloid progenitor cells. For example, plasmacytoid dendritic cells are differentiated from bone marrow using recombinant human-FLT3L[167]. Therefore, if increasing concentrations of FLT3L can outcompete Su mediated cytotoxicity or lead to maturation of pDCs, this would further suggest that Su is reducing the viability of DCs, as seen in the tumour, in a FLT3R dependent mechanism.

Another important aspect in understanding the mechanism of Su/ORV therapy is to determine the cell-type that is infected in the tumour microenvironment. To this end, tumours

infected with ORV±Su can be imaged at various time points using intra-vital microscopy (IVM). IVM not only allows us to detect virus-infected cell (GFP^+), but also enables immune-phenotyping of these cells. IVM would enable the visualization of the tumour microenvironment and quantify differences between Su treated tumours and ORV treated tumours. These experiments would allow us to further understand the mechanism behind Su's action. However, to further improve the clinical outcome of this therapy, we need to determine whether co-therapy improves outcome of metastatic disease in the 4T1 model.

4T1 is a spontaneously metastasizing model of breast cancer, which starts forming metastatic lesions between day 3 and day 7 after implantation[168]. To further understand the clinical relevance of this study, we need to study Su and ORV co-therapy in the context of metastatic lesions. Breast cancer patients undergo mastectomy prior to chemotherapeutic intervention. Therefore, studying the effect of Su/ORV co-therapy after surgical removal of the primary tumour may allow us to determine whether the co-therapy leads to the generation of systemic anti-tumour immunity. To this end, 4T1-Fluc tumours would be established, treated with ORV±Su and then the tumours would be surgically removed at the end of the treatment term. This would allow TAAs to be released in the tumour and activation of $CD8^+$ T cells. Animals would then be imaged twice a week to monitor their metastatic burden. Animals will be sacrificed when they exhibit signs of distress such as weight loss, reduced grooming, reduced movement and laboured breathing. Metastatic lesions can be quantified using immunohistochemistry and India ink infusion to determine if there are any differences in the number of metastatic lesions between monotherapy and co-therapy.

3.5 Conclusion and Significance

In conclusion, this study strongly suggests that Su can improve ORV infection by reducing IFN production in the tumour microenvironment. Taken together, this provides rationale for combining Su with OV therapy. Sunitinib is well characterized in the clinic as the FDA approved chemotherapy agent for mRCC and Imatinib resistant GIST. Oncolytic rhabdoviruses, VSV-hIFNβ (Indiana strain) and Maraba-MG1-MAGEA3 are currently in clinical trials. Since both of these reagents are readily available in the clinical setting, it is plausible that the combination therapy can be tested as an arm of therapy in the on going Phase I clinical trials. In addition, sunitinib may also improve tumour control with other oncolytic virus therapies such as Adenovirus (H101) that is approved in China. Other groups such as Donald McDonald in collaboration with Sillajen have also shown an improvement in the infection of vaccinia virus in pancreatic neuro-endocrine tumours *in vivo*[91]. This further supports that idea that sunitinib may be used in combination with other oncolytic platforms. Other viruses reliant on defects in type I IFN signalling can also be combined with sunitinib such as Newcastle Disease Virus[169,170].

REFERENCES:

1. Kaufman, H. L., Kohlhapp, F. J. & Zloza, A. Oncolytic viruses: a new class of immunotherapy drugs. *Nat Rev Drug Discov* **14,** 642–662 (2015).
2. Stojdl, D. *et al.* Exploiting tumor-specific defects in the interferon pathway with a previously unknown oncolytic virus. *Nat. Med.* **6,** 821–5 (2000).
3. Stojdl, D. F. *et al.* VSV strains with defects in their ability to shutdown innate immunity are potent systemic anti-cancer agents. *Cancer Cell* **4,** 263–275 (2003).
4. Pol, J. G. *et al.* Maraba virus as a potent oncolytic vaccine vector. *Mol. Ther.* **22,** 420–9 (2014).
5. Samuel, C. E. Antiviral actions of interferons. *Clinical Microbiology Reviews* **14,** 778–809 (2001).
6. Jha, B. K., Dong, B., Nguyen, C. T., Polyakova, I. & Silverman, R. H. Suppression of antiviral innate immunity by sunitinib enhances oncolytic virotherapy. *Mol. Ther.* **21,** 1749–1757 (2013).
7. Russell, S. J., Peng, K.-W. & Bell, J. C. Oncolytic virotherapy. *Nat. Biotechnol.* **30,** 658–70 (2012).
8. Zamarin, D. *et al.* Localized oncolytic virotherapy overcomes systemic tumor resistance to immune checkpoint blockade immunotherapy. *Sci. Transl. Med.* **6,** 226ra32 (2014).
9. Mansour, M., Palese, P. & Zamarin, D. Oncolytic specificity of Newcastle disease virus is mediated by selectivity for apoptosis-resistant cells. *J. Virol.* **85,** 6015–23 (2011).
10. Yu, W. & Fang, H. Clinical trials with oncolytic adenovirus in China. *Curr. Cancer Drug Targets* **7,** 141–148 (2007).
11. Coffey, M. C., Strong, J. E., Forsyth, P. a & Lee, P. W. Reovirus therapy of tumors with activated Ras pathway. *Science (80-.).* **282,** 1332–1334 (1998).
12. Stojdl, D. F. *et al.* Exploiting tumor-specific defects in the interferon pathway with a previously unknown oncolytic virus. *Nat. Med.* **6,** 821–825 (2000).
13. Willmon, C. L. *et al.* Expression of IFN-beta enhances both efficacy and safety of oncolytic vesicular stomatitis virus for therapy of mesothelioma. *Cancer Res.* **69,** 7713–20 (2009).
14. Kim, K. H. *et al.* A phase i clinical trial of Ad5/3-??24, a novel serotype-chimeric, infectivity-enhanced, conditionally-replicative adenovirus (CRAd), in patients with recurrent ovarian cancer. *Gynecol. Oncol.* **130,** 518–524 (2013).
15. Bell, J. & McFadden, G. Viruses for tumor therapy. *Cell Host Microbe* **15,** 260–265 (2014).
16. Kirn, D. Oncolytic virotherapy for cancer with the adenovirus dl1520 (Onyx-015): results of phase I and II trials. *Expert Opin Biol Ther* **1,** 525–538 (2001).
17. Garber, K. China Approves World's First Oncolytic Virus Therapy For Cancer Treatment. *J. Natl. Cancer Inst.* **98 ,** 298–300 (2006).
18. Ranki, T. *et al.* Local treatment of a pleural mesothelioma tumor with ONCOS-102

induces a systemic antitumor CD8 + T-cell response, prominent infiltration of CD8 + lymphocytes and Th1 type polarization. *Oncoimmunology* **3,** e958937 (2014).
19. Burke, J. M. *et al.* A first in human phase 1 study of CG0070, a GM-CSF expressing oncolytic adenovirus, for the treatment of nonmuscle invasive bladder cancer. *J. Urol.* **188,** 2391–2397 (2012).
20. Andtbacka, R. H. I. *et al.* Talimogene laherparepvec improves durable response rate in patients with advanced melanoma. *J. Clin. Oncol.* **33,** 2780–2788 (2015).
21. Markert, J. M. *et al.* A phase 1 trial of oncolytic HSV-1, G207, given in combination with radiation for recurrent GBM demonstrates safety and radiographic responses. *Mol. Ther.* **22,** 1048–55 (2014).
22. Markert, J. M. *et al.* Phase Ib trial of mutant herpes simplex virus G207 inoculated pre- and post-tumor resection for recurrent GBM. *Mol. Ther.* **17,** 199–207 (2009).
23. Goshima, F. *et al.* Oncolytic viral therapy with a combination of HF10, a herpes simplex virus type 1 variant and granulocyte-macrophage colony-stimulating factor for murine ovarian cancer. *Int. J. Cancer* **134,** 2865–2877 (2014).
24. Sahin, T. T. *et al.* Impact of novel oncolytic virus HF10 on cellular components of the tumor microenviroment in patients with recurrent breast cancer. *Cancer Gene Ther.* **19,** 229–237 (2012).
25. Esaki, S., Goshima, F., Kimura, H., Murakami, S. & Nishiyama, Y. Enhanced antitumoral activity of oncolytic herpes simplex virus with gemcitabine using colorectal tumor models. *Int. J. Cancer* **132,** 1592–1601 (2013).
26. Learmonth, K., Braidwood, L., Woll, P. & Conner, J. Abstract B033: Cytokine responses following intrapleural administration of oncolytic HSV SEPREHVIR® in patients with malignant pleural mesothelioma. *Cancer Immunol. Res.* **4 ,** B033–B033 (2016).
27. Liu, H. *et al.* Preclinical evaluation of herpes simplex virus armed with granulocyte-macrophage colony-stimulating factor in pancreatic carcinoma. *World J. Gastroenterol.* **19,** 5138–43 (2013).
28. Heo, J. *et al.* Randomized dose-finding clinical trial of oncolytic immunotherapeutic vaccinia JX-594 in liver cancer. *Nat Med* **19,** 329–336 (2013).
29. Sborov, D. W. *et al.* A Phase 1 Trial of Single Agent Reolysin in Patients with Relapsed Multiple Myeloma. *Clin Cancer Res* **20,** 5946–5955 (2014).
30. Mita, A. C., Argiris, A., Coffey, M., Gill, G. & Mita, M. Abstract C70: A phase 2 study of intravenous administration of REOLYSIN® (reovirus type 3 dearing) in combination with paclitaxel (P) and carboplatin (C) in patients with squamous cell carcinoma of the lung. *Mol. Cancer Ther.* **12 ,** C70–C70 (2013).
31. Galanis, E. *et al.* Phase I Trial of Intraperitoneal Administration of an Oncolytic Measles Virus Strain Engineered to Express Carcinoembryonic Antigen for Recurrent Ovarian Cancer. *Cancer Res.* **70 ,** 875–882 (2010).
32. Zamarin, D. *et al.* Enhancement of oncolytic properties of recombinant newcastle disease virus through antagonism of cellular innate immune responses. *Mol. Ther.* **17,** 697–706 (2009).
33. Freeman, A. I. *et al.* Phase I/II Trial of Intravenous NDV-HUJ Oncolytic Virus in Recurrent Glioblastoma Multiforme. *Mol Ther* **13,** 221–228 (2006).
34. Yuan, M., Wong, Y., Au, G. & Shafren, D. Combination of intravenously delivered cavatak (coxsackievirus A21) and immune-checkpoint blockade significantly reduces

tumor growth and tumor rechallenge. *J. Immunother. Cancer* **3,** P342–P342 (2015).
35. Brun, J. *et al.* Identification of genetically modified Maraba virus as an oncolytic rhabdovirus. *Mol. Ther.* **18,** 1440–1449 (2010).
36. Desjardins, A. *et al.* ONCOLYTIC POLIO/RHINOVIRUS RECOMBINANT (PVSRIPO) IN RECURRENT GLIOBLASTOMA (GBM): FIRST PHASE I CLINICAL TRIAL EVALUATING THE INTRATUMORAL ADMINISTRATION. *Neuro-Oncology* **16 ,** iii43–iii43 (2014).
37. Dobrikova, E. Y. *et al.* Recombinant oncolytic poliovirus eliminates glioma in vivo without genetic adaptation to a pathogenic phenotype. *Mol. Ther.* **16,** 1865–72 (2008).
38. Parato, K. a *et al.* The Oncolytic Poxvirus JX-594 Selectively Replicates in and Destroys Cancer Cells Driven by Genetic Pathways Commonly Activated in Cancers. *Mol. Ther.* **20,** 749–758 (2012).
39. Sadler, A. J. & Williams, B. R. G. Interferon-inducible antiviral effectors. *Nat. Rev. Immunol.* **8,** 559–568 (2008).
40. Sato, M. *et al.* Distinct and essential roles of transcription factors IRF-3 and IRF-7 in response to viruses for IFN-alpha/beta gene induction. *Immunity* **13,** 539–548 (2000).
41. Holcik, M. Could the eIF2α-Independent Translation Be the Achilles Heel of Cancer? *Front. Oncol.* **5,** 264 (2015).
42. Desmet, E. A., Anguish, L. J. & Parker, J. S. L. Virus-mediated compartmentalization of the host translational machinery. *MBio* **5,** (2014).
43. Williams, B. R. PKR; a sentinel kinase for cellular stress. *Oncogene* **18,** 6112–6120 (1999).
44. Teng, Y. *et al.* Inhibition of eIF2α dephosphorylation enhances TRAIL-induced apoptosis in hepatoma cells. *Cell Death Dis.* **5,** e1060 (2014).
45. Moerdyk-Schauwecker, M. *et al.* Resistance of pancreatic cancer cells to oncolytic vesicular stomatitis virus: role of type I interferon signaling. *Virology* **436,** 221–34 (2013).
46. Westcott, M. M. *et al.* Interferon Beta and Interferon Alpha 2a Differentially Protect Head and Neck Cancer Cells from Vesicular Stomatitis Virus-Induced Oncolysis. *J. Virol.* **89,** 7944–54 (2015).
47. Jayakar, H. R., Jeetendra, E. & Whitt, M. A. Rhabdovirus assembly and budding. *Virus Research* **106,** 117–132 (2004).
48. Finkelshtein, D., Werman, A., Novick, D., Barak, S. & Rubinstein, M. LDL receptor and its family members serve as the cellular receptors for vesicular stomatitis virus. *Proc. Natl. Acad. Sci. U. S. A.* **110,** 7306–11 (2013).
49. Whitt, M. A. Generation of VSV pseudotypes using recombinant ??G-VSV for studies on virus entry, identification of entry inhibitors, and immune responses to vaccines. *J. Virol. Methods* **169,** 365–374 (2010).
50. Ahmed, M. *et al.* Ability of the matrix protein of vesicular stomatitis virus to suppress beta interferon gene expression is genetically correlated with the inhibition of host RNA and protein synthesis. *J Virol* **77,** 4646–4657 (2003).
51. Lyles, D. S. Cytopathogenesis and inhibition of host gene expression by RNA viruses. *Microbiol. Mol. Biol. Rev.* **64,** 709–24 (2000).
52. Black, B. L. & Lyles, D. S. Vesicular stomatitis virus matrix protein inhibits host cell-directed transcription of target genes in vivo. *J. Virol.* **66,** 4058–4064 (1992).
53. Ferran, M. C. & Lucas-Lenard, J. M. The vesicular stomatitis virus matrix protein inhibits

transcription from the human beta interferon promoter. *J. Virol.* **71,** 371–377 (1997).
54. Ahmed, M. *et al.* Ability of the matrix protein of vesicular stomatitis virus to suppress beta interferon gene expression is genetically correlated with the inhibition of host RNA and protein synthesis. *J. Virol.* **77,** 4646–4657 (2003).
55. Desforges, M. *et al.* Different host-cell shutoff strategies related to the matrix protein lead to persistence of vesicular stomatitis virus mutants on fibroblast cells. *Virus Res.* **76,** 87–102 (2001).
56. Gaddy, D. F. & Lyles, D. S. Vesicular stomatitis viruses expressing wild-type or mutant M proteins activate apoptosis through distinct pathways. *J. Virol.* **79,** 4170–4179 (2005).
57. Gaddy, D. F. & Lyles, D. S. Oncolytic vesicular stomatitis virus induces apoptosis via signaling through PKR, Fas, and Daxx. *J. Virol.* **81,** 2792–804 (2007).
58. Miyamoto, S. *et al.* Coxsackievirus B3 Is an Oncolytic Virus with Immunostimulatory Properties That Is Active against Lung Adenocarcinoma. *Cancer Res.* **72 ,** 2609–2621 (2012).
59. Diaconu, I. *et al.* Immune response is an important aspect of the antitumor effect produced by a CD40L-encoding oncolytic adenovirus. *Cancer Res.* **72,** 2327–2338 (2012).
60. Simmons, D. P. *et al.* Type I IFN drives a distinctive dendritic cell maturation phenotype that allows continued class II MHC synthesis and antigen processing. *J. Immunol.* **188,** 3116–26 (2012).
61. Longman, R. S. *et al.* Dendritic-cell maturation alters intracellular signaling networks, enabling differential effects of IFN-??/?? on antigen cross-presentation. *Blood* **109,** 1113–1122 (2007).
62. Bartlett, D. L. *et al.* Oncolytic viruses as therapeutic cancer vaccines. *Mol. Cancer* **12,** 103 (2013).
63. Bridle, B. W. *et al.* Oncolytic vesicular stomatitis virus quantitatively and qualitatively improves primary CD8(+) T-cell responses to anticancer vaccines. *Oncoimmunology* **2,** e26013 (2013).
64. Diaz, R. M. *et al.* Oncolytic immunovirotherapy for melanoma using vesicular stomatitis virus. *Cancer Res.* **67,** 2840–2848 (2007).
65. Lemay, C. G. *et al.* Harnessing oncolytic virus-mediated antitumor immunity in an infected cell vaccine. *Mol. Ther.* **20,** 1791–9 (2012).
66. Angarita, F. a., Acuna, S. a., Ottolino-Perry, K., Zerhouni, S. & McCart, J. A. Mounting a strategic offense: Fighting tumor vasculature with oncolytic viruses. *Trends Mol. Med.* **19,** 378–392 (2013).
67. Breitbach, C. J. *et al.* Targeting tumor vasculature with an oncolytic virus. *Mol. Ther.* **19,** 886–94 (2011).
68. Breitbach, C. J. *et al.* Targeting tumor vasculature with an oncolytic virus. *Mol. Ther.* **19,** 886–894 (2011).
69. Breitbach, C. J. *et al.* Oncolytic vaccinia virus disrupts tumor-associated vasculature in humans. *Cancer Res.* **73,** 1265–1275 (2013).
70. Arulanandam, R. *et al.* VEGF-Mediated Induction of PRD1-BF1/Blimp1 Expression Sensitizes Tumor Vasculature to Oncolytic Virus Infection. *Cancer Cell* **28,** 210–224 (2015).
71. Bose, A. *et al.* Sunitinib facilitates the activation and recruitment of therapeutic anti-tumor immunity in concert with specific vaccination. *Int. J. Cancer* **129,** 2158–2170 (2011).

72. Bunt, S. K., Sinha, P., Clements, V. K., Leips, J. & Ostrand-Rosenberg, S. Inflammation induces myeloid-derived suppressor cells that facilitate tumor progression. *J. Immunol.* **176,** 284–290 (2006).
73. Schoggins, J. W. & Rice, C. M. Interferon-stimulated genes and their antiviral effector functions. *Curr. Opin. Virol.* **1,** 519–525 (2011).
74. Parato, K. A., Senger, D., Forsyth, P. A. J. & Bell, J. C. Recent progress in the battle between oncolytic viruses and tumours. *Nat. Rev. Cancer* **5,** 965–976 (2005).
75. Shayakhmetov, D. M., Di Paolo, N. C. & Mossman, K. L. Recognition of virus infection and innate host responses to viral gene therapy vectors. *Mol. Ther.* **18,** 1422–1429 (2010).
76. Kawai, T. & Akira, S. TLR signaling. *Cell Death Differ.* **13,** 816–25 (2006).
77. Loo, Y. M. & Gale, M. Immune Signaling by RIG-I-like Receptors. *Immunity* **34,** 680–692 (2011).
78. Dixit, E. & Kagan, J. C. Intracellular Pathogen Detection by RIG-I-Like Receptors. *Adv. Immunol.* **117,** 99–125 (2013).
79. Kawai, T. *et al.* IPS-1, an adaptor triggering RIG-I- and Mda5-mediated type I interferon induction. *Nat Immunol* **6,** 981–988 (2005).
80. Platanias, L. C. Mechanisms of type-I- and type-II-interferon-mediated signalling. *Nat. Rev. Immunol.* **5,** 375–86 (2005).
81. Mellman, I., Coukos, G. & Dranoff, G. Cancer immunotherapy comes of age. *Nature* **480,** 480–489 (2011).
82. McGray, a J. R. *et al.* Immunotherapy-induced CD8(+) T Cells Instigate Immune Suppression in the Tumor. *Mol. Ther.* **22,** 206–18 (2014).
83. Gabrilovich, D. I. & Nagaraj, S. Myeloid-derived suppressor cells as regulators of the immune system. *Nat. Rev. Immunol.* **9,** 162–174 (2009).
84. Fujimura, T., Kambayashi, Y. & Aiba, S. Crosstalk between regulatory T cells (Tregs) and myeloid derived suppressor cells (MDSCs) during melanoma growth. *Oncoimmunology* **1,** 1433–1434 (2012).
85. Sideras, K. *et al.* Role of the immune system in pancreatic cancer progression and immune modulating treatment strategies. *Cancer Treat. Rev.* **40,** 513–522 (2014).
86. Thomas, D. a & Massagué, J. TGF-beta directly targets cytotoxic T cell functions during tumor evasion of immune surveillance. *Cancer Cell* **8,** 369–80 (2005).
87. Le Bœuf, F. *et al.* Model-based rational design of an oncolytic virus with improved therapeutic potential. *Nat. Commun.* **4,** 1974 (2013).
88. Beug, S. T. *et al.* Smac mimetics and innate immune stimuli synergize to promote tumor death. *Nat. Biotechnol.* **32,** 182–190 (2014).
89. Faivre, S., Demetri, G., Sargent, W. & Raymond, E. Molecular basis for sunitinib efficacy and future clinical development. *Nat. Rev. Drug Discov.* **6,** 734–745 (2007).
90. Zhou, Q., Guo, P. & Gallo, J. M. Impact of angiogenesis inhibition by sunitinib on tumor distribution of temozolomide. *Clin. Cancer Res.* **14,** 1540–1549 (2008).
91. McDonald, C. E. *et al.* Abstract 296: Synergistic actions of oncolytic vaccinia virus and sunitinib on pancreatic neuroendocrine tumors in RIP-Tag2 mice. *Cancer Res* **75,** 296 (2015).
92. Goodman, V. L. *et al.* Approval summary: Sunitinib for the treatment of imatinib refractory or intolerant gastrointestinal stromal tumors and advanced renal cell carcinoma. *Clin. Cancer Res.* **13,** 1367–1373 (2007).

93. Swords, R., Freeman, C. & Giles, F. Targeting the FMS-like tyrosine kinase 3 in acute myeloid leukemia. *Leukemia* **26,** 2176–2185 (2012).
94. Aparicio-Gallego, G. *et al.* New insights into molecular mechanisms of sunitinib-associated side effects. *Mol. Cancer Ther.* **10,** 2215–23 (2011).
95. Murray, L. J. *et al.* SU11248 inhibits tumor growth and CSF-1R-dependent osteolysis in an experimental breast cancer bone metastasis model. *Clin. Exp. Metastasis* **20,** 757–766 (2003).
96. Jha, B. K. *et al.* Inhibition of RNase L and RNA-dependent protein kinase (PKR) by sunitinib impairs antiviral innate immunity. *J. Biol. Chem.* **286,** 26319–26326 (2011).
97. Finke, J. *et al.* MDSC as a mechanism of tumor escape from sunitinib mediated anti-angiogenic therapy. *Int. Immunopharmacol.* **11,** 853–858 (2011).
98. Finke, J. H. *et al.* Modification of the tumor microenvironment as a novel target of renal cell carcinoma therapeutics. *Cancer J.* **19,** 353–364 (2013).
99. Hosoi, A. *et al.* Adoptive cytotoxic T lymphocyte therapy triggers a counter-regulatory immunosuppressive mechanism via recruitment of myeloid-derived suppressor cells. *Int. J. Cancer* **134,** 1810–1822 (2014).
100. Finke, J. *et al.* MDSC as a mechanism of tumor escape from sunitinib mediated anti-angiogenic therapy. *Int. Immunopharmacol.* **11,** 856–861 (2011).
101. Ko, J. S. *et al.* Sunitinib mediates reversal of myeloid-derived suppressor cell accumulation in renal cell carcinoma patients. *Clin. Cancer Res.* **15,** 2148–2157 (2009).
102. Kollmannsberger, C. *et al.* Sunitinib therapy for metastatic renal cell carcinoma: recommendations for management of side effects. *Can. Urol. Assoc. J.* **1,** S41–S54 (2007).
103. Donskov, F. *et al.* Sunitinib-associated hypertension and neutropenia as efficacy biomarkers in metastatic renal cell carcinoma patients. *Br. J. Cancer* **113,** 1571–1580 (2015).
104. Rautiola, J., Donskov, F., Peltola, K., Joensuu, H. & Bono, P. Sunitinib-induced hypertension, neutropenia and thrombocytopenia as predictors of good prognosis in metastatic renal cell carcinoma patients. *BJU Int.* **Epub ahead,** n/a–n/a (2014).
105. Faivre, S. *et al.* Safety, pharmacokinetic, and antitumor activity of SU11248, a novel oral multitarget tyrosine kinase inhibitor, in patients with cancer. *J. Clin. Oncol.* **24,** 25–35 (2006).
106. Kingston, D. *et al.* The concerted action of GM-CSF and Flt3-ligand on in vivo dendritic cell homeostasis. *Blood* **114,** 835–843 (2009).
107. Kikushige, Y. *et al.* Human Flt3 is expressed at the hematopoietic stem cell and the granulocyte/macrophage progenitor stages to maintain cell survival. *J. Immunol.* **180,** 7358–7367 (2008).
108. McKenna, H. J. *et al.* Mice lacking flt3 ligand have deficient hematopoiesis affecting hematopoietic progenitor cells, dendritic cells, and natural killer cells. *Blood* **95,** 3489–3497 (2000).
109. Kim, K. T., Levis, M. & Small, D. Constitutively activated FLT3 phosphorylates BAD partially through Pim-1. *Br. J. Haematol.* **134,** 500–509 (2006).
110. Grafone, T., Palmisano, M., Nicci, C. & Storti, S. An overview on the role of FLT3-tyrosine kinase receptor in acute myeloid leukemia: Biology and treatment. *Oncology Reviews* **6,** 64–74 (2012).

111. Liu, K. *et al.* In vivo analysis of dendritic cell development and homeostasis. *Science* **324,** 392–397 (2009).
112. Woller, N., Gürlevik, E., Ureche, C.-I., Schumacher, A. & Kühnel, F. Oncolytic viruses as anticancer vaccines. *Front. Oncol.* **4,** 188 (2014).
113. Lemay, C. G. *et al.* Harnessing Oncolytic Virus-mediated Antitumor Immunity in an Infected Cell Vaccine. *Mol. Ther.* **20,** 1791–1799 (2012).
114. Diebold, S. S. *et al.* Viral infection switches non-plasmacytoid dendritic cells into high interferon producers. *Nature* **424,** 324–328 (2003).
115. Asselin-Paturel, C. *et al.* Mouse type I IFN-producing cells are immature APCs with plasmacytoid morphology. *Nat. Immunol.* **2,** 1144–1150 (2001).
116. Ludewig, B. CD169+ macrophages take the bullet : Nature Immunology : Nature Publishing Group. *Nat. Immunol.* (2011). at <http://www.nature.com/ni/journal/v13/n1/full/ni.2189.html?WT.ec_id=NI-201201>
117. Anderson, B. D., Nakamura, T., Russell, S. J. & Peng, K. W. High CD46 receptor density determines preferential killing of tumor cells by oncolytic measles virus. *Cancer Res.* **64,** 4919–4926 (2004).
118. Jiang, Y., Li, Y. & Zhu, B. T-cell exhaustion in the tumor microenvironment. *Cell Death Dis.* **6,** e1792 (2015).
119. Wu, X. *et al.* Immune microenvironment profiles of tumor immune equilibrium and immune escape states of mouse sarcoma. *Cancer Lett.* **340,** 124–133 (2013).
120. Xin, H. *et al.* Sunitinib inhibition of Stat3 induces renal cell carcinoma tumor cell apoptosis and reduces immunosuppressive cells. *Cancer Res.* **69,** 2506–2513 (2009).
121. O'Farrell, A. M. *et al.* SU11248 is a novel FLT3 tyrosine kinase inhibitor with potent activity in vitro and in vivo. *Blood* **101,** 3597–3605 (2003).
122. Diallo, J. S., Vähä-Koskela, M., Le Boeuf, F. & Bell, J. Propagation, purification, and in vivo testing of oncolytic vesicular stomatitis virus strains. *Methods Mol. Biol.* **797,** 127–140 (2012).
123. Weischenfeldt, J. & Porse, B. Bone marrow-derived macrophages (BMM): Isolation and applications. *Cold Spring Harb. Protoc.* **3,** (2008).
124. Savina, A. *et al.* NOX2 Controls Phagosomal pH to Regulate Antigen Processing during Crosspresentation by Dendritic Cells. *Cell* **126,** 205–218 (2006).
125. Veldhoen, M., Moncrieffe, H., Hocking, R. J., Atkins, C. J. & Stockinger, B. Modulation of dendritic cell function by naive and regulatory CD4+ T cells. *J Immunol* **176,** 6202–6210 (2006).
126. Celis, J. E. *et al.* Proteomic characterization of the interstitial fluid perfusing the breast tumor microenvironment: a novel resource for biomarker and therapeutic target discovery. *Mol. Cell. Proteomics* **3,** 327–344 (2004).
127. Ko, J. S. *et al.* Direct and differential suppression of myeloid-derived suppressor cell subsets by sunitinib is compartmentally constrained. *Cancer Res.* **70,** 3526–3536 (2010).
128. Karsunky, H., Merad, M., Cozzio, a., Weissman, I. L. & Manz, M. G. Flt3 Ligand Regulates Dendritic Cell Development from Flt3+ Lymphoid and Myeloid-committed Progenitors to Flt3+ Dendritic Cells In Vivo. *J. Exp. Med.* **198,** 305–313 (2003).
129. DuPré, S. A., Redelman, D. & Hunter, K. W. The mouse mammary carcinoma 4T1: characterization of the cellular landscape of primary tumours and metastatic tumour foci. *Int. J. Exp. Pathol.* **88,** 351–360 (2007).

130. Liu, Y.-P., Suksanpaisan, L., Steele, M. B., Russell, S. J. & Peng, K.-W. Induction of antiviral genes by the tumor microenvironment confers resistance to virotherapy. *Sci. Rep.* **3,** 2375 (2013).
131. Zucchini, N. *et al.* Individual plasmacytoid dendritic cells are major contributors to the production of multiple innate cytokines in an organ-specific manner during viral infection. *Int. Immunol.* **20,** 45–56 (2008).
132. Swiecki, M., Gilfillan, S., Vermi, W., Wang, Y. & Colonna, M. Plasmacytoid dendritic cell ablation impacts early interferon responses and antiviral NK and CD8(+) T cell accrual. *Immunity* **33,** 955–966 (2010).
133. Gary Gilliland, D. & Griffin, J. D. The roles of FLT3 in hematopoiesis and leukemia. *Blood* **100,** 1532–1542 (2002).
134. Colonna, M., Trinchieri, G. & Liu, Y.-J. Plasmacytoid dendritic cells in immunity. *Nat. Immunol.* **5,** 1219–26 (2004).
135. Bernhard, C. A., Ried, C., Kochanek, S. & Brocker, T. CD169+ macrophages are sufficient for priming of CTLs with specificities left out by cross-priming dendritic cells. *Proc. Natl. Acad. Sci.* **112,** 5461–5466 (2015).
136. Pejawar, S. S., Parks, G. D. & Alexander-Miller, M. A. Abortive versus productive viral infection of dendritic cells with a paramyxovirus results in differential upregulation of select costimulatory molecules. *J. Virol.* **79,** 7544–57 (2005).
137. Escudier, B. *et al.* Phase II study of sunitinib administered in a continuous once-daily dosing regimen in patients with cytokine-refractory metastatic renal cell carcinoma. *J. Clin. Oncol.* **27,** 4068–4075 (2009).
138. Motzer, R. J. *et al.* Randomized phase II trial of sunitinib on an intermittent versus continuous dosing schedule as first-line therapy for advanced renal cell carcinoma. *J. Clin. Oncol.* **30,** 1371–7 (2012).
139. Haznedar, J. O. *et al.* Single- and multiple-dose disposition kinetics of sunitinib malate, a multitargeted receptor tyrosine kinase inhibitor: comparative plasma kinetics in non-clinical species. *Cancer Chemother. Pharmacol.* **64,** 691–706 (2009).
140. Ryan, C. W. Dosing strategies and optimization of targeted therapy in advanced renal cell carcinoma. *J. Oncol. Pharm. Pract.* (2015). doi:10.1177/1078155215618769
141. Tan, H. S. *et al.* Efficacy and Safety of an Attenuated-Dose Sunitinib Regimen in Metastatic Renal Cell Carcinoma: Results from a Prospective Registry in Singapore. *Clin. Genitourin. Cancer* **13,** e285–e295 (2015).
142. Matsumoto, S. *et al.* Antiangiogenic agent sunitinib transiently increases tumor oxygenation and suppresses cycling hypoxia. *Cancer Res.* **71,** 6350–6359 (2011).
143. Kato, H. *et al.* Cell type-specific involvement of RIG-I in antiviral response. *Immunity* **23,** 19–28 (2005).
144. Asselin-Paturel, C. & Trinchieri, G. Production of type I interferons: plasmacytoid dendritic cells and beyond. *J. Exp. Med.* **202,** 461–465 (2005).
145. Xiang, Y. *et al.* Effects of RNase L Mutations Associated with Prostate Cancer on Apoptosis Induced by 2???,5???-Oligoadenylates. *Cancer Res.* **63,** 6795–6801 (2003).
146. Liu, S. *et al.* Phosphorylation of innate immune adaptor proteins MAVS, STING, and TRIF induces IRF3 activation. *Science* **347,** aaa2630 (2015).
147. Huang, B. *et al.* Toll-like receptors on tumor cells facilitate evasion of immune surveillance. *Cancer Res.* **65,** 5009–5014 (2005).

148. Yan, W. *et al.* Control of PERK eIF2alpha kinase activity by the endoplasmic reticulum stress-induced molecular chaperone P58IPK. *Proc. Natl. Acad. Sci. U. S. A.* **99,** 15920–15925 (2002).
149. Gabrilovich, D. I., Ostrand-Rosenberg, S. & Bronte, V. Coordinated regulation of myeloid cells by tumours. *Nat. Rev. Immunol.* **12,** 253–68 (2012).
150. Banchereau, J. *et al.* Immunobiology of dendritic cells. *Annu. Rev. Immunol.* **18,** 767–811 (2000).
151. Merad, M., Sathe, P., Helft, J., Miller, J. & Mortha, A. The dendritic cell lineage: ontogeny and function of dendritic cells and their subsets in the steady state and the inflamed setting. *Annu. Rev. Immunol.* **31,** 563–604 (2013).
152. Sitnicka, E. *et al.* Key role of flt3 ligand in regulation of the common lymphoid progenitor but not in maintenance of the hematopoietic stem cell pool. *Immunity* **17,** 463–472 (2002).
153. Nagasawa, T. Microenvironmental niches in the bone marrow required for B-cell development. *Nat. Rev. Immunol.* **6,** 107–116 (2006).
154. Stirewalt, D. L. & Radich, J. P. The role of FLT3 in haematopoietic malignancies. *Nat. Rev. Cancer* **3,** 650–665 (2003).
155. Sathe, P., Vremec, D., Wu, L., Corcoran, L. & Shortman, K. Convergent differentiation: Myeloid and lymphoid pathways to murine plasmacytoid dendritic cells. in *Blood* **121,** 11–19 (2013).
156. Yang, G.-X. *et al.* Plasmacytoid dendritic cells of different origins have distinct characteristics and function: studies of lymphoid progenitors versus myeloid progenitors. *J. Immunol.* **175,** 7281–7287 (2005).
157. Mancuso, G. *et al.* Bacterial recognition by TLR7 in the lysosomes of conventional dendritic cells. *Nat. Immunol.* **10,** 587–594 (2009).
158. Wang, X. *et al.* Differential requirement for the IKKβ/NF-κB signaling module in regulating TLR- versus RLR-induced type 1 IFN expression in dendritic cells. *J. Immunol.* **193,** 2538–45 (2014).
159. Nakashima, T. & Takayanagi, H. Osteoimmunology: Crosstalk between the immune and bone systems. *J. Clin. Immunol.* **29,** 555–567 (2009).
160. Crouse, J., Kalinke, U. & Oxenius, A. Regulation of antiviral T cell responses by type I interferons. *Nat. Rev. Immunol.* **15,** 231–242 (2015).
161. Luft, T. *et al.* Type I IFNs enhance the terminal differentiation of dendritic cells. *J. Immunol.* **161,** 1947–53 (1998).
162. Bose, A. *et al.* Sunitinib facilitates the activation and recruitment of therapeutic anti-tumor immunity in concert with specific vaccination. *Int. J. Cancer* **129,** 2158–2170 (2011).
163. Hipp, M. M. *et al.* Sorafenib, but not sunitinib, affects function of dendritic cells and induction of primary immune responses. *Blood* **111,** 5610–5620 (2008).
164. Dhondt, K. P. *et al.* Type I interferon signaling protects mice from lethal henipavirus infection. *J. Infect. Dis.* **207,** 142–51 (2013).
165. Ma, F. *et al.* Positive feedback regulation of type I IFN production by the IFN-inducible DNA sensor cGAS. *J. Immunol.* **194,** 1545–54 (2015).
166. Johnson, S. A. & Hunter, T. Kinomics: methods for deciphering the kinome. *Nat. Methods* **2,** 17–25 (2005).
167. Brawand, P. *et al.* Murine plasmacytoid pre-dendritic cells generated from Flt3 ligand-supplemented bone marrow cultures are immature APCs. *J. Immunol. (Baltimore, Md.*

1950) **169,** 6711–6719 (2002).
168. Aslakson, C. J. & Miller, F. R. Selective events in the metastatic process defined by analysis of the sequential dissemination of subpopulations of a mouse mammary tumor. *Cancer Res.* **52,** 1399–1405 (1992).
169. Wilden, H., Fournier, P., Zawatzky, R. & Schirrmacher, V. Expression of RIG-I, IRF3, IFN-?? and IRF7 determines resistance or susceptibility of cells to infection by Newcastle Disease Virus. *Int. J. Oncol.* **34,** 971–982 (2009).
170. Krishnamurthy, S., Takimoto, T., Scroggs, R. A. & Portner, A. Differentially regulated interferon response determines the outcome of Newcastle disease virus infection in normal and tumor cell lines. *J. Virol.* **80,** 5145–5155 (2006).

APPENDIX:

Appendix 1: Supplemental Figures

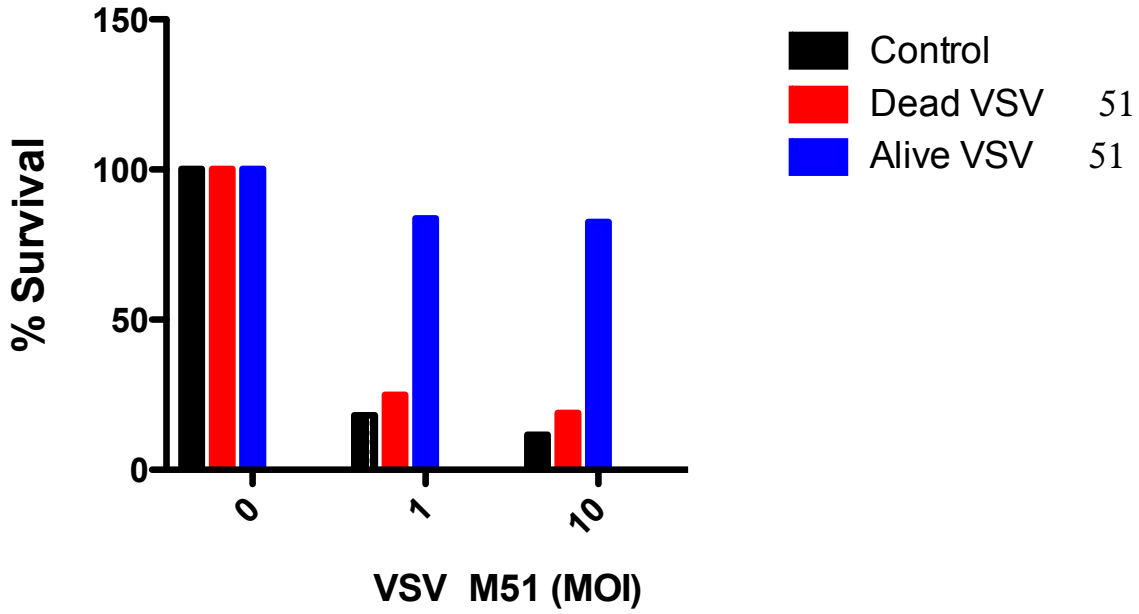

Figure S1: 4T1 cells are competent in producing and responding to interferon.

4T1 cells were treated with PBS, dead VSVΔ51 or active VSVΔ51 at a MOI of 0.1 for 18-20 hours. Subsequently, conditioned medium was collected and UV irradiated to inactivate the virus. Following this, naïve 4T1 cells were treated with the conditioned medium overnight and infected with virus thus the following day at MOIs 0,1,10 and alamar blue assay was performed 48 hours post infection.

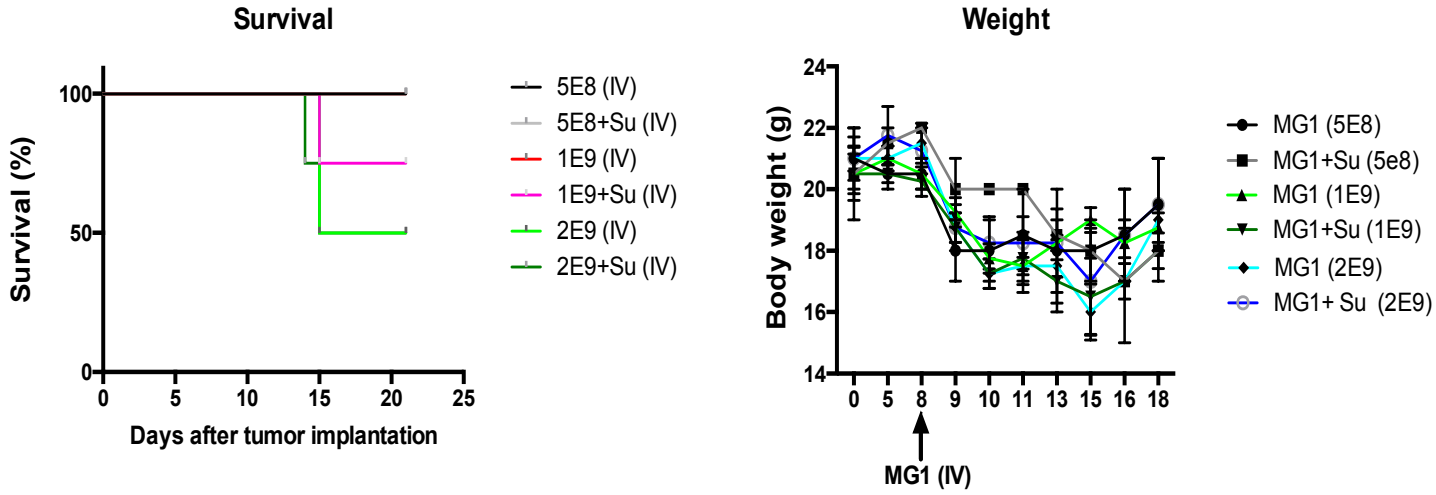

Figure S2: Sunitinib may increase the MTD of Maraba-MG1 when MG1 is administered intravenously.

Balb/c mice bearing 4T1 tumours were treated with sunitinib starting at day 5 and then injected with three different concentrations of Maraba- MG1 intravenously. The experiments in this study were done using 5E8 PFU MG1 but the virus was administered intratumorally. The end points were based on virus related adverse effects such as hind limb paralysis and > 20% body weight loss.

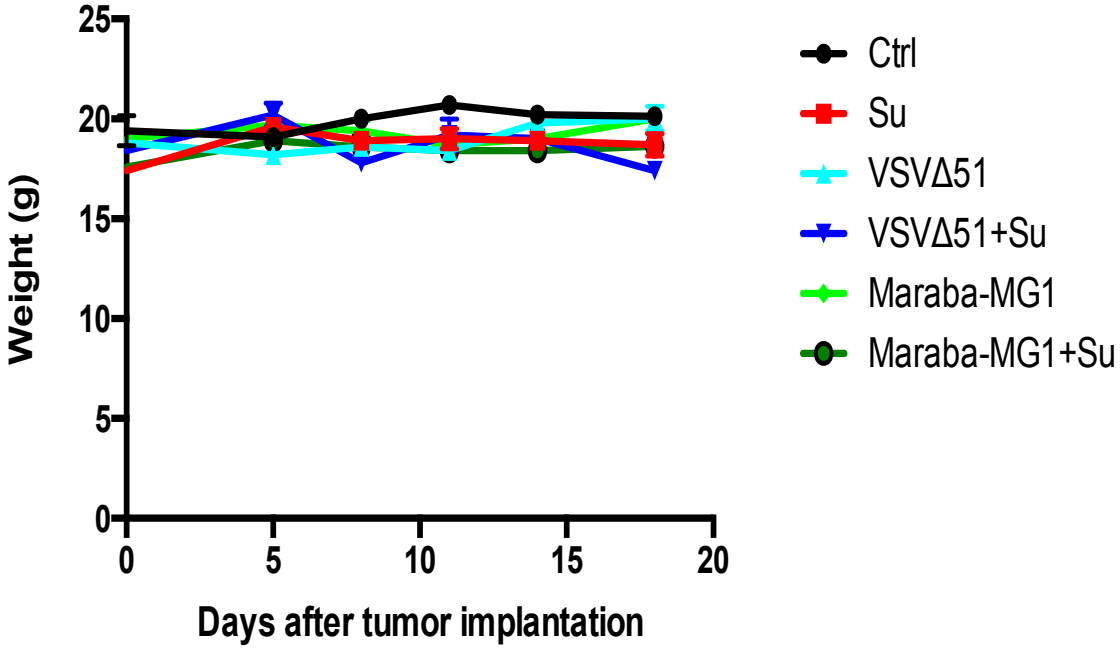

Figure S3: Body weight of animals treated with ORV+/- Su

4T1 tumour bearing animals treated with ORV+/- Su did not lose significant amounts of body weight and the therapy was well tolerated. There is transient weight loss after the first virus infection, however the mice gain their weight back between 48-72 hours post infection

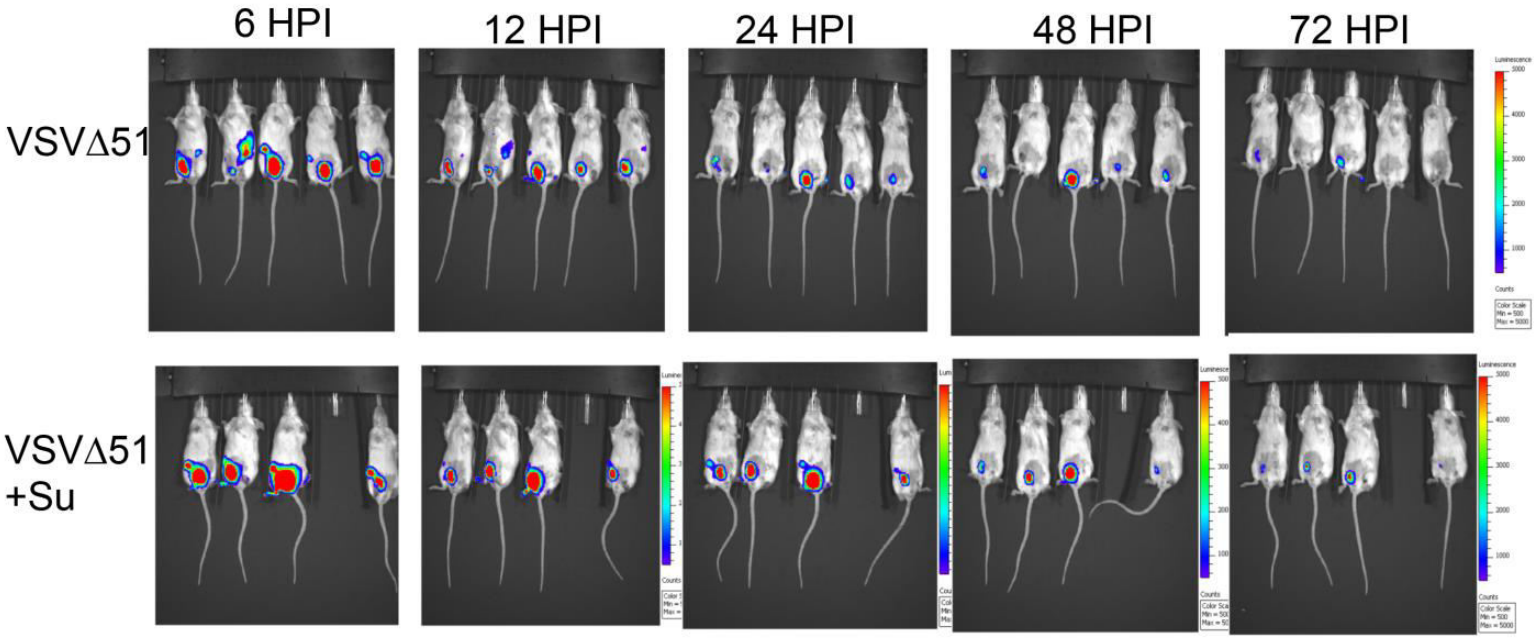

Figure S4: Sunitinib improves VSVΔ51 infection in the tumour.

4T1 cells were implanted in Balb/c mice and sunitinib treatment was started at day 5 after inoculation. 5E8 PFU of VSVΔ51-fluc was injected in the tumour and imaging was performed at the times indicated above. There is an increase in the virus signal in the group that is treated with sunitinib at the early stages of infection as well as the later time points. The increase in the virus titre persists which indicates that there is a reduction in the clearance or the virus progeny is able to successfully infect more cells with sunitinib that without sunitinib.

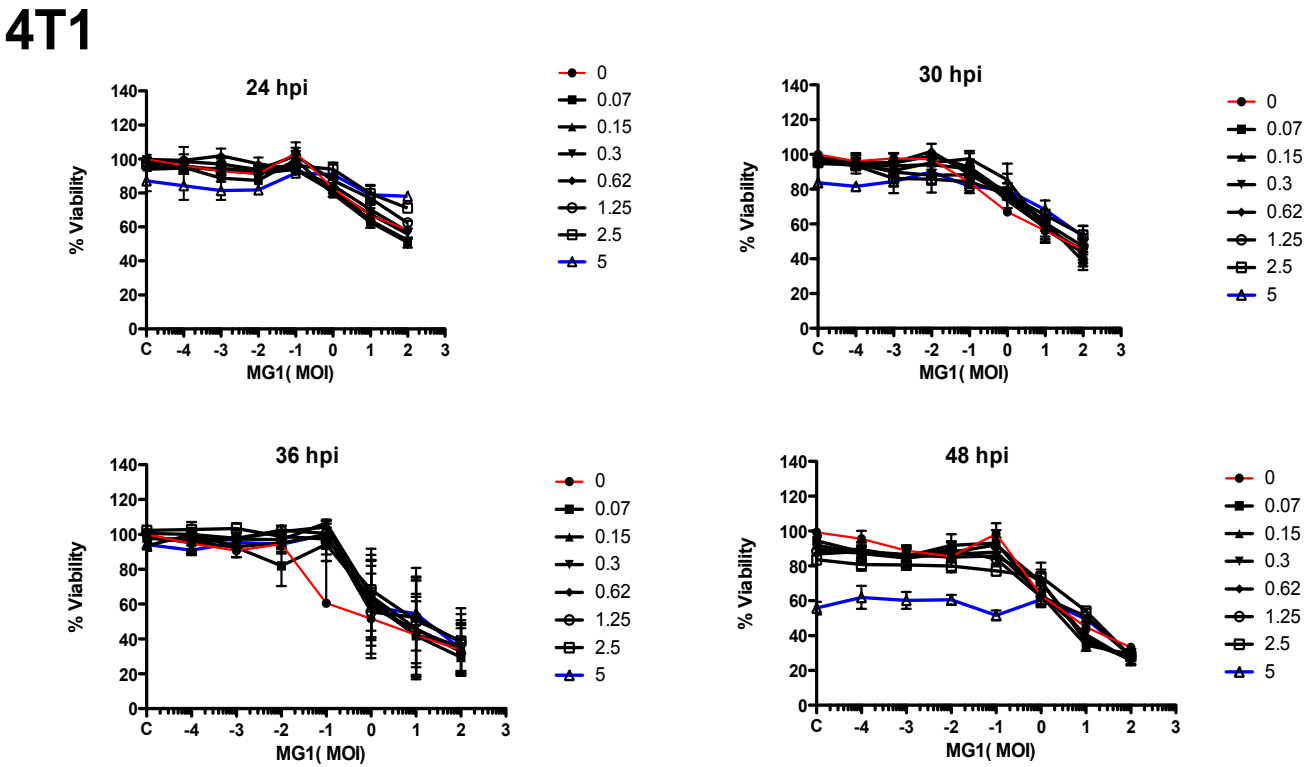

Figure S5: MG1 and sunitinib do not synergize in 4T1 cells

4T1 cells were treated with sunitinib at various concentrations for 2hrs prior to treating them with Maraba-MG1 at different MOIs ranging form 1E-4 to 1E2. Alamar blue assays were performed at several time points (24, 30, 36 and 48 hpi). There is no difference in the percentage of cell death when the concentration of sunitinib is increased.

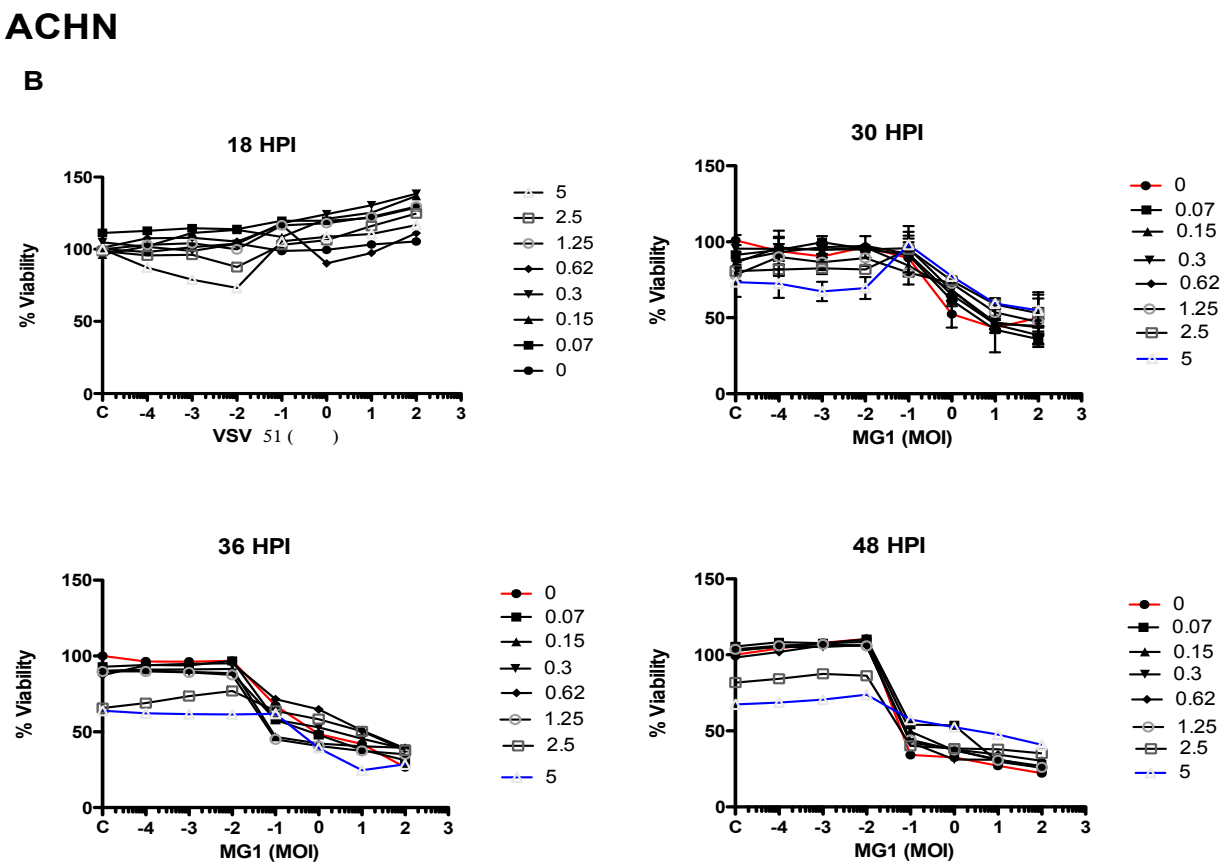

Figure S6: Sunitinib and Maraba-MG1 do not synergize in ACHN cells

ACHN cells were treated with sunitinib at various concentrations for 2hrs prior to treating them with Maraba-MG1 at different MOIs ranging form 1E-4 to 1E2. Alamar blue assays were performed at several time points (24, 30, 36 and 48 hpi). There is no difference in the percentage of cell death when the concentration of sunitinib is increased.

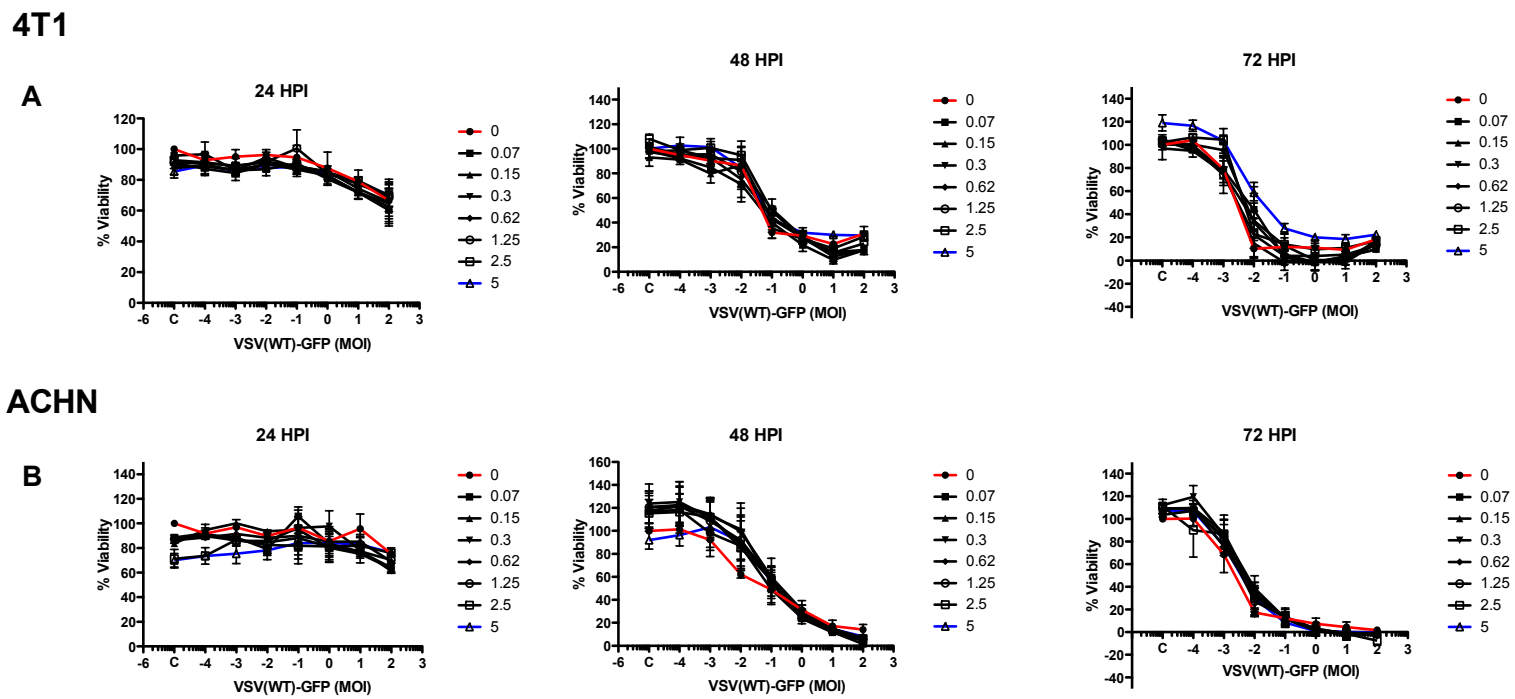

Figure S7: Sunitinib and WT-VSV do not synergize in 4T1 and ACHN cells

4T1 and ACHN cells were treated with sunitinib at various concentrations for 2hrs prior to treating them with wild-type VSV at different MOIs ranging from 1E-4 to 1E2. Alamar blue assays were performed at several time points (24, 48 and 72 hpi). There is no difference in the percentage of cell death when the concentration of sunitinib is increased.

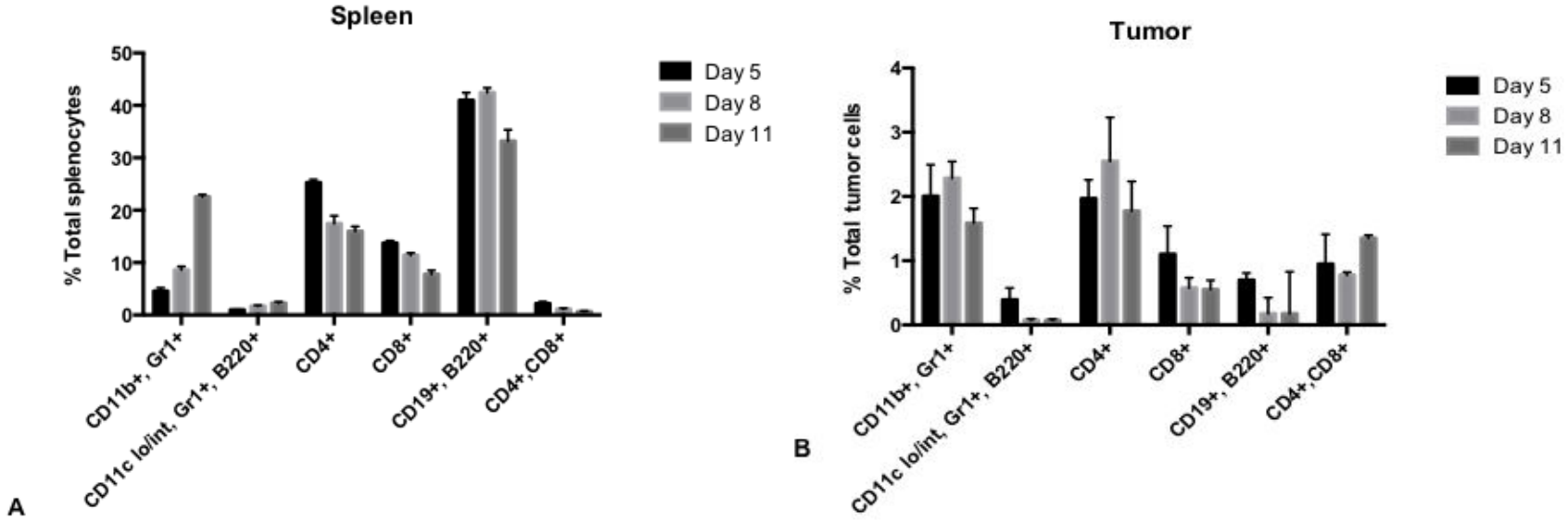

Figure S8: Percentage of myeloid cells increase in the spleen as 4T1 tumours grow.

Mean± SEM of myeloid and lymphoid cells expressed as a per cent CD45+ in 4T1 tumour bearing 6-8 weeks old Balb/c mice with no treatment (n=5/time point). (A) Spleen samples analysed for a series of myeloid cells (CD11b+ Gr1+, CD11c lo/int Gr1+ B220+) and lymphoid cells (CD4+, CD8+, CD19+ B220+, and CD4+CD8+) in 4T1 tumour bearing animals on day 5, 8 and 11 days post inoculation. (B) Tumor samples analysed for a series of myeloid cells (CD11b+ Gr1+, CD11c lo/int Gr1+ B220+) and lymphoid cells (CD4+, CD8+, CD19+ B220+, and CD4+CD8+) in 4T1 tumour bearing animals on day 5, 8 and 11 days post inoculation.

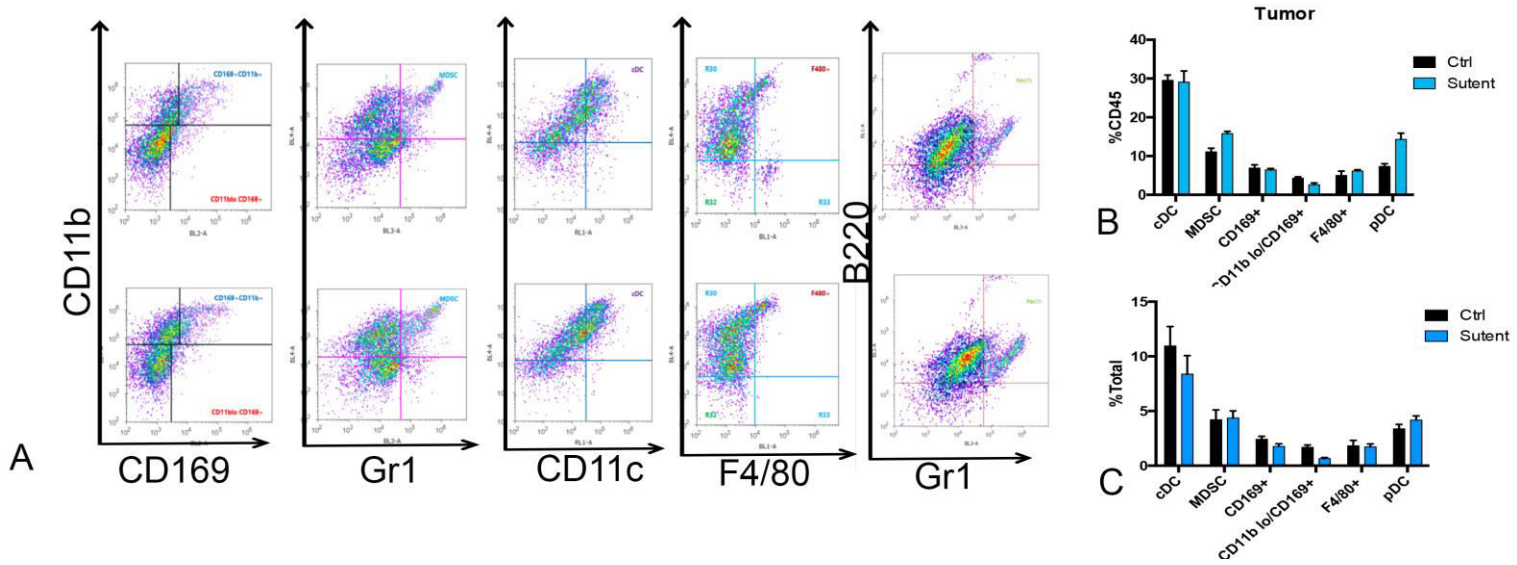

Figure S9: Sunitinib treatment does not reduce the number of myeloid cells in the tumour after three cosecutive days of treatment.

4T1 tumours were treated with vehicle (Ctrl) or Su (40mg/kg). Tumors were harvested day 8 post tumour implantation, treated with collagenase IV and DNAse I and flow cytometry was performed. Initial gate was set to include all cells and doublets were excluded, daughter plots were generated based on CD45+ cells. Representative plots of CD169+ Mϕ (CD169+ CD11b+), MDSCs (CD11b+ Gr1+), cDCs (CD11b+ CD11c+), F4/80+ Mϕ and plasmacytoid dendritic cells in the tumor (L→R)(A). These cells were then plotted as %CD45+ cells(B) or % total splenocytes (C). Data represented as mean± SEM of % CD45+ cells. One-way ANOVA was applied to whether data was statistically significant (n=5 mice/ group).

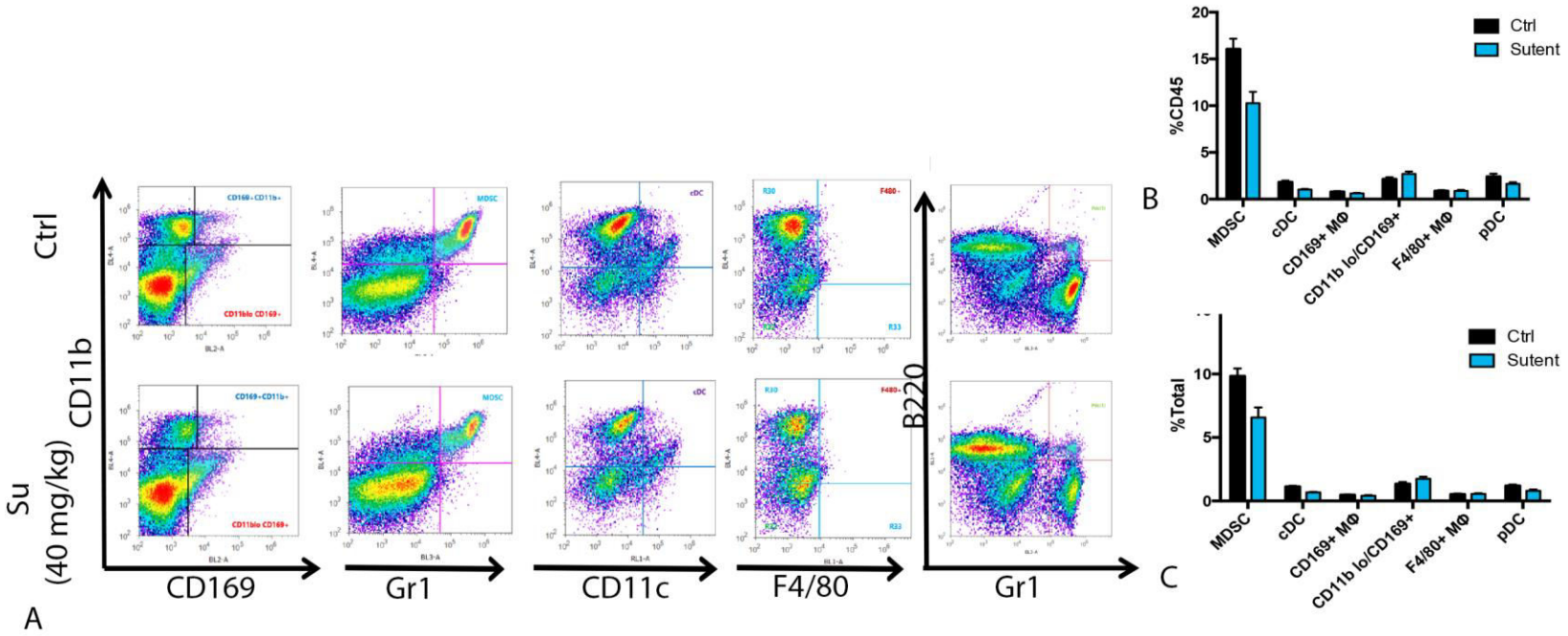

Figure S10: Sunitinib leads to a trend in the reduction of myeloid cells in the spleen after three days of treatment.

4T1 tumour bearing animals were treated with vehicle (Ctrl) or Su (40mg/kg). Spleens were harvested day 8 post tumour implantation and flow cytometry was performed. Initial gate was set to include all cells and doublets were excluded, daughter plots were generated based on CD45+ cells. Representative plots of CD169+ Mϕ (CD169+ CD11b+), MDSCs (CD11b+ Gr1+), cDCs (CD11b+ CD11c+), F4/80+ Mϕ and plasmacytoid dendritic cells in the spleen (L→R)(A). These cells were then plotted as %CD45+ cells (B) or % total splenocytes (C). Data represented as mean± SEM of % CD45+ cells. Data represented as mean± SEM of % CD45+ cells. One-way ANOVA was applied to whether data was statistically significant (n=5 mice/ group).

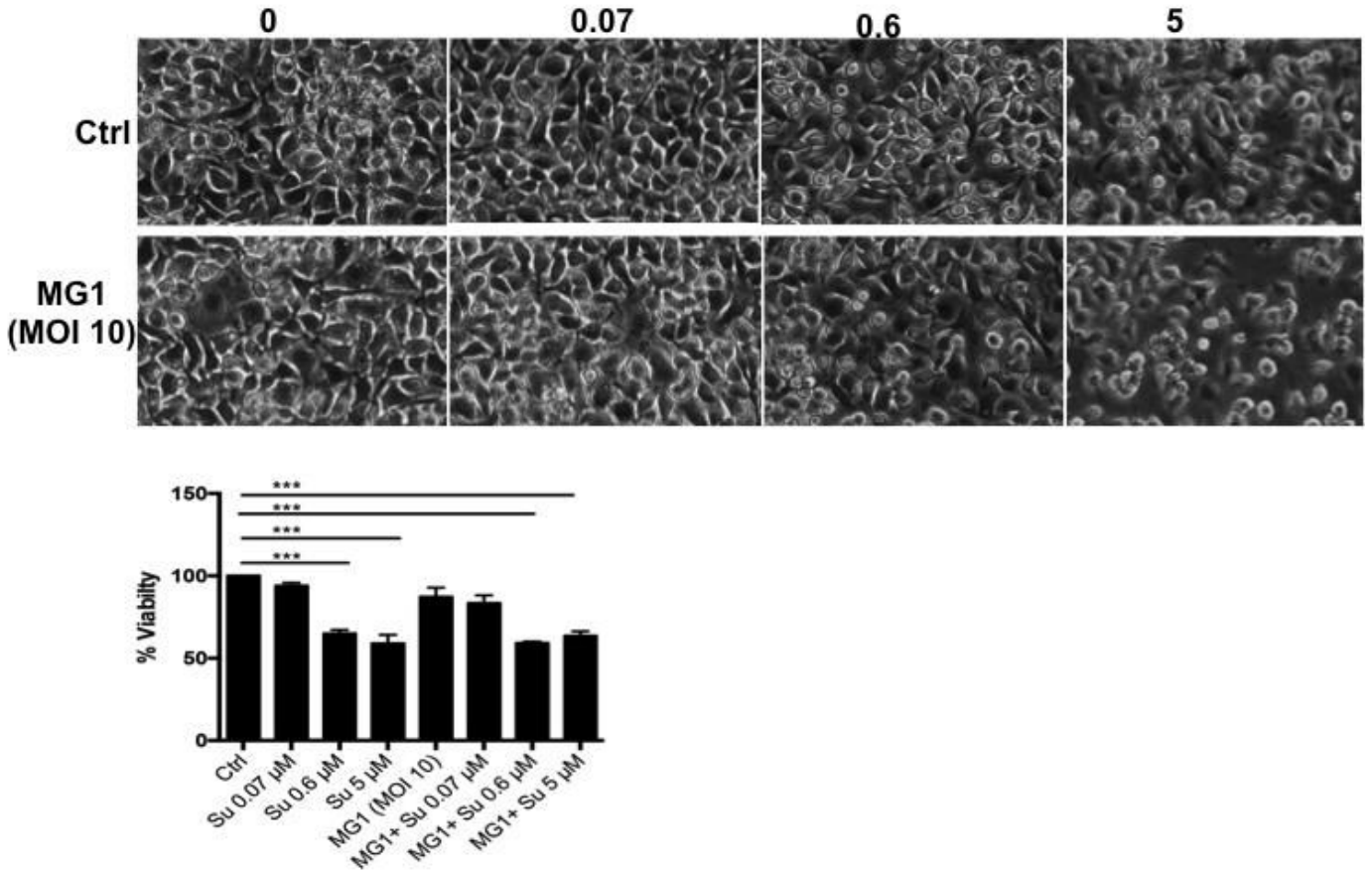

Figure S11: Su reduces the viability of BMDMs

BMDMs were derived from bone marrow of C57/BL6 mice and treated with Su at 0.078µM, 0.625µM and 5µM for 2 hours prior to Maraba-MG1 infection (MOI 10). Alamar blue assay was performed at 24 hpi to determine viability. (A) Representative images of BMDMs 24 hpi with Maraba-MG1 (MOI 10) ±sunitinib. B) Viability of BMDMs at 24 hpi calculated as % control (n=3/ group), Data represented as mean± SEM (*p<0.05, ** p<0.01, ***p<0.001).

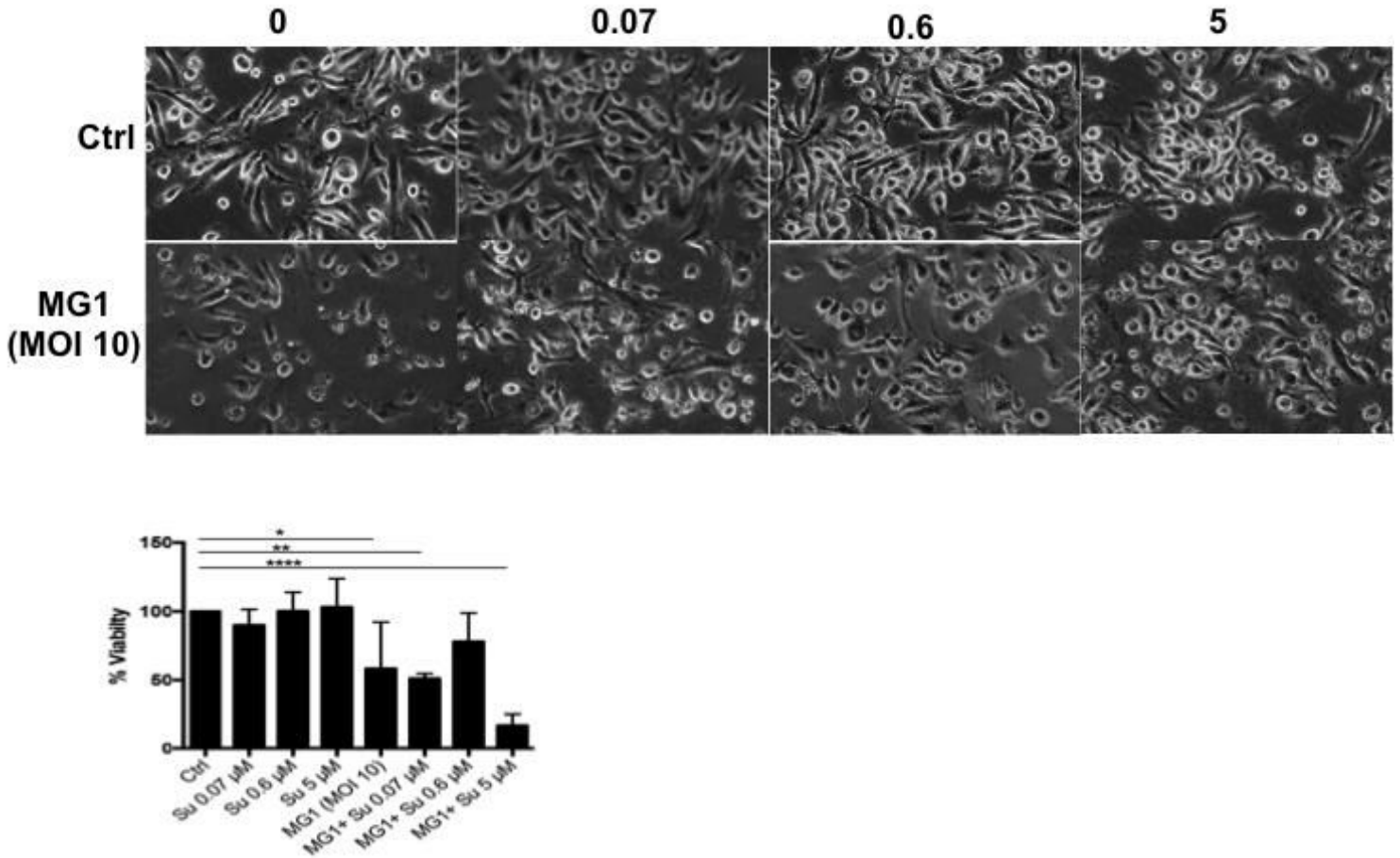

Figure S12: Maraba-MG1 reduces the viability of BMDCs

BMDCs were derived from bone marrow of C57/BL6 mice and treated with Su at 0.078µM, 0.625µM and 5µM for 2 hours prior to Maraba-MG1 infection (MOI 10). Alamar blue assay was performed at 24 hpi to determine viability. (A) Representative images of BMDMs 24 hpi with Maraba-MG1 (MOI 10) ±sunitinib. (B) Viability of BMDMs at 24 hpi calculated as % control (n=3/ group), Data represented as mean± SEM (*$p<0.05$, ** $p<0.01$, ***$p<0.001$).

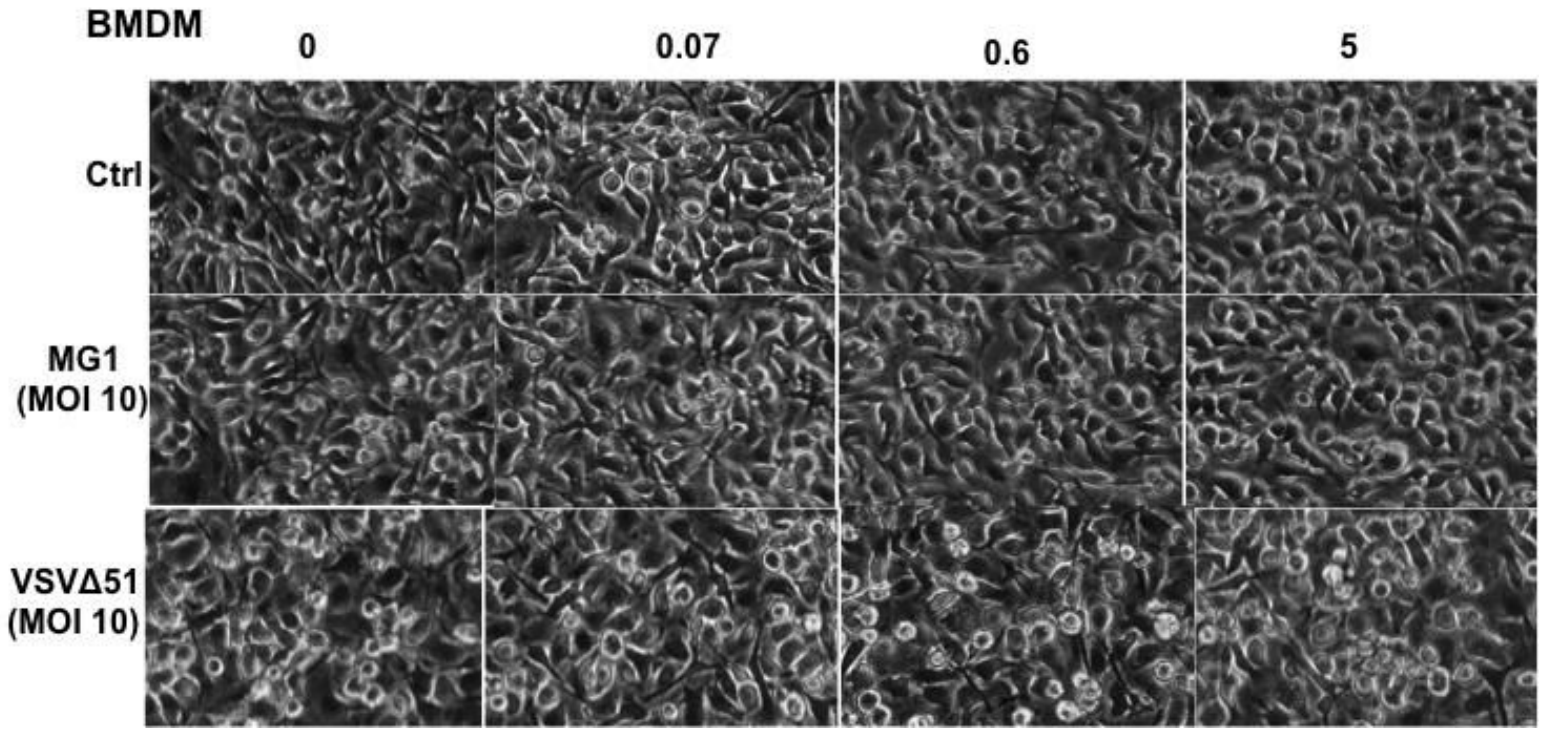

Figure S13: BMDM viability is not reduced at 6 hours post infection.

There is no observable cell-death in Su+ORV treated BMDMs after 6 hpi, however there is a reduction in the production of type I IFN.

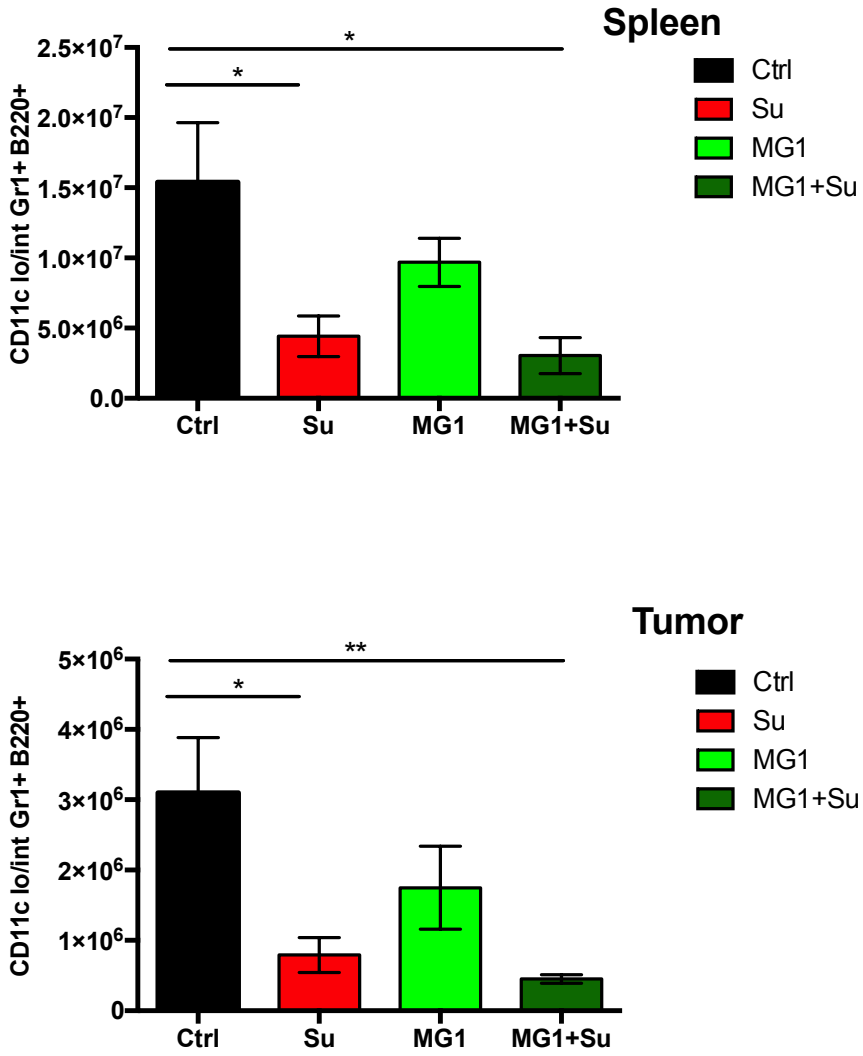

Figure S14 Plasmacytoid dendritic cells are reduced in the spleen and tumour with sunitinib treatment when expressed as absolute numbers

Sunitinib treatment reduced the number of plasmacytoid dendritic cells in the spleen and the tumour after six days of treatment. Although, there is no difference when this data is expressed at percent CD45 or percent total, there is a significant drop in the number of plasmacytoid dendritic cells in the tumour and in the spleen.